



Measurement of single top-quark production in the s-channel in proton–proton collisions at $\sqrt{s} = 13$ TeV with the ATLAS detector

The ATLAS Collaboration

A measurement of single top-quark production in the s-channel is performed in proton–proton collisions at a centre-of-mass energy of 13 TeV with the ATLAS detector at the CERN Large Hadron Collider. The dataset corresponds to an integrated luminosity of 139 fb^{-1} . The analysis is performed on events with an electron or muon, missing transverse momentum and exactly two b -tagged jets in the final state. A discriminant based on matrix element calculations is used to separate single-top-quark s-channel events from the main background contributions, which are top-quark pair production and W -boson production in association with jets. The observed (expected) signal significance over the background-only hypothesis is 3.3 (3.9) standard deviations, and the measured cross-section is $\sigma = 8.2^{+3.5}_{-2.9} \text{ pb}$, consistent with the Standard Model prediction of $\sigma^{\text{SM}} = 10.32^{+0.40}_{-0.36} \text{ pb}$.

Contents

1	Introduction	2
2	ATLAS detector	3
3	Data and simulation samples	4
4	Event reconstruction and selection	6
5	Background estimation	8
6	Matrix element method	9
7	Systematic uncertainties	14
8	Signal extraction	15
9	Results	16
10	Conclusion	20

1 Introduction

In proton–proton (pp) collisions, top quarks are produced predominantly in pairs via the strong interaction, but also singly via the electroweak interaction through a Wtb vertex. Single top-quark production is therefore a powerful probe for the top quark electroweak couplings. In the Standard Model (SM), three different production mechanisms are possible at leading-order (LO) in perturbative theory: an exchange of a virtual W boson either in the t-channel or in the s-channel, or the associated production of a top quark and a W boson (tW). Figure 1 shows the dominant Feynman diagram for s-channel single top-quark production, in which a top quark is produced with a bottom anti-quark in the final state. This mode plays an important role in searches for new phenomena that could be modelled as anomalous couplings or in effective field theories [1, 2].

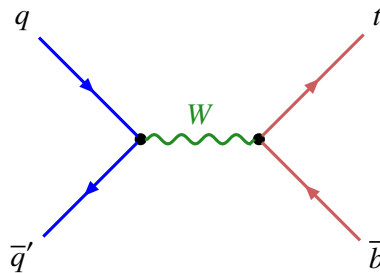


Figure 1: Feynman diagram for the dominant hard scattering process at leading-order in QCD of s-channel single top-quark production. The quarks in the initial (final) state are shown in blue (red), and the exchanged W boson is shown in green.

Single top-quark production in proton–antiproton collisions was first observed by the CDF and D0 collaborations in combined measurements of the s-channel and t-channel [3, 4]. The s-channel production mode alone was later observed in a combination of the results from the two collaborations [5]. At the Large Hadron Collider (LHC), the production of single top quarks in pp collisions was observed by the CMS and ATLAS collaborations in t-channel production at a centre-of-mass energy of $\sqrt{s} = 7$ TeV [6, 7], and in tW associated production at $\sqrt{s} = 8$ TeV [8, 9]. Both production modes were later measured at $\sqrt{s} = 13$ TeV [10–13]. For s-channel production, searches were performed by the CMS Collaboration, combining $\sqrt{s} = 7$ TeV and $\sqrt{s} = 8$ TeV data, leading to an observed (expected) significance of 2.5 (1.1) standard deviations [14], and by the ATLAS Collaboration with $\sqrt{s} = 8$ TeV data, leading to an observed (expected) significance of 3.2 (3.9) standard deviations [15], over the background-only hypothesis.

In this paper, a measurement of the single-top-quark s-channel production cross-section in pp collisions at $\sqrt{s} = 13$ TeV is presented. In the SM, the s-channel single-top-quark cross-section in pp collisions at $\sqrt{s} = 13$ TeV, calculated at next-to-leading order (NLO) in quantum chromodynamics (QCD), is $\sigma^{\text{SM}} = 10.32^{+0.40}_{-0.36}$ pb (cf. Section 3). The increase in the cross-section for this process between $\sqrt{s} = 8$ TeV and $\sqrt{s} = 13$ TeV is slightly larger than for W -boson production, which is the second dominant source of background; it is however not as large as for $t\bar{t}$ production, which is the dominant source. Using predictions based on the same techniques as those described in Section 3, the ratio of the s-channel single-top-quark cross-section to the W -boson cross-section is $1.4 \cdot 10^{-4}$ ($1.7 \cdot 10^{-4}$), and to the $t\bar{t}$ cross-section is $2.1 \cdot 10^{-2}$ ($1.2 \cdot 10^{-2}$), at $\sqrt{s} = 8$ TeV ($\sqrt{s} = 13$ TeV). This analysis is therefore more challenging as the centre-of-mass energy increases.

The top quark decays almost exclusively into a W boson and a b -quark. This analysis considers only the leptonic decays (electron or muon) of the W boson, because the fully hadronic final states are dominated by multijet background. Some of the events containing a W boson decaying into a τ -lepton which subsequently decays leptonically are also selected. At LO the final state contains two jets with large transverse momenta: one jet containing b -hadrons (called a b -jet) originating from the decay of the top quark into a b -quark, and another b -jet from the Wtb vertex producing the top quark. Thus the experimental signature consists of an isolated electron or muon, large missing transverse momentum due to the undetected neutrino from the W -boson decay, and two jets with large transverse momentum (p_T) which are both identified as containing b -hadrons (b -tagged). To extract the signal events amidst the copious background, a ‘matrix element method’ discriminant [16, 17] is used, which assigns to each selected event a probability of being signal, estimated by means of exact matrix element calculations at LO for signal and background processes. This strategy has been shown to provide better sensitivity than the boosted decision trees used in previous searches for s-channel production [15, 18].

2 ATLAS detector

ATLAS [19] is a multipurpose particle detector at the LHC with a forward–backward symmetric cylindrical geometry and a near 4π coverage in solid angle.¹ It consists of an inner tracking detector surrounded

¹ ATLAS uses a right-handed coordinate system with its origin at the nominal interaction point (IP) in the centre of the detector and the z -axis along the beam pipe. The x -axis points from the IP to the centre of the LHC ring, and the y -axis points upwards. Cylindrical coordinates (r, ϕ) are used in the transverse plane, ϕ being the azimuthal angle around the z -axis. The rapidity is defined as $y = (1/2) \ln[(E + p_z)/(E - p_z)]$ where E is the energy and p_z is the longitudinal component of the momentum along the beam pipe. The pseudorapidity is defined in terms of the polar angle θ as $\eta = -\ln \tan(\theta/2)$. Angular distance is measured in units of $\Delta R \equiv \sqrt{(\Delta\eta)^2 + (\Delta\phi)^2}$.

by a thin superconducting solenoid providing a 2 T axial magnetic field, electromagnetic and hadron calorimeters, and a muon spectrometer. The inner tracking detector covers the pseudorapidity range $|\eta| < 2.5$. It consists of silicon pixel, silicon microstrip, and transition radiation tracking detectors. Lead/liquid-argon (LAr) sampling calorimeters provide electromagnetic (EM) energy measurements with high granularity. A steel/scintillator-tile hadron calorimeter covers the central pseudorapidity range ($|\eta| < 1.7$). The endcap and forward regions are instrumented with LAr calorimeters for both the EM and hadronic energy measurements up to $|\eta| = 4.9$. The muon spectrometer surrounds the calorimeters and is based on three large superconducting air-core toroidal magnets with eight coils each. The field integral of the toroids ranges between 2.0 and 6.0 T m across most of the detector. The muon spectrometer includes a system of precision tracking chambers and fast detectors for triggering. A two-level trigger system is used to select events. The first-level trigger is implemented in hardware and uses a subset of the detector information to accept events at a rate below 100 kHz. This is followed by a software-based trigger that reduces the accepted event rate to 1 kHz on average depending on the data-taking conditions. An extensive software suite [20] is used in the reconstruction and analysis of real and simulated data, in detector operations, and in the trigger and data acquisition systems of the experiment.

3 Data and simulation samples

The data for this analysis were collected with the ATLAS detector at the LHC between 2015 and 2018, in pp collisions at $\sqrt{s} = 13$ TeV, using single-lepton triggers, and correspond to an integrated luminosity of 139 fb^{-1} . Only events for which the LHC beams were in stable-collision mode and all relevant subsystems were operational are considered [21].

Monte Carlo (MC) simulation is used to model signal and background processes. Events were simulated using either the full ATLAS detector simulation [22] based on GEANT4 [23] or a faster simulation where the full GEANT4 simulation of the calorimeter response is replaced by a detailed parameterisation of the shower shapes [22]. To simulate the effects of multiple interactions in the same and neighbouring bunch crossings (pile-up), additional interactions were generated using PYTHIA 8.186 [24] with a set of tuned parameters called the A3 tune [25] and overlaid onto the simulated hard-scatter event. Simulated events are reweighted to match the pile-up conditions observed in the full dataset, and are processed through the same reconstruction algorithms and analysis chain as the data.

Events of single-top-quark s-channel, t-channel, and tW events, as well as $t\bar{t}$ events, were generated at NLO in QCD using the POWHEG BOX v2 generator [26–32] for the nominal prediction of these processes. The top-quark mass was set to $m_t = 172.5$ GeV. For single-top-quark s-channel and tW production, and for $t\bar{t}$ production, the samples were generated in the five-flavour scheme and using the NNPDF3.0_{NLO} parton distribution function (PDF) sets [33], and for single-top-quark t-channel production, the samples were generated in the four-flavour scheme and using the NNPDF3.0_{NLO_nf4} PDF sets. The parton shower, hadronisation, and underlying event were added using PYTHIA 8.230 with the A14 tune [34] and the NNPDF2.3_{LO} PDF sets [35]. The decays of b - and c -hadrons were simulated using the EVTGEN 1.6.0 program [36]. For $t\bar{t}$ production, the h_{damp} parameter² in POWHEG BOX was set to $1.5 \cdot m_t$. For tW production, the diagram removal (DR) scheme, in which all doubly resonant NLO tW diagram amplitudes are removed [37], was employed to handle interference with $t\bar{t}$ diagrams.

² The h_{damp} parameter is a resummation damping factor and one of the parameters that control the matching of POWHEG matrix elements to the parton shower and thus effectively regulates the high- p_T radiation against which the $t\bar{t}$ system recoils.

Alternative simulation samples are used to estimate modelling uncertainties of top-quark processes (cf. Section 7). For the dominant $t\bar{t}$ background process, two alternative samples are used: one produced with POWHEG BOX v2 but with the h_{damp} parameter set to $3 \cdot m_t$ in order to estimate the impact of varying the resummation, and the other produced with MADGRAPH5_AMC@NLO to assess the effect of changing the matching of NLO matrix elements (MEs) to the parton shower. For tW production, another sample produced with POWHEG BOX v2 but using the diagram subtraction scheme, where a gauge-invariant subtraction term modifies the NLO tW cross-section to locally cancel out the $t\bar{t}$ contribution [37], is used to evaluate the impact of using a different algorithm to remove the overlap with $t\bar{t}$ production. For these three samples, PYTHIA 8.230 is used for the parton shower and hadronisation. Furthermore, for each of the four top-quark processes, another sample was produced with POWHEG BOX v2 with the same settings as for the nominal POWHEG BOX + PYTHIA 8 samples, but with HERWIG 7.04 instead of PYTHIA 8.230 in order to assess the impact of using a different parton shower and hadronisation model. These samples used the H7UE tune [38, 39] and MMHT2014LO PDF set [40] with HERWIG 7.04, and EVTGEN 1.6.0 for b - and c -hadrons decays.

Samples of leptonic W - and Z -boson (V) events where the boson decays leptonically, and semileptonic diboson (VV) events where one boson decays leptonically and the other hadronically, were simulated with the SHERPA 2.2.1 [41] generator. In the Z -boson events samples, the invariant mass of the two leptons are required to be larger than 40 GeV. For V production, MEs with NLO (LO) accuracy in QCD for up to two (four) parton emissions were used, while for VV production, MEs with NLO (LO) accuracy for up to one (three) parton emission(s) were used. The MEs were calculated with the Comix [42] and OPENLOOPS [43–45] libraries, and matched to the SHERPA parton shower [46] using the MEPS@NLO prescription [47–50]. The NNPDF3.0NNLO set of PDFs was used, along with a dedicated set of tuned parton-shower parameters developed by the SHERPA authors.

The simulated event samples above described are normalised to the integrated luminosity corresponding to the analysed data sample, and using theory predictions for the cross-sections of the individual processes, as described below. The predicted cross-section for the s-channel single-top-quark signal is $\sigma^{\text{SM}} = 10.32^{+0.29}_{-0.24}(\text{scales}) \pm 0.27(\text{PDF} + \alpha_s)$ pb = $10.32^{+0.40}_{-0.36}(\text{total})$ pb, calculated at NLO in QCD with HATHOR 2.1 [51, 52], where the uncertainties due to PDFs and α_s were calculated using the PDF4LHC prescription [53] with the MSTW2008NLO 68% CL [54, 55], CT10NLO [56] and NNPDF2.3NLO [35] PDF sets, and were added in quadrature to the effect of the scale uncertainty, defined by taking the envelope of the cross-section values obtained by independently varying the renormalisation and factorisation scales upwards and downwards by a factor of 2 while preventing the two scales from differing by more than a factor of 2. For $t\bar{t}$ production, the predicted cross-section of 832^{+40}_{-46} pb is used, calculated at next-to-next-to-leading order (NNLO) in QCD including the resummation of next-to-next-to-leading logarithmic (NNLL) soft-gluon terms with TOP++ 2.0 [57–63], where the uncertainty accounts for the effect of the PDF and α_s uncertainties calculated using the PDF4LHC15 prescription [53] with the MSTW2008NNLO [54, 55], CT10NNLO [56, 64] and NNPDF2.3LO [35] PDF sets, summed in quadrature with the effect of the scale uncertainty. The t-channel single-top-quark cross-section is 217^{+9}_{-8} pb, calculated at NLO in QCD with HATHOR 2.1 [51, 52], where the uncertainty accounts for the effect of the PDF and α_s uncertainties calculated using the PDF4LHC15 prescription with the MSTW2008NLO 68% CL, CT10NLO, and NNPDF2.3NLO PDF sets, summed in quadrature with the effect of the scale uncertainty. The tW cross-section is calculated at NLO in QCD with NNLL soft-gluon corrections [65, 66], giving a value of 71.7 ± 3.8 pb, where the uncertainty accounts for the effect of the PDF uncertainty calculated using the MSTW2008NNLO 90% CL PDF set, summed in quadrature with the effect of the scale uncertainty. These predicted cross-sections for top-quark processes are calculated for a top-quark mass of $m_t = 172.5$ GeV. The V +jets MC samples are normalised to cross-sections predicted at NNLO in QCD [67]: 60.2 nb for $W(\rightarrow \ell\nu_\ell)$ + jets and 6.32 nb

for $Z(\rightarrow \ell^+\ell^-) + \text{jets}$, calculated using the FEWZ program [68] with the MSTW2008_{NNLO} PDF set. The diboson MC samples are normalised to the cross-section predicted by the SHERPA 2.2.1 [41] generator.

To model the instrumental background from fake and non-prompt electrons (cf. Section 5), dijet events were simulated using PYTHIA 8.186 with the A14 tune and the NNPDF2.3_{LO} PDF sets, and using the EVTGEN 1.2.0 program to model the decays of bottom and charm hadrons. Here, $2 \rightarrow 2$ QCD processes were generated, including multijet, $qg \rightarrow q\gamma$, $q\bar{q} \rightarrow g\gamma$, electroweak (W/Z) and $t\bar{t}$ production processes. This simulated sample was filtered at generator level to enrich the sample with jets which are likely to resemble electron signatures in the detector: events are kept if particles (excluding neutrinos and muons) deposit at least 17 GeV of energy into a square area $\eta \times \phi = 0.1 \times 0.1$, mimicking the highly localised energy deposits characteristic of electrons.

4 Event reconstruction and selection

Events are required to have at least one primary vertex with two or more tracks with $p_T > 0.5$ GeV. If more than one vertex is found, the hard-scattering primary vertex is selected as the one with the highest sum of squared transverse momenta of associated tracks [69].

Events were recorded using single-lepton triggers with either a low p_T threshold and a lepton isolation requirement, or a higher threshold but a looser identification criterion and without any isolation requirement. The lowest p_T threshold in the single-muon trigger was 20 (26) GeV [70] for data taken in 2015 (2016–2018), while in the single-electron trigger it was 24 (26) GeV [71].

Electrons are reconstructed from tracks in the inner tracking detector (ID) associated with topological clusters of energy depositions in the calorimeter [72] and are required to have $p_T > 10$ GeV and $|\eta| < 2.47$. Candidates in the calorimeter barrel–endcap transition region ($1.37 < |\eta| < 1.52$) are excluded. Electrons must satisfy the *Medium* likelihood identification criterion. Muon candidates are identified by matching ID tracks to full tracks or track segments reconstructed in the muon spectrometer, using the *Loose* identification criterion [73]. Muons are required to have $p_T > 10$ GeV and $|\eta| < 2.5$. Lepton tracks must match the primary vertex of the event, i.e. they have to satisfy $|z_0 \sin(\theta)| < 0.5$ mm and $|d_0/\sigma(d_0)| < 5$ (3) for electrons (muons), where z_0 is the longitudinal impact parameter relative to the primary vertex and d_0 (with uncertainty $\sigma(d_0)$) is the transverse impact parameter relative to the beam line.

Jets are reconstructed from noise-suppressed topological clusters of calorimeter energy depositions [74] calibrated at the electromagnetic scale [75], using the anti- k_t [76, 77] algorithm with a radius parameter of 0.4. The average energy contribution from pile-up is subtracted according to the jet area and jets are calibrated as described in Ref. [75] with a series of simulation-based corrections and in situ techniques. Jets are required to satisfy $p_T > 20$ GeV and $|\eta| < 4.5$. The effect of pile-up is reduced by a so-called jet vertex tagger (JVT) algorithm, applied on jets with $p_T < 120$ GeV and $|\eta| < 2.5$, that uses tracking information to reject calorimeter-based jets that are not consistent with originating from the primary vertex [78].

Jets containing b -hadrons are b -tagged in the $|\eta| < 2.5$ range corresponding to the tracker acceptance, with the MV2c10 multivariate algorithm [79], which combines information about the transverse impact parameters of displaced tracks and the topological properties of secondary and tertiary decay vertices reconstructed within the jet. In this analysis, two working points are used, defined by different thresholds for the MV2c10 discriminant, and corresponding to 85% and 77% efficiencies for b -jets with $p_T > 20$ GeV as determined in simulated $t\bar{t}$ events. The corresponding rejection rate is 2.7 (4.9) for c -jets (containing c -hadrons and no b -hadrons), and 25 (110) for light-jets (containing no c - or b -hadrons), for the 85%

(77%) efficiency working point. Correction factors are applied to the simulated events to compensate for differences between data and simulation in the b -tagging efficiency for b -, c -, and light-jets [79–81].

An overlap removal procedure is applied to prevent double-counting of objects. The closest jet within $\Delta R_y = \sqrt{(\Delta y)^2 + (\Delta \phi)^2} = 0.2$ of a selected electron is removed. If the nearest jet surviving that selection is within $\Delta R_y = 0.4$ of the electron, the electron is discarded. Muons are usually removed if they are separated from the nearest jet by $\Delta R_y < 0.4$, since this reduces the background from heavy-flavour decays inside jets. However, if this jet has fewer than three associated tracks, the muon is kept and the jet is removed instead; this avoids an inefficiency for high-energy muons undergoing significant energy loss in the calorimeter.

The missing transverse momentum (with magnitude E_T^{miss}) is reconstructed as the negative vector sum of the p_T of all the selected electrons, muons, and jets described above, with an extra ‘soft term’ built from additional tracks associated with the primary vertex, to make it resilient to pile-up contamination [82].

Events are required to have exactly one lepton with $p_T > 30$ GeV, and at least two jets with $p_T > 25$ GeV and $|\eta| < 2.5$. The selected lepton is required to match a corresponding object at trigger level. More stringent identification and isolation criteria are applied to increase background rejection: events are kept if the selected electron (muon) satisfies the *Tight (Medium)* identification and the *Gradient* [72, 83] isolation criteria. To reduce the contribution of multijet production, which is dominant at low transverse momentum and low transverse mass of the W boson³ (denoted by m_T^W), events are required to have $E_T^{\text{miss}} > 35$ GeV and $m_T^W > 30$ GeV. Events are categorised into four non-overlapping analysis regions, using additional selection criteria described in the following.

The signal region (SR) targets the s-channel single-top signal topology and is used to perform the statistical analysis presented in Section 8. In the SR, events contain exactly two jets with $p_T > 30$ GeV and $|\eta| < 2.5$, both b -tagged using the 77% efficiency working point, and at least one of them is required to have $p_T > 40$ GeV. In order to reduce the contamination from the dilepton channel of $t\bar{t}$ production (see Section 5), events are rejected if they contain additional leptons with $10 \text{ GeV} < p_T < 30 \text{ GeV}$, regardless the more stringent identification and isolation criteria described in the previous paragraph. To reduce the contamination from t-channel single-top production, and from the semileptonic channel of $t\bar{t}$ events, events are rejected if they contain additional jets with $20 \text{ GeV} < p_T < 30 \text{ GeV}$ or with $2.5 < |\eta| < 4.5$.

The W + jets validation region (W + jets VR) is enriched in W + jets events by using a less stringent b -tagging requirement, and is used to assess the modelling of the W + jets background (cf. Section 5). In the W + jets VR, events contain exactly two jets, both with $p_T > 30$ GeV and b -tagged using the 85% efficiency working point, but at least one of these two jets must fail the 77% working point requirement in order to ensure that none of the selected events satisfies the SR requirements. Events are also required to contain no additional lepton with $10 \text{ GeV} < p_T < 30 \text{ GeV}$ regardless the more stringent identification and isolation criteria.

Two validation regions are enriched in $t\bar{t}$ events in order to assess the modelling of this process. In the $t\bar{t}$ 3-jets VR and $t\bar{t}$ 4-jets VR, events are required to have, respectively, exactly three and exactly four jets with $p_T > 25$ GeV and $|\eta| < 2.5$, two of which must be b -tagged using the 77% efficiency working point.

³ The transverse mass of the W boson, m_T^W , is computed from the lepton transverse momentum, p_T^ℓ and the difference in azimuthal angle, $\Delta\phi(\ell, E_T^{\text{miss}})$ as $m_T^W = \sqrt{2E_T^{\text{miss}}p_T^\ell[1 - \cos(\Delta\phi(\ell, E_T^{\text{miss}}))]}$.

5 Background estimation

Several processes with a final state that is identical or very similar to the single-top s-channel signal are sources of background events for this analysis. The largest background source is $t\bar{t}$ production, which is difficult to distinguish from the signal since such events contain real top-quark decays. In the dileptonic decay mode, $t\bar{t}$ events can mimic the final-state signature of the signal if one of the two leptons is unidentified, whereas the semileptonic decay mode contributes to the selected samples if only two jets are reconstructed. The second most important background source is W + jets production. Such events have the same signature as the signal if two jets produced in association with the W boson are b -jets. Furthermore, W -boson production in association with c - or light-jets contributes due to misidentification of such jets as b -jets; this represents 3% of the expected W + jets yield. Single top-quark production in the t-channel also leads to a sizeable background contribution, while associated tW production has a smaller event yield. Both Z + jets and diboson production are minor background sources. These background processes, as well as the signal, are modelled using MC event samples and normalised to cross-sections predicted in the SM, as described in Section 3, before the signal extraction fit described in Section 8.

In addition, multijet production contributes to the selected events, when jets, non-prompt leptons from heavy-flavour decays, or electrons from photon conversion, are misidentified as prompt isolated leptons. The modelling of this background in the electron (muon) channel relies on the so-called jet-electron (anti-muon) method described in Refs. [84, 85], in which a dedicated simulated (data) event sample is used as a model for the shapes of the different distributions. The normalisation of the multijet background is extracted from data for both channels, using a dedicated fit described in this section. Both normalisations and shapes are later used as input for the signal extraction fit described in Section 8.

In the case of the jet-electron model, a dedicated selection is imposed on the MC simulated dijet events sample described in Section 3, in order to select the events with jets that are likely to resemble a lepton in the detector. Such jets are required to deposit a large amount of their energy in the electromagnetic calorimeter, and are treated as electrons in the event selection. In order to reduce the uncertainty due to the size of the MC sample, the b -tagging requirements imposed on two of the jets in the event selection described in Section 4 are not applied. In the case of the anti-muon model, a dedicated data sample is used. Some of the muon identification criteria, related to the energy loss in the calorimeter, to the longitudinal impact parameter, or to the tracking and calorimeter isolation, are inverted or changed [73, 84], resulting in a sample that is enriched with events containing fake or non-prompt muons from multijet events.

The jet-electron and anti-muon event samples are then used to estimate the multijet background normalisation in a binned maximum-likelihood fit, using variables chosen to provide good separation between the background sources: the E_T^{miss} distribution in the electron channel, and the m_T^W distribution in the muon channel. For this purpose, the region definitions are modified in order to increase the number of multijet background events in the selected sample: the requirements on E_T^{miss} in the electron channel, and on m_T^W in the muon channel, are not applied. A simultaneous fit of the electron and muon channels is performed in the SR to extract the normalisations of both the jet-electron and anti-muon samples, which are allowed to float freely and independently in the fit. The obtained multijet normalisation is used in the SR as an initial value for the signal extraction fit described in Section 8. The normalisation of the W + jets contribution is also allowed to float freely in the fit, and so is the normalisation of the top-quark processes. The latter are grouped together in one template where the relative contributions are fixed to their SM predictions, as they show similar E_T^{miss} and m_T^W distributions. The normalisation factors extracted for the W + jets and top-quark processes in this fit are, however, not used for the signal extraction fit described in Section 8. The normalisations of the other processes are fixed to their SM predictions. The fit is repeated in each of

the three VRs to extract the multijet normalisation in these regions. In the $W+$ jets VR ($t\bar{t}$ 3-jets VR and $t\bar{t}$ 4-jets VR), the normalisation of the $W+$ jets contribution (top-quark processes contribution) is allowed to float freely, while the normalisations of the other processes are fixed to their SM predictions. The multijet normalisation obtained in the three VRs is used to validate the modelling of the discriminant, as described in Section 6.

Figures 2 and 3 show the E_T^{miss} and m_T^W distributions in the electron and muon channels respectively, after the fit of the multijet background in each region. In these distributions, the uncertainties in the background normalisations described in Section 7 are included, as well as 6% and 40% uncertainties in the $t\bar{t}$ and $W+$ jets background normalisations, motivated respectively by the uncertainty in the $t\bar{t}$ cross-section prediction (cf. Section 3) and the value of the $W+$ jets normalisation factor extracted in the fit – while they are eventually treated as unconstrained parameters in the statistical analysis of the signal cross-section (cf. Section 8). The predictions after the fit are in agreement with the data, given the statistical and systematic uncertainties. The trends seen at low E_T^{miss} or m_T^W values for the best fit distribution would not impact the signal extraction fit, for which the $E_T^{\text{miss}} > 35$ GeV and $m_T^W > 30$ GeV requirements are applied (cf. Section 4). Furthermore, the trends seen at high E_T^{miss} or m_T^W values are consistent with the mismodelling, seen in other analyses [86], of $t\bar{t}$ events by MC generators at NLO in QCD, which predict harder top-quark p_T spectra than observed in data, and which are typically covered by the relevant $t\bar{t}$ modelling systematic uncertainties described in Section 7.

6 Matrix element method

The matrix element method (MEM) [16, 17] directly uses theoretical calculations to compute a per-event signal probability. This technique was used for the observation of single top-quark production in proton–antiproton collisions at the Tevatron [3, 4, 87–89], and in finding evidence of single top-quark s-channel production in proton–proton collisions in ATLAS [15]. The discrimination between signal and background is based on the computation of likelihood values $\mathcal{P}(X | H_{\text{proc}})$ for the hypothesis that a measured event with final state X defined by the presence of certain reconstructed objects, is of a certain process type H_{proc} . The likelihoods can be computed by means of the factorisation theorem from the corresponding partonic cross-sections of the hard scattering process, as follows:

$$\mathcal{P}(X | H_{\text{proc}}) = \int d\Phi \frac{1}{\sigma_{H_{\text{proc}}}} \frac{d\sigma_{H_{\text{proc}}}}{d\Phi} T_{H_{\text{proc}}}(X | \Phi).$$

The normalised fully differential cross-section $(1/\sigma_{H_{\text{proc}}})(d\sigma_{H_{\text{proc}}}/d\Phi)$ gives the probability density for a scattering process H_{proc} to lead to a parton-level final state Φ as a function of the four-momenta of all outgoing particles. The mapping between the measured final state X and the parton-level state Φ is implemented by transfer functions $T_{H_{\text{proc}}}(X | \Phi)$ which take into account the detector energy-resolution functions, the reconstruction efficiencies for the electron, the muon and the jets, and the b -tagging efficiencies, as a function of the parton-level transverse momenta and pseudorapidities, and the efficiency of the E_T^{miss} selection as a function of the neutrino transverse momentum. The permutations between the partons and the reconstructed objects are taken into account by summing over the possible configurations which contribute to the differential cross-section [87, 89].

The phase-space integration of the differential partonic cross-sections is performed by using the Monte Carlo integration algorithm Vegas [90] from the Cuba program library [91]. The required PDF sets are taken from the LHAPDF5 package [92], while the computation of the scattering amplitudes is based on

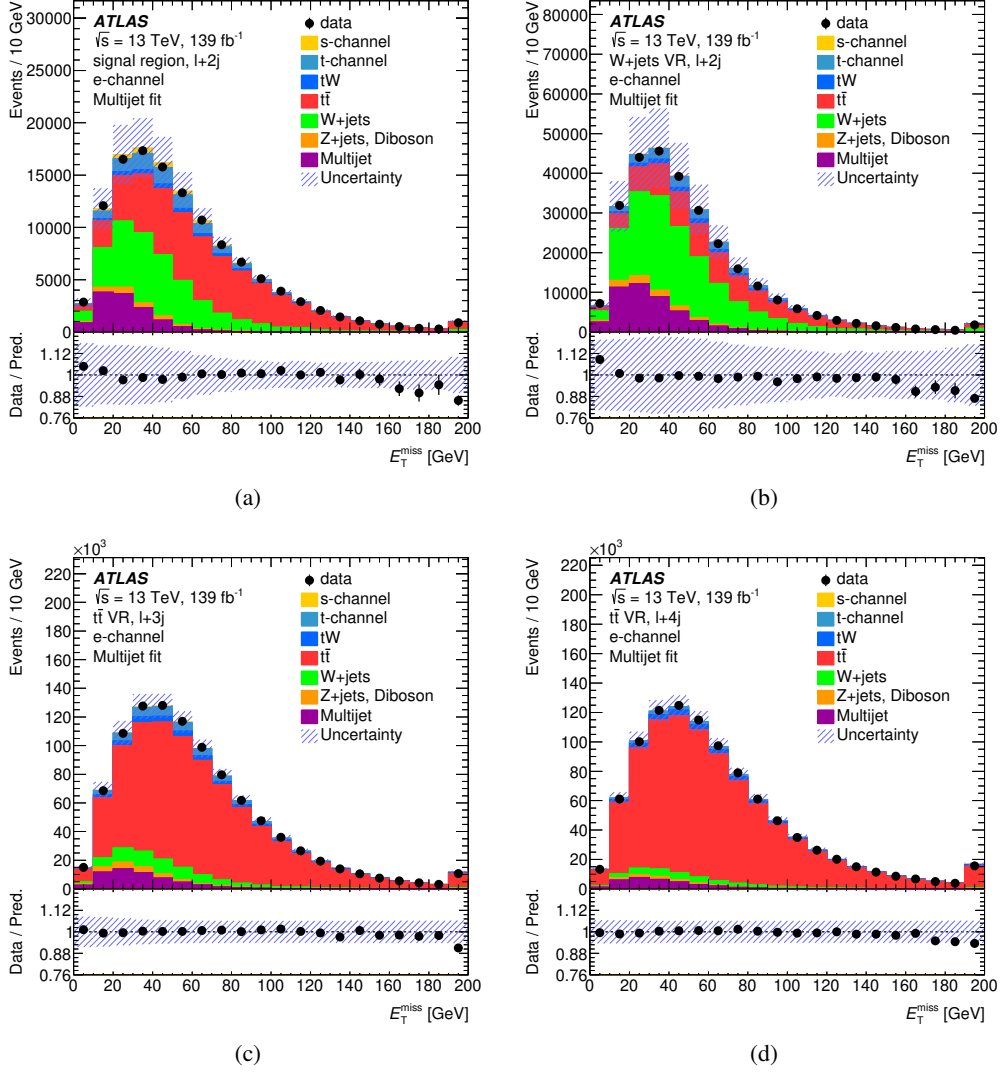


Figure 2: Distribution of E_T^{miss} after the fit of the multijet backgrounds, in the electron channel, in the (a) signal region, (b) W +jets VR, (c) $t\bar{t}$ 3-jets VR, and (d) $t\bar{t}$ 4-jets VR without applying the requirement on E_T^{miss} . Simulated events are normalised to the expected number of events given the integrated luminosity, after applying the normalisation factors obtained in the multijet fit. The last bin includes the overflow. The uncertainty bands indicate the simulation's statistical uncertainty, the normalisation uncertainties for different processes (40% for W +jets production, 30% for multijet background and 6% for top-quark processes) and the multijet background shape uncertainty in each bin, summed in quadrature. The lower panels show the ratio of the data to the prediction.

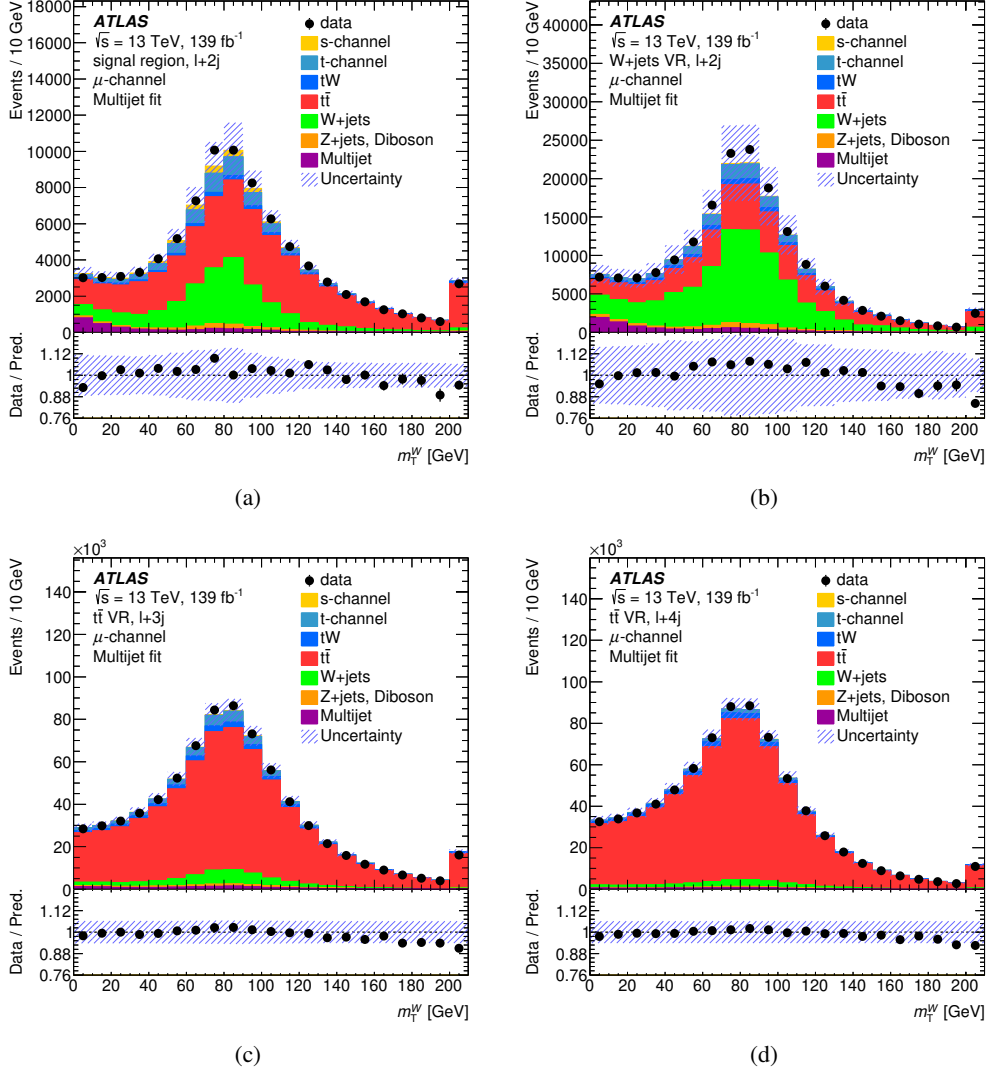


Figure 3: Distribution of m_T^W after the fit of the multijet backgrounds, in the muon channel, in the (a) signal region, (b) W+jets VR, (c) $t\bar{t}$ 3-jets VR, and (d) $t\bar{t}$ 4-jets VR without applying the requirement on m_T^W . Simulated events are normalised to the expected number of events given the integrated luminosity, after applying the normalisation factors obtained in the multijet fit. The last bin includes the overflow. The uncertainty bands indicate the simulation's statistical uncertainty, the normalisation uncertainties for different processes (40% for W+jets production, 30% for multijet background and 6% for top-quark processes) and the multijet background shape uncertainty in each bin, summed in quadrature. The lower panels show the ratio of the data to the prediction.

code from the MCFM program [93]. The functional forms and parameterisations of the ATLAS detector resolutions used for the transfer functions are those used in the KLFilter kinematic fit framework [94, 95]. The parameters are derived from event samples produced using the ATLAS detector simulation.

In total, eight different processes, all having at least one charged lepton, one neutrino, and two quarks in the final state, are considered for the computation of the likelihood values: two processes for the s-channel single-top-quark signal (one with two final-state partons corresponding to the b -quarks in the LO diagram, and one with three final-state partons in which a real radiation correction is included), one process for the t-channel single-top-quark background (which is modelled in the four-flavour scheme only), two processes for $t\bar{t}$ production (for the semileptonic and dileptonic final states, which are evaluated separately), and three processes for the remaining W -boson background production (one process with two associated light-jets, one process with one light-jet and one c -jet, and one process with two b -jets). The scattering matrix elements for all considered processes are calculated using LO amplitudes.

From the likelihood values of these processes the probability $P(S|X)$ for a measured event X to be a signal event S can be computed with Bayes' theorem by:

$$P(S|X) = \frac{\sum_i P(S_i) \mathcal{P}(X|S_i)}{\sum_i P(S_i) \mathcal{P}(X|S_i) + \sum_j P(B_j) \mathcal{P}(X|B_j)}.$$

Here, S_i and B_j denote all signal and background processes that are considered. The a priori probabilities $P(S_i)$ and $P(B_j)$ are taken to be the expected event fractions from the various processes contributing to the signal region, as obtained from Monte Carlo simulations; variations of these factors were observed to have negligible impact on the sensitivity. The final state X of the measured events have the SR topology: one electron or muon, two b -tagged jets, and missing transverse momentum. The value of $P(S|X)$ is taken as the discriminant in the signal extraction. Figure 4 shows its expected distribution for the s-channel single-top-quark signal and for the $t\bar{t}$ and W +jets background contributions in the SR, with the same binning and range as used for the signal extraction described in Section 8.

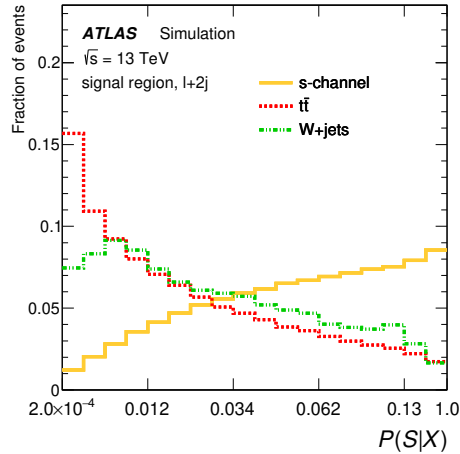


Figure 4: Expected distributions of the MEM discriminant $P(S|X)$ in the SR, for the s-channel single-top signal, and for the $t\bar{t}$ and W +jets backgrounds, for MEM discriminant values larger than 2.0×10^{-4} . Each distribution is normalised to unity. The binning is the same as the optimised binning used in the signal extraction fit, resulting in a non-linear horizontal scale.

In order to validate the s-channel MEM discriminant $P(S|X)$, it is computed in the three validation regions. For the $t\bar{t}$ VRs, in which events with three or four jets are selected, only the two b -tagged jets are considered

for the MEM discriminant computation, since most of the considered processes have only two outgoing partons. For the jet-electron sample, in which the b -tagging requirement is not applied (cf. Section 5), only the two leading jets are considered. Figure 5 compares the discriminant distribution in data with that in simulation for the three VRs, using the same optimised binning as used for the signal extraction fit in the SR described in Section 8. In these distributions, produced prior to the signal extraction fit, the uncertainty band includes the normalisation uncertainties of all processes, including the signal and the $t\bar{t}$ and W +jets backgrounds, as well as the simulation's statistical uncertainty. Good modelling is observed in the three validation regions.

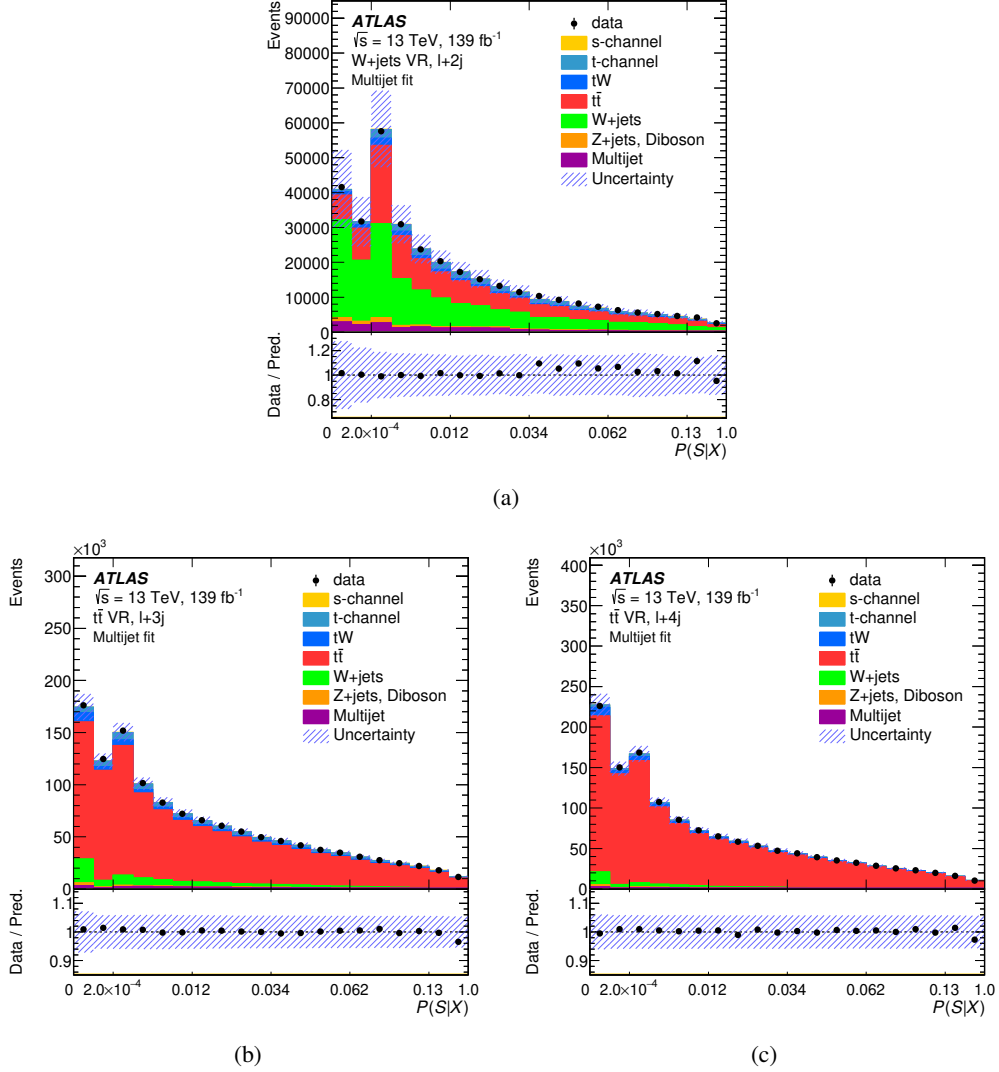


Figure 5: Distributions of the MEM discriminant $P(S|X)$ in the (a) W +jets VR, (b) $t\bar{t}$ 3-jets VR, and (c) $t\bar{t}$ 4-jets VR. Simulated events are normalised to the expected number of events given the integrated luminosity, after applying the normalisation factors obtained in the multijet fit presented in Section 5. The uncertainty bands indicate the simulation's statistical uncertainty and the normalisation uncertainties for the various processes in each bin, summed in quadrature. The ratio of the observed number to the predicted number of events in each bin is shown in the lower panel, with different vertical axis ranges. The binning is the same as the optimised binning used in the signal extraction fit described in Section 8, resulting in a non-linear horizontal scale.

7 Systematic uncertainties

Systematic uncertainties affect the signal acceptance and the background normalisations. Furthermore, most of them affect the shape of the MEM discriminant distribution because they affect the four-momenta of the reconstructed objects, or their efficiencies. Uncertainties related to the detector and to the modelling of the signal and background processes are taken into account. In the statistical analysis, an independent nuisance parameter is assigned to each source of systematic uncertainty. Several of the systematic uncertainties are decomposed into components from multiple independent sources.

The uncertainty in the combined 2015–2018 integrated luminosity is 1.7% [96], obtained using the LUCID-2 detector [97] for the primary luminosity measurement. An uncertainty associated with the modelling of pile-up in the simulation is included to cover the difference between the predicted and measured inelastic cross-section values [98].

The jet energy scale uncertainty is derived by combining information from test-beam data, LHC collision data and simulation, and the jet energy resolution uncertainty is obtained by combining dijet p_T -balance measurements and simulation [75]. Additional considerations related to jet flavour, pile-up corrections, η dependence and high- p_T jets are included. A total of 31 independent contributions are considered for the jet energy scale uncertainty, and 9 for the jet energy resolution uncertainty. The efficiency of the JVT algorithm to identify and remove jets from pile-up is measured with $Z \rightarrow \mu^+\mu^-$ events in data using techniques similar to those used in Ref. [78].

The efficiency to correctly tag b -jets is measured using dileptonic $t\bar{t}$ events [79]. The mis-tag rate for c -jets is measured using semileptonic $t\bar{t}$ events, exploiting the c -jets from the hadronic W -boson decays using techniques similar to those in Ref. [80]. The mis-tag rate for light-jets is measured using a negative-tag method, similar to that in Ref. [81], applied to Z + jets events. Uncertainties on this efficiency and these mis-tag rates are due to reconstructed object calibrations and to the modelling of the different processes, and are decomposed into sets of uncorrelated sources of uncertainty: 45, 20, and 20 components for b -, c - and light-jets, respectively.

Uncertainties associated with leptons arise from the trigger, reconstruction, identification, and isolation, as well as the lepton momentum scale and resolution. Efficiencies are measured, and calibrations of the scale and resolution are performed, using leptons in $Z \rightarrow \ell^+\ell^-$ and $J/\psi \rightarrow \ell^+\ell^-$ events [72, 83]. Systematic uncertainties in these measurements account for 22 independent sources.

All uncertainties related to the energy scales or resolution of the reconstructed objects are propagated to the calculation of the missing transverse momentum. Three additional uncertainties associated with the scale and resolution of the soft term are also included.

The modelling of the cross-section and acceptance of the two dominant backgrounds, $t\bar{t}$ and W +jets production, is affected by several systematic uncertainties. Therefore, the normalisations of these processes are measured in the signal extraction fit (cf. Section 8), and no constraints are placed on these two freely floating parameters. For single-top t -channel and tW production, uncertainties in the theoretical cross-sections of 4% and 5%, respectively, are propagated to the statistical analysis. For Z +jets and diboson processes, an uncertainty of 60% is considered, including $\pm 5\%$ for the inclusive cross-section summed in quadrature with $\pm 24\%$ per additional jet and $\pm 50\%$ for the heavy-flavour component [15, 99, 100]. Finally, an uncertainty of 30% is assigned to the normalisation of the multijet background, motivated by the change in the multijet normalisation when altering various settings in the multijet fit described in Section 5, or by comparisons with other methods of estimating this background, as used in previous analyses [84, 85].

Uncertainties due to the modelling of the different processes are taken into account. For each of the single-top s-channel, t-channel and tW processes, and the $t\bar{t}$ process, four sources related to the modelling of initial- and final-state radiation (ISR/FSR) are considered: two independent sources estimated by separately varying the renormalisation and factorisation scales in the ME generator by factors of 0.5 and 2, one source estimated by varying the renormalisation scale for QCD emission in the initial-state radiation in PYTHIA 8 (corresponding to the Var3c variation of the A14 tune [34]), and one source estimated by halving and doubling the renormalisation scale for QCD emission in the final-state radiation in PYTHIA 8. One additional source is also estimated for each of these four top-quark processes to account for the parton shower and hadronisation model, by comparing the nominal POWHEG BOX+PYTHIA 8 MC sample with a POWHEG BOX+HERWIG 7.04 sample. The uncertainty associated with the algorithm removing the overlap between tW and $t\bar{t}$ production at NLO [37] is assessed by comparing the nominal POWHEG BOX+PYTHIA 8 tW sample produced using the diagram removal scheme with an alternative sample produced with the same generator but using the diagram subtraction scheme. For the dominant $t\bar{t}$ background, two additional sources are considered: one source related to soft gluon resummation is estimated by setting the h_{damp} parameter to $3.0 \cdot m_t$, instead of the nominal $1.5 \cdot m_t$, in the POWHEG BOX+PYTHIA 8 $t\bar{t}$ MC sample, and one source related to the matching of the ME to the parton shower is estimated by comparing the nominal POWHEG BOX+PYTHIA 8 $t\bar{t}$ MC sample with a MADGRAPH5_AMC@NLO+PYTHIA 8 sample. One source of uncertainty related to the shape of the W +jets background is evaluated by using the envelope of the independent variations of the renormalisation and factorisation scales in the ME of the W +jets MC sample. Two sources of uncertainty affecting the shape of the multijet background are considered, one for the electron channel and one for the muon channel. These two sources are estimated by varying the criteria related to the fraction of energy deposited in the electromagnetic calorimeter for the jet-electron model, and to the tracking isolation in the anti-muon model, respectively (cf. Section 5). All these modelling uncertainties may affect both the shape of the MEM discriminant and the normalisation of each process, except for $t\bar{t}$ and W +jets, for which the normalisation is extracted in the fit.

The choice of PDFs affects the modelling of top-quark processes, and these uncertainties are evaluated using the PDF4LHC15 combined PDF error sets [53], which contain 30 symmetric eigenvectors. Four independent sets of 30 uncertainty sources are considered, one for each process. For single-top t-channel production, the PDF4LHC15_nlo_nf4_30 set is used, while for single-top s-channel and tW production, and $t\bar{t}$ production, the PDF4LHC15_nlo_30 set is used.

8 Signal extraction

The single-top-quark s-channel production cross-section is measured by means of a binned profile maximum-likelihood fit of the MEM discriminant in the signal region. The binning of the MEM discriminant is optimised in the signal region using the procedure described in Ref. [101], in order to maximise the expected sensitivity while keeping the total statistical uncertainty of the predicted number of events in each bin at a level adjusted to avoid biases due to fluctuations. This results in bins of unequal width, with wider bins in regions with a large signal contribution, while preserving a sufficiently large number of background events in each bin. In this paper, MEM discriminant distributions are presented with a non-linear horizontal scale, in such a way that the histogram bins appear to have a constant width. Values of $P(S|X)$ lower than 2.0×10^{-4} are not taken into account for the signal extraction because of the very low signal-to-background ratio in this range; this rejects 21% (18%) of the expected $t\bar{t}$ (W +jets) background events, while the expected signal yield is reduced by less than 1%. The electron and muon channels, which have similar sensitivity to the signal, are merged regardless of the lepton charge or flavour or of the various

data-taking periods of the LHC, while preserving correlations of the later described nuisance parameters associated to systematic uncertainties, in order to measure the combined production cross-section of single top quarks and top antiquarks.

The binned likelihood function $\mathcal{L}(\mu, \theta)$ used in the fit consists of a product of Poisson probability terms over the signal region histogram bins. The likelihood function depends on the signal strength μ , defined as $\mu = \sigma/\sigma^{\text{SM}}$, where σ is the observed signal production cross-section, and on a set of nuisance parameters θ , which characterise the effects of systematic uncertainties in the signal and background predictions. They are implemented in the likelihood function as Gaussian priors, with the exception of the unconstrained normalisation factors for the $t\bar{t}$ and W +jets backgrounds. The statistical uncertainty in the predictions, which incorporates the statistical uncertainty arising from the limited number of simulated events, is included in the likelihood function in the form of additional nuisance parameters, one for each of the considered bins, and constrained by Poisson priors. The test statistic t_μ is defined as the profile likelihood ratio: $t_\mu = -2 \ln(\mathcal{L}(\mu, \hat{\theta}_\mu)/\mathcal{L}(\hat{\mu}, \hat{\theta}))$, where $\hat{\mu}$ and $\hat{\theta}$ are the values of the parameters which maximise the likelihood function, and $\hat{\theta}_\mu$ are the values of the nuisance parameters which maximise the likelihood function for a given value of μ [102]. This test statistic, implemented in a framework based on RooStats [103, 104] and HistFactory [105], is used to assess the compatibility of the observed data with the background-only hypothesis, and to make statistical inferences about μ .

9 Results

A comparison of the MEM discriminant distributions in data and simulation is shown in Figure 6, before and after the fit to data. The uncertainty in the total prediction before the fit in Figure 6(a) is dominated by signal modelling, the jet energy resolution and scale, ISR/FSR in top-quark processes, and $t\bar{t}$ modelling uncertainties. The distribution after the fit in Figure 6(b) shows good agreement within the total uncertainty band, and the global goodness of fit calculated using the saturated model [106] is 10.3%. The measured distribution of the MEM discriminant for the signal contribution is shown in Figure 7, and is compared with the data after the subtraction of all background contributions. The expected event yields for the different processes, before and after the fit, are shown in Table 1, together with the observed event yield in data. The measured $t\bar{t}$ and W +jets normalisation factors are $0.81^{+0.13}_{-0.12}$ and $1.37^{+0.35}_{-0.31}$, respectively; their correlation is 51%, and their respective correlations with the signal cross-section are 55% and 27%. After the fit, none of the other nuisance parameters is pulled by more than 0.8 standard deviation, constrained to less than 74% of its pre-fit impact on the cross-section by the fit, or has a correlation with the fitted cross-section larger than 33%.

Several tests were performed in order to assess the robustness of this fit, called 'baseline fit' in this paragraph. First, instead of being left unconstrained, the $t\bar{t}$ and W +jets normalisations were assigned an uncertainty on their cross-sections. In such case, the nuisance parameters associated to these uncertainties were pulled in the same directions as the normalisation factors in the baseline fit. Second, a fit of the background-only hypothesis to the data was performed, keeping only bins of the discriminant distribution in which the expected signal-to-background ratio does not exceed 5%. In such a fit, the $t\bar{t}$ and W +jets normalisation factors were pulled by values compatible to those obtained in the baseline fit. Furthermore, the post-fit nuisance parameters of this background-only fit were propagated to the signal and background MC samples, with signal cross-section set to its prediction from theory, in order to build a 'realistic' pseudo-data set. A signal-plus-background fit to this pseudo-data set was then performed, and the measured cross-section was compatible with the predicted cross-section. Finally, the linearity of the statistical model was checked,

by performing fits to pseudo-data sets produced from the nominal predictions (Asimov datasets), where the expected signal cross-section was increased or decreased. In such fits, the measured and expected cross-sections were in agreement.

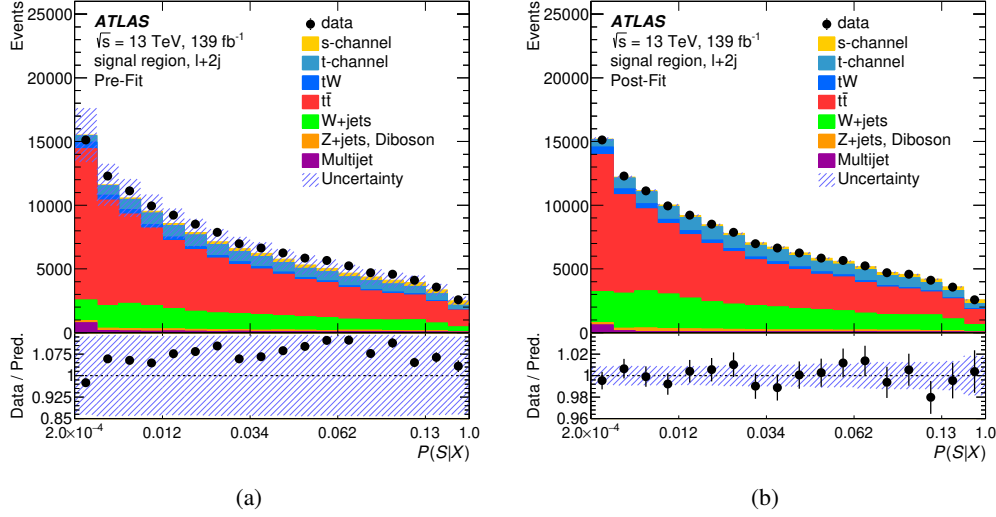


Figure 6: Distributions of the MEM discriminant $P(S|X)$ in the SR (a) before and (b) after the fit to data, for MEM discriminant values larger than 2.0×10^{-4} . The lower panels show the ratio of the data to the prediction, with different vertical axis ranges. The uncertainty bands indicate the total uncertainties and their correlations in each bin. The uncertainties in the $t\bar{t}$ and W +jets normalisation factors, as well as in the s-channel signal cross-section, are not defined pre-fit and therefore only included in the post-fit uncertainties in (b). The binning is the same as the optimised binning used in the fit, resulting in a non-linear horizontal scale.

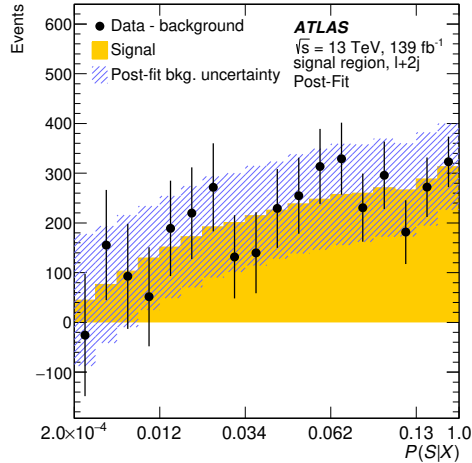


Figure 7: Distribution of the MEM discriminant $P(S|X)$ in the SR after the fit to data, for MEM discriminant values larger than 2.0×10^{-4} , after subtraction of all backgrounds. The fitted distribution for the simulation of the signal is shown together with the post-fit uncertainty in the backgrounds. The binning is the same as the optimised binning used in the fit, resulting in a non-linear horizontal scale.

Process	Event yield	
	Pre-fit	Post-fit
s-channel	$4\,200 \pm 710$	$3\,700 \pm 1\,100$
t-channel	$13\,000 \pm 2\,000$	$15\,000 \pm 2\,300$
tW	$3\,680 \pm 970$	$4\,250 \pm 1\,100$
$t\bar{t}$	$76\,000 \pm 12\,000$	$70\,600 \pm 4\,200$
W + jets	$21\,500 \pm 2\,900$	$32\,200 \pm 5\,000$
Z + jets, VV	$2\,400 \pm 1\,400$	$2\,900 \pm 1\,600$
Multijet	$2\,150 \pm 650$	$1\,700 \pm 540$
Total	$123\,000 \pm 17\,000$	$130\,310 \pm 620$
Data	130 310	

Table 1: Pre-fit and post-fit event yields in the SR, for MEM discriminant values larger than 2.0×10^{-4} . The central value of the event yield for each process is calculated by summing the values of the discriminant bin contents, using the nominal expected yield for the pre-fit value, and the best-fit estimate for the post-fit value. The error includes statistical and systematic uncertainties summed in quadrature. All sources of systematic uncertainties are included, taking into account correlations and anti-correlations in the post-fit case. The uncertainties in the $t\bar{t}$ and W + jets normalisation factors, as well as in the s-channel signal cross-section, are not defined pre-fit and therefore only included in the post-fit uncertainties.

The measured cross-section is $\sigma = 8.2 \pm 0.6$ (stat.) $_{-2.8}^{+3.4}$ (syst.) pb = $8.2_{-2.9}^{+3.5}$ (total) pb, which is compatible with the SM prediction of $\sigma^{\text{SM}} = 10.32_{-0.36}^{+0.40}$ pb. A summary of the main sources of uncertainty is presented in Table 2. The largest contribution arises from the $t\bar{t}$ normalisation. Uncertainties in the jet energy scale and resolution, and in the signal generator modelling, also play an important role, followed by the modelling of ISR/FSR in top-quark processes, the statistical uncertainty of the MC predictions, the $t\bar{t}$ generator modelling uncertainties, and the flavour-tagging uncertainties. The observed signal significance is 3.3 standard deviations above the background-only hypothesis, while the expected significance is 3.9 standard deviations.

Source	$\Delta\sigma/\sigma$ [%]
$t\bar{t}$ normalisation	+24/-17
$t\bar{t}$ shape modelling	+18/-15
ISR/FSR	+13/-11
PS & had.	+12/-10
ME/PS matching	+10/-8
h_{damp}	< 1
s-channel modelling	+18/-8
PS & had.	+18/-8
ISR/FSR	+3/-1
Jet energy resolution	+18/-12
Jet energy scale	+18/-13
MC statistics	+13/-11
Flavour tagging	+12/-10
W+ jets normalisation	+11/-8
PDFs	+10/-9
$t\bar{t}$	+10/-9
s-channel	± 1
t-channel	± 1
tW	± 1
t-channel modelling	± 6
PS & had.	± 5
ISR/FSR	± 4
W+ jets μ_r/μ_f shape	+6/-5
Normalisation of other processes	+6/-5
Pile-up	+5/-3
Luminosity	+4/-3
tW modelling	+1/-2
PS & had.	± 1
$t\bar{t}$ overlap	± 1
ISR/FSR	± 1
Missing transverse momentum	± 1
Multijet shape modelling	± 1
Other detector sources	± 1
Systematic uncertainties	+42/-34
Statistical uncertainty	± 8
Total	+42/-35

Table 2: Observed impact of the different sources of uncertainty on the measured s-channel signal cross-section, grouped by categories. The impact of each category is obtained by repeating the fit after having fixed the set of nuisance parameters corresponding to that category, subtracting the square of the resulting uncertainty from the square of the uncertainty found in the full fit, and calculating the square root. The statistical uncertainty is obtained by repeating the fit after having fixed all nuisance parameters, including the $t\bar{t}$ and W+ jets normalisation factors. 'PS & had.' refers to the parton shower and hadronisation model, 'ME/PS matching' to the matching of the ME to the parton shower, and ' $t\bar{t}$ overlap' to the algorithm removing the overlap between tW and $t\bar{t}$ production at NLO, as described in Section 7.

10 Conclusion

A measurement of the s-channel single-top-quark production cross-section in pp collisions at a centre-of-mass energy of 13 TeV recorded by the ATLAS detector at the LHC is presented. The analysis was performed using data collected in 2015–2018 corresponding to an integrated luminosity of 139 fb^{-1} . The selected events contain one electron or muon, two jets which are both b -tagged, and missing transverse momentum. The matrix element method was used to obtain a discriminant to separate the signal from the background events, and the signal was extracted using a profile likelihood fit. The measured signal cross-section, combining top-quark and top-antiquark production, is $\sigma = 8.2_{-2.9}^{+3.5} \text{ pb}$, in agreement with the SM prediction of $\sigma^{\text{SM}} = 10.3 \pm 0.4 \text{ pb}$. The observed (expected) signal significance is 3.3 (3.9) standard deviations above the background-only hypothesis. This result provides a measurement of the cross-section of this process at a new centre-of-mass energy, which allows the energy dependence of this observable to be probed.

Acknowledgements

We thank CERN for the very successful operation of the LHC, as well as the support staff from our institutions without whom ATLAS could not be operated efficiently.

We acknowledge the support of ANPCyT, Argentina; YerPhI, Armenia; ARC, Australia; BMWFW and FWF, Austria; ANAS, Azerbaijan; CNPq and FAPESP, Brazil; NSERC, NRC and CFI, Canada; CERN; ANID, Chile; CAS, MOST and NSFC, China; Minciencias, Colombia; MEYS CR, Czech Republic; DNRF and DNSRC, Denmark; IN2P3-CNRS and CEA-DRF/IRFU, France; SRNSFG, Georgia; BMBF, HGF and MPG, Germany; GSRI, Greece; RGC and Hong Kong SAR, China; ISF and Benoziyo Center, Israel; INFN, Italy; MEXT and JSPS, Japan; CNRST, Morocco; NWO, Netherlands; RCN, Norway; MEiN, Poland; FCT, Portugal; MNE/IFA, Romania; MESTD, Serbia; MSSR, Slovakia; ARRS and MIZŠ, Slovenia; DSI/NRF, South Africa; MICINN, Spain; SRC and Wallenberg Foundation, Sweden; SERI, SNSF and Cantons of Bern and Geneva, Switzerland; MOST, Taiwan; TENMAK, Türkiye; STFC, United Kingdom; DOE and NSF, United States of America. In addition, individual groups and members have received support from BCKDF, CANARIE, Compute Canada and CRC, Canada; PRIMUS 21/SCI/017 and UNCE SCI/013, Czech Republic; COST, ERC, ERDF, Horizon 2020 and Marie Skłodowska-Curie Actions, European Union; Investissements d’Avenir Labex, Investissements d’Avenir IDEX and ANR, France; DFG and AvH Foundation, Germany; Herakleitos, Thales and Aristeia programmes co-financed by EU-ESF and the Greek NSRF, Greece; BSF-NSF and MINERVA, Israel; Norwegian Financial Mechanism 2014-2021, Norway; NCN and NAWA, Poland; La Caixa Banking Foundation, CERCA Programme Generalitat de Catalunya and PROMETEO and GenT Programmes Generalitat Valenciana, Spain; Göran Gustafssons Stiftelse, Sweden; The Royal Society and Leverhulme Trust, United Kingdom.

The crucial computing support from all WLCG partners is acknowledged gratefully, in particular from CERN, the ATLAS Tier-1 facilities at TRIUMF (Canada), NDGF (Denmark, Norway, Sweden), CC-IN2P3 (France), KIT/GridKA (Germany), INFN-CNAF (Italy), NL-T1 (Netherlands), PIC (Spain), ASGC (Taiwan), RAL (UK) and BNL (USA), the Tier-2 facilities worldwide and large non-WLCG resource providers. Major contributors of computing resources are listed in Ref. [107].

References

- [1] T. M. P. Tait and C.-P. Yuan, *Single top quark production as a window to physics beyond the standard model*, *Phys. Rev. D* **63** (2000) 014018, arXiv: [hep-ph/0007298](#).
- [2] Q.-H. Cao, J. Wudka and C.-P. Yuan, *Search for new physics via single top production at the LHC*, *Phys. Lett. B* **658** (2007) 50, arXiv: [0704.2809 \[hep-ph\]](#).
- [3] CDF Collaboration, *First Observation of Electroweak Single Top Quark Production*, *Phys. Rev. Lett.* **103** (2009) 092002, arXiv: [0903.0885 \[hep-ex\]](#).
- [4] D0 Collaboration, *Observation of Single Top Quark Production*, *Phys. Rev. Lett.* **103** (2009) 092001, arXiv: [0903.0850 \[hep-ex\]](#).
- [5] CDF and D0 Collaborations, *Observation of s -channel production of single top quarks at the Tevatron*, *Phys. Rev. Lett.* **112** (2014) 231803, arXiv: [1402.5126 \[hep-ex\]](#).
- [6] CMS Collaboration, *Measurement of the single-top-quark t -channel cross section in pp collisions at $\sqrt{s} = 7$ TeV*, *JHEP* **12** (2012) 035, arXiv: [1209.4533 \[hep-ex\]](#).
- [7] ATLAS Collaboration, *Measurement of the t -channel single top-quark production cross section in pp collisions at $\sqrt{s} = 7$ TeV with the ATLAS detector*, *Phys. Lett. B* **717** (2012) 330, arXiv: [1205.3130 \[hep-ex\]](#).
- [8] CMS Collaboration, *Observation of the Associated Production of a Single Top Quark and a W Boson in pp Collisions at $\sqrt{s} = 8$ TeV*, *Phys. Rev. Lett.* **112** (2014) 231802, arXiv: [1401.2942 \[hep-ex\]](#).
- [9] ATLAS Collaboration, *Measurement of the production cross-section of a single top quark in association with a W boson at 8 TeV with the ATLAS experiment*, *JHEP* **01** (2016) 064, arXiv: [1510.03752 \[hep-ex\]](#).
- [10] CMS Collaboration, *Cross section measurement of t -channel single top quark production in pp collisions at $\sqrt{s} = 13$ TeV*, *Phys. Lett. B* **772** (2017) 752, arXiv: [1610.00678 \[hep-ex\]](#).
- [11] ATLAS Collaboration, *Measurement of the inclusive cross-sections of single top-quark and top-antiquark t -channel production in pp collisions at $\sqrt{s} = 13$ TeV with the ATLAS detector*, *JHEP* **04** (2017) 086, arXiv: [1609.03920 \[hep-ex\]](#).
- [12] CMS Collaboration, *Observation of tW production in the single-lepton channel in pp collisions at $\sqrt{s} = 13$ TeV*, *JHEP* **11** (2021) 111, arXiv: [2109.01706 \[hep-ex\]](#).
- [13] ATLAS Collaboration, *Measurement of the cross-section for producing a W boson in association with a single top quark in pp collisions at $\sqrt{s} = 13$ TeV with ATLAS*, *JHEP* **01** (2018) 063, arXiv: [1612.07231 \[hep-ex\]](#).
- [14] CMS Collaboration, *Search for s channel single top quark production in pp collisions at $\sqrt{s} = 7$ and 8 TeV*, *JHEP* **09** (2016) 027, arXiv: [1603.02555 \[hep-ex\]](#).
- [15] ATLAS Collaboration, *Evidence for single top-quark production in the s -channel in proton–proton collisions at $\sqrt{s} = 8$ TeV with the ATLAS detector using the Matrix Element Method*, *Phys. Lett. B* **756** (2016) 228, arXiv: [1511.05980 \[hep-ex\]](#).

- [16] K. Kondo, *Dynamical Likelihood Method for Reconstruction of Events With Missing Momentum. 1: Method and Toy Models*, *J. Phys. Soc. Jap.* **57** (1988) 4126.
- [17] K. Kondo, *Dynamical likelihood method for reconstruction of events with missing momentum. 2: Mass spectra for $2 \rightarrow 2$ processes*, *J. Phys. Soc. Jap.* **60** (1991) 836.
- [18] ATLAS Collaboration, *Search for s -channel single top-quark production in proton–proton collisions at $\sqrt{s} = 8$ TeV with the ATLAS detector*, *Phys. Lett. B* **740** (2015) 118, arXiv: [1410.0647 \[hep-ex\]](#).
- [19] ATLAS Collaboration, *The ATLAS Experiment at the CERN Large Hadron Collider*, *JINST* **3** (2008) S08003.
- [20] ATLAS Collaboration, *The ATLAS Collaboration Software and Firmware*, ATL-SOFT-PUB-2021-001, 2021, URL: <https://cds.cern.ch/record/2767187>.
- [21] ATLAS Collaboration, *ATLAS data quality operations and performance for 2015–2018 data-taking*, *JINST* **15** (2020) P04003, arXiv: [1911.04632 \[physics.ins-det\]](#).
- [22] ATLAS Collaboration, *The ATLAS Simulation Infrastructure*, *Eur. Phys. J. C* **70** (2010) 823, arXiv: [1005.4568 \[physics.ins-det\]](#).
- [23] S. Agostinelli et al., *GEANT4 – a simulation toolkit*, *Nucl. Instrum. Meth. A* **506** (2003) 250.
- [24] T. Sjöstrand et al., *An introduction to PYTHIA 8.2*, *Comput. Phys. Commun.* **191** (2015) 159, arXiv: [1410.3012 \[hep-ph\]](#).
- [25] ATLAS Collaboration, *The Pythia 8 A3 tune description of ATLAS minimum bias and inelastic measurements incorporating the Donnachie–Landshoff diffractive model*, ATL-PHYS-PUB-2016-017, 2016, URL: <https://cds.cern.ch/record/2206965>.
- [26] P. Nason, *A new method for combining NLO QCD with shower Monte Carlo algorithms*, *JHEP* **11** (2004) 040, arXiv: [hep-ph/0409146](#).
- [27] S. Frixione, P. Nason and C. Oleari, *Matching NLO QCD computations with parton shower simulations: the POWHEG method*, *JHEP* **11** (2007) 070, arXiv: [0709.2092 \[hep-ph\]](#).
- [28] S. Alioli, P. Nason, C. Oleari and E. Re, *A general framework for implementing NLO calculations in shower Monte Carlo programs: the POWHEG BOX*, *JHEP* **06** (2010) 043, arXiv: [1002.2581 \[hep-ph\]](#).
- [29] S. Alioli, P. Nason, C. Oleari and E. Re, *NLO single-top production matched with shower in POWHEG: s - and t -channel contributions*, *JHEP* **09** (2009) 111, arXiv: [0907.4076 \[hep-ph\]](#), Erratum: *JHEP* **02** (2010) 011.
- [30] R. Frederix, E. Re and P. Torrielli, *Single-top t -channel hadroproduction in the four-flavour scheme with POWHEG and aMC@NLO*, *JHEP* **09** (2012) 130, arXiv: [1207.5391 \[hep-ph\]](#).
- [31] E. Re, *Single-top Wt -channel production matched with parton showers using the POWHEG method*, *Eur. Phys. J. C* **71** (2011) 1547, arXiv: [1009.2450 \[hep-ph\]](#).
- [32] S. Frixione, G. Ridolfi and P. Nason, *A positive-weight next-to-leading-order Monte Carlo for heavy flavour hadroproduction*, *JHEP* **09** (2007) 126, arXiv: [0707.3088 \[hep-ph\]](#).

- [33] The NNPDF Collaboration, R. D. Ball et al., *Parton distributions for the LHC run II*, *JHEP* **04** (2015) 040, arXiv: [1410.8849 \[hep-ph\]](#).
- [34] ATLAS Collaboration, *ATLAS Pythia 8 tunes to 7 TeV data*, ATL-PHYS-PUB-2014-021, 2014, URL: <https://cds.cern.ch/record/1966419>.
- [35] NNPDF Collaboration, R. D. Ball et al., *Parton distributions with LHC data*, *Nucl. Phys. B* **867** (2013) 244, arXiv: [1207.1303 \[hep-ph\]](#).
- [36] D. J. Lange, *The EvtGen particle decay simulation package*, *Nucl. Instrum. Meth. A* **462** (2001) 152.
- [37] S. Frixione, E. Laenen, P. Motylinski, C. White and B. R. Webber, *Single-top hadroproduction in association with a W boson*, *JHEP* **07** (2008) 029, arXiv: [0805.3067 \[hep-ph\]](#).
- [38] M. Bähr et al., *Herwig++ physics and manual*, *Eur. Phys. J. C* **58** (2008) 639, arXiv: [0803.0883 \[hep-ph\]](#).
- [39] J. Bellm et al., *Herwig 7.0/Herwig++ 3.0 release note*, *Eur. Phys. J. C* **76** (2016) 196, arXiv: [1512.01178 \[hep-ph\]](#).
- [40] L. A. Harland-Lang, A. D. Martin, P. Motylinski and R. S. Thorne, *Parton distributions in the LHC era: MMHT 2014 PDFs*, *Eur. Phys. J. C* **75** (2015) 204, arXiv: [1412.3989 \[hep-ph\]](#).
- [41] E. Bothmann et al., *Event generation with Sherpa 2.2*, *SciPost Phys.* **7** (2019) 034, arXiv: [1905.09127 \[hep-ph\]](#).
- [42] T. Gleisberg and S. Höche, *Comix, a new matrix element generator*, *JHEP* **12** (2008) 039, arXiv: [0808.3674 \[hep-ph\]](#).
- [43] F. Buccioni et al., *OpenLoops 2*, *Eur. Phys. J. C* **79** (2019) 866, arXiv: [1907.13071 \[hep-ph\]](#).
- [44] F. Cascioli, P. Maierhöfer and S. Pozzorini, *Scattering Amplitudes with Open Loops*, *Phys. Rev. Lett.* **108** (2012) 111601, arXiv: [1111.5206 \[hep-ph\]](#).
- [45] A. Denner, S. Dittmaier and L. Hofer, *COLLIER: A fortran-based complex one-loop library in extended regularizations*, *Comput. Phys. Commun.* **212** (2017) 220, arXiv: [1604.06792 \[hep-ph\]](#).
- [46] S. Schumann and F. Krauss, *A parton shower algorithm based on Catani–Seymour dipole factorisation*, *JHEP* **03** (2008) 038, arXiv: [0709.1027 \[hep-ph\]](#).
- [47] S. Höche, F. Krauss, M. Schönherr and F. Siegert, *A critical appraisal of NLO+PS matching methods*, *JHEP* **09** (2012) 049, arXiv: [1111.1220 \[hep-ph\]](#).
- [48] S. Höche, F. Krauss, M. Schönherr and F. Siegert, *QCD matrix elements + parton showers. The NLO case*, *JHEP* **04** (2013) 027, arXiv: [1207.5030 \[hep-ph\]](#).
- [49] S. Catani, F. Krauss, B. R. Webber and R. Kuhn, *QCD Matrix Elements + Parton Showers*, *JHEP* **11** (2001) 063, arXiv: [hep-ph/0109231](#).
- [50] S. Höche, F. Krauss, S. Schumann and F. Siegert, *QCD matrix elements and truncated showers*, *JHEP* **05** (2009) 053, arXiv: [0903.1219 \[hep-ph\]](#).

- [51] M. Aliev et al., *HATHOR – HAdronic Top and Heavy quarks crOSS section calculator*, *Comput. Phys. Commun.* **182** (2011) 1034, arXiv: [1007.1327 \[hep-ph\]](#).
- [52] P. Kant et al., *HatHor for single top-quark production: Updated predictions and uncertainty estimates for single top-quark production in hadronic collisions*, *Comput. Phys. Commun.* **191** (2015) 74, arXiv: [1406.4403 \[hep-ph\]](#).
- [53] J. Butterworth et al., *PDF4LHC recommendations for LHC Run II*, *J. Phys. G* **43** (2016) 023001, arXiv: [1510.03865 \[hep-ph\]](#).
- [54] A. D. Martin, W. J. Stirling, R. S. Thorne and G. Watt, *Parton distributions for the LHC*, *Eur. Phys. J. C* **63** (2009) 189, arXiv: [0901.0002 \[hep-ph\]](#).
- [55] A. D. Martin, W. J. Stirling, R. S. Thorne and G. Watt, *Uncertainties on α_S in global PDF analyses and implications for predicted hadronic cross sections*, *Eur. Phys. J. C* **64** (2009) 653, arXiv: [0905.3531 \[hep-ph\]](#).
- [56] H.-L. Lai et al., *New parton distributions for collider physics*, *Phys. Rev. D* **82** (2010) 074024, arXiv: [1007.2241 \[hep-ph\]](#).
- [57] M. Beneke, P. Falgari, S. Klein and C. Schwinn, *Hadronic top-quark pair production with NNLL threshold resummation*, *Nucl. Phys. B* **855** (2012) 695, arXiv: [1109.1536 \[hep-ph\]](#).
- [58] M. Cacciari, M. Czakon, M. Mangano, A. Mitov and P. Nason, *Top-pair production at hadron colliders with next-to-next-to-leading logarithmic soft-gluon resummation*, *Phys. Lett. B* **710** (2012) 612, arXiv: [1111.5869 \[hep-ph\]](#).
- [59] P. Bärnreuther, M. Czakon and A. Mitov, *Percent-Level-Precision Physics at the Tevatron: Next-to-Next-to-Leading Order QCD Corrections to $q\bar{q} \rightarrow t\bar{t} + X$* , *Phys. Rev. Lett.* **109** (2012) 132001, arXiv: [1204.5201 \[hep-ph\]](#).
- [60] M. Czakon and A. Mitov, *NNLO corrections to top-pair production at hadron colliders: the all-fermionic scattering channels*, *JHEP* **12** (2012) 054, arXiv: [1207.0236 \[hep-ph\]](#).
- [61] M. Czakon and A. Mitov, *NNLO corrections to top pair production at hadron colliders: the quark-gluon reaction*, *JHEP* **01** (2013) 080, arXiv: [1210.6832 \[hep-ph\]](#).
- [62] M. Czakon, P. Fiedler and A. Mitov, *Total Top-Quark Pair-Production Cross Section at Hadron Colliders Through $O(\alpha_S^4)$* , *Phys. Rev. Lett.* **110** (2013) 252004, arXiv: [1303.6254 \[hep-ph\]](#).
- [63] M. Czakon and A. Mitov, *Top++: A program for the calculation of the top-pair cross-section at hadron colliders*, *Comput. Phys. Commun.* **185** (2014) 2930, arXiv: [1112.5675 \[hep-ph\]](#).
- [64] J. Gao et al., *CT10 next-to-next-to-leading order global analysis of QCD*, *Phys. Rev. D* **89** (2014) 033009, arXiv: [1302.6246 \[hep-ph\]](#).
- [65] N. Kidonakis, *Two-loop soft anomalous dimensions for single top quark associated production with a W^- or H^-* , *Phys. Rev. D* **82** (2010) 054018, arXiv: [1005.4451 \[hep-ph\]](#).
- [66] N. Kidonakis, ‘Top Quark Production’, *Proceedings, Helmholtz International Summer School on Physics of Heavy Quarks and Hadrons (HQ 2013)* (JINR, Dubna, Russia, 15th–28th July 2013) 139, arXiv: [1311.0283 \[hep-ph\]](#).

- [67] C. Anastasiou, L. Dixon, K. Melnikov and F. Petriello, *High-precision QCD at hadron colliders: Electroweak gauge boson rapidity distributions at next-to-next-to leading order*, [Phys. Rev. D **69** \(2004\) 094008](#), arXiv: [hep-ph/0312266](#).
- [68] K. Melnikov and F. Petriello, *Electroweak gauge boson production at hadron colliders through $O(\alpha_s^2)$* , [Phys. Rev. D **74** \(2006\) 114017](#), arXiv: [hep-ph/0609070](#).
- [69] ATLAS Collaboration, *Reconstruction of primary vertices at the ATLAS experiment in Run 1 proton–proton collisions at the LHC*, [Eur. Phys. J. C **77** \(2017\) 332](#), arXiv: [1611.10235 \[hep-ex\]](#).
- [70] ATLAS Collaboration, *Performance of the ATLAS muon triggers in Run 2*, [JINST **15** \(2020\) P09015](#), arXiv: [2004.13447 \[hep-ex\]](#).
- [71] ATLAS Collaboration, *Performance of electron and photon triggers in ATLAS during LHC Run 2*, [Eur. Phys. J. C **80** \(2020\) 47](#), arXiv: [1909.00761 \[hep-ex\]](#).
- [72] ATLAS Collaboration, *Electron and photon performance measurements with the ATLAS detector using the 2015–2017 LHC proton–proton collision data*, [JINST **14** \(2019\) P12006](#), arXiv: [1908.00005 \[hep-ex\]](#).
- [73] ATLAS Collaboration, *Muon reconstruction and identification efficiency in ATLAS using the full Run 2 pp collision data set at $\sqrt{s} = 13$ TeV*, [Eur. Phys. J. C **81** \(2021\) 578](#), arXiv: [2012.00578 \[hep-ex\]](#).
- [74] ATLAS Collaboration, *Topological cell clustering in the ATLAS calorimeters and its performance in LHC Run 1*, [Eur. Phys. J. C **77** \(2017\) 490](#), arXiv: [1603.02934 \[hep-ex\]](#).
- [75] ATLAS Collaboration, *Jet energy scale and resolution measured in proton–proton collisions at $\sqrt{s} = 13$ TeV with the ATLAS detector*, [Eur. Phys. J. C **81** \(2020\) 689](#), arXiv: [2007.02645 \[hep-ex\]](#).
- [76] M. Cacciari, G. P. Salam and G. Soyez, *The anti- k_t jet clustering algorithm*, [JHEP **04** \(2008\) 063](#), arXiv: [0802.1189 \[hep-ph\]](#).
- [77] M. Cacciari, G. P. Salam and G. Soyez, *FastJet user manual*, [Eur. Phys. J. C **72** \(2012\) 1896](#), arXiv: [1111.6097 \[hep-ph\]](#).
- [78] ATLAS Collaboration, *Performance of pile-up mitigation techniques for jets in pp collisions at $\sqrt{s} = 8$ TeV using the ATLAS detector*, [Eur. Phys. J. C **76** \(2016\) 581](#), arXiv: [1510.03823 \[hep-ex\]](#).
- [79] ATLAS Collaboration, *ATLAS b -jet identification performance and efficiency measurement with $t\bar{t}$ events in pp collisions at $\sqrt{s} = 13$ TeV*, [Eur. Phys. J. C **79** \(2019\) 970](#), arXiv: [1907.05120 \[hep-ex\]](#).
- [80] ATLAS Collaboration, *Measurement of b -tagging efficiency of c -jets in $t\bar{t}$ events using a likelihood approach with the ATLAS detector*, ATLAS-CONF-2018-001, 2018, URL: <https://cds.cern.ch/record/2306649>.
- [81] ATLAS Collaboration, *Calibration of light-flavour b -jet mistagging rates using ATLAS proton–proton collision data at $\sqrt{s} = 13$ TeV*, ATLAS-CONF-2018-006, 2018, URL: <https://cds.cern.ch/record/2314418>.

- [82] ATLAS Collaboration, *Performance of missing transverse momentum reconstruction with the ATLAS detector using proton–proton collisions at $\sqrt{s} = 13$ TeV*, *Eur. Phys. J. C* **78** (2018) 903, arXiv: [1802.08168 \[hep-ex\]](#).
- [83] ATLAS Collaboration, *Muon reconstruction performance of the ATLAS detector in proton–proton collision data at $\sqrt{s} = 13$ TeV*, *Eur. Phys. J. C* **76** (2016) 292, arXiv: [1603.05598 \[hep-ex\]](#).
- [84] ATLAS Collaboration, *Estimation of non-prompt and fake lepton backgrounds in final states with top quarks produced in proton–proton collisions at $\sqrt{s} = 8$ TeV with the ATLAS Detector*, ATLAS-CONF-2014-058, 2014, URL: <https://cds.cern.ch/record/1951336>.
- [85] ATLAS Collaboration, *Fiducial, total and differential cross-section measurements of t-channel single top-quark production in pp collisions at 8 TeV using data collected by the ATLAS detector*, *Eur. Phys. J. C* **77** (2017) 531, arXiv: [1702.02859 \[hep-ex\]](#).
- [86] ATLAS Collaboration, *Measurement of the $t\bar{t}$ production cross-section in the lepton+jets channel at $\sqrt{s} = 13$ TeV with the ATLAS experiment*, *Phys. Lett. B* **810** (2020) 135797, arXiv: [2006.13076 \[hep-ex\]](#).
- [87] CDF Collaboration, *Measurement of the Single Top Quark Production Cross Section at CDF*, *Phys. Rev. Lett.* **101** (2008) 252001, arXiv: [0809.2581 \[hep-ex\]](#).
- [88] D0 Collaboration, *Evidence for production of single top quarks and first direct measurement of $|V_{tb}|$* , *Phys. Rev. Lett.* **98** (2007) 181802, arXiv: [hep-ex/0612052](#).
- [89] D0 Collaboration, *Evidence for production of single top quarks*, *Phys. Rev. D* **78** (2008) 012005, arXiv: [0803.0739 \[hep-ex\]](#).
- [90] G. P. Lepage, *A new algorithm for adaptive multidimensional integration*, *J. Comput. Phys.* **27** (1978) 192.
- [91] T. Hahn, *The CUBA library*, *Nucl. Instrum. Meth. A* **559** (2006) 273, arXiv: [hep-ph/0509016](#).
- [92] J. Butterworth, G. Dissertori, S. Dittmaier, D. de Florian, N. Glover et al., *Les Houches 2013: Physics at TeV Colliders: Standard Model Working Group Report*, (2014), arXiv: [1405.1067 \[hep-ph\]](#).
- [93] J. M. Campbell and R. K. Ellis, *MCFM for the Tevatron and the LHC*, *Nucl. Phys. B Proc. Suppl.* **205-206** (2010) 10, arXiv: [1007.3492 \[hep-ph\]](#).
- [94] ATLAS Collaboration, *Measurement of the charge asymmetry in top quark pair production in pp collisions at $\sqrt{s} = 7$ TeV using the ATLAS detector*, *Eur. Phys. J. C* **72** (2012) 2039, arXiv: [1203.4211 \[hep-ex\]](#).
- [95] J. Erdmann et al., *A likelihood-based reconstruction algorithm for top-quark pairs and the KLFitter framework*, *Nucl. Instrum. Meth. A* **748** (2014) 18, arXiv: [1312.5595 \[hep-ex\]](#).
- [96] ATLAS Collaboration, *Luminosity determination in pp collisions at $\sqrt{s} = 13$ TeV using the ATLAS detector at the LHC*, ATLAS-CONF-2019-021, 2019, URL: <https://cds.cern.ch/record/2677054>.
- [97] G. Avoni et al., *The new LUCID-2 detector for luminosity measurement and monitoring in ATLAS*, *JINST* **13** (2018) P07017.

- [98] ATLAS Collaboration, *Measurement of the Inelastic Proton–Proton Cross Section at $\sqrt{s} = 13$ TeV with the ATLAS Detector at the LHC*, *Phys. Rev. Lett.* **117** (2016) 182002, arXiv: [1606.02625 \[hep-ex\]](#).
- [99] S. D. Ellis, R. Kleiss and W. J. Stirling, *W's, Z's and Jets*, *Phys. Lett. B* **154** (1985) 435.
- [100] F. A. Berends, H. Kuijff, B. Tausk and W. T. Giele, *On the production of a W and jets at hadron colliders*, *Nucl. Phys. B* **357** (1991) 32.
- [101] ATLAS Collaboration, *Search for the $b\bar{b}$ decay of the Standard Model Higgs boson in associated (W/Z)H production with the ATLAS detector*, *JHEP* **01** (2015) 069, arXiv: [1409.6212 \[hep-ex\]](#).
- [102] G. Cowan, K. Cranmer, E. Gross and O. Vitells, *Asymptotic formulae for likelihood-based tests of new physics*, *Eur. Phys. J. C* **71** (2011) 1554, arXiv: [1007.1727 \[physics.data-an\]](#), Erratum: *Eur. Phys. J. C* **73** (2013) 2501.
- [103] W. Verkerke and D. Kirkby, *The RooFit toolkit for data modeling*, 2003, arXiv: [physics/0306116 \[physics.data-an\]](#).
- [104] L. Moneta et al., *The RooStats project*, *PoS ACAT2010* (2011) 057, arXiv: [1009.1003 \[physics.data-an\]](#).
- [105] K. Cranmer, G. Lewis, L. Moneta, A. Shibata and W. Verkerke, *HistFactory: A tool for creating statistical models for use with RooFit and RooStats*, CERN-OPEN-2012-016, 2012, URL: <https://cds.cern.ch/record/1456844>.
- [106] R. D. Cousins, *Generalization of chisquare goodness-of-fit test for binned data using saturated models, with application to histograms*, (2013), URL: http://www.physics.ucla.edu/~cousins/stats/cousins_saturated.pdf.
- [107] ATLAS Collaboration, *ATLAS Computing Acknowledgements*, ATL-SOFT-PUB-2021-003, 2021, URL: <https://cds.cern.ch/record/2776662>.

The ATLAS Collaboration

G. Aad ¹⁰¹, B. Abbott ¹¹⁹, D.C. Abbott ¹⁰², K. Abeling ⁵⁵, S.H. Abidi ²⁹, A. Aboulhorma ^{35e}, H. Abramowicz ¹⁵⁰, H. Abreu ¹⁴⁹, Y. Abulaiti ¹¹⁶, A.C. Abusleme Hoffman ^{136a}, B.S. Acharya ^{68a,68b,o}, B. Achkar ⁵⁵, C. Adam Bourdarios ⁴, L. Adamczyk ^{84a}, L. Adamek ¹⁵⁴, S.V. Addepalli ²⁶, J. Adelman ¹¹⁴, A. Adiguzel ^{21c}, S. Adorni ⁵⁶, T. Adye ¹³³, A.A. Affolder ¹³⁵, Y. Afik ³⁶, M.N. Agaras ¹³, J. Agarwala ^{72a,72b}, A. Aggarwal ⁹⁹, C. Agheorghiesei ^{27c}, J.A. Aguilar-Saavedra ^{129f}, A. Ahmad ³⁶, F. Ahmadov ^{38,w}, W.S. Ahmed ¹⁰³, S. Ahuja ⁹⁴, X. Ai ⁴⁸, G. Aielli ^{75a,75b}, I. Aizenberg ¹⁶⁷, M. Akbiyik ⁹⁹, T.P.A. Åkesson ⁹⁷, A.V. Akimov ³⁷, K. Al Khoury ⁴¹, G.L. Alberghi ^{23b}, J. Albert ¹⁶³, P. Albicocco ⁵³, M.J. Alconada Verzini ⁸⁹, S. Alderweireldt ⁵², M. Aleksa ³⁶, I.N. Aleksandrov ³⁸, C. Alexa ^{27b}, T. Alexopoulos ¹⁰, A. Alfonsi ¹¹³, F. Alfonsi ^{23b}, M. Alhroob ¹¹⁹, B. Ali ¹³¹, S. Ali ¹⁴⁷, M. Aliev ³⁷, G. Alimonti ^{70a}, W. Alkakhri ⁵⁵, C. Allaire ³⁶, B.M.M. Allbrooke ¹⁴⁵, P.P. Allport ²⁰, A. Aloisio ^{71a,71b}, F. Alonso ⁸⁹, C. Alpigiani ¹³⁷, E. Alunno Camelia ^{75a,75b}, M. Alvarez Estevez ⁹⁸, M.G. Alvigi ^{71a,71b}, Y. Amaral Coutinho ^{81b}, A. Ambler ¹⁰³, C. Amelung ³⁶, C.G. Ames ¹⁰⁸, D. Amidei ¹⁰⁵, S.P. Amor Dos Santos ^{129a}, S. Amoroso ⁴⁸, K.R. Amos ¹⁶¹, C.S. Amrouche ⁵⁶, V. Ananiev ¹²⁴, C. Anastopoulos ¹³⁸, T. Andeen ¹¹, J.K. Anders ¹⁹, S.Y. Andrean ^{47a,47b}, A. Andreazza ^{70a,70b}, S. Angelidakis ⁹, A. Angerami ^{41,y}, A.V. Anisenkov ³⁷, A. Annovi ^{73a}, C. Antel ⁵⁶, M.T. Anthony ¹³⁸, E. Antipov ¹²⁰, M. Antonelli ⁵³, D.J.A. Antrim ^{17a}, F. Anulli ^{74a}, M. Aoki ⁸², T. Aoki ¹⁵², J.A. Aparisi Pozo ¹⁶¹, M.A. Aparo ¹⁴⁵, L. Aperio Bella ⁴⁸, C. Appelt ¹⁸, N. Aranzabal ³⁶, V. Araujo Ferraz ^{81a}, C. Arcangeletti ⁵³, A.T.H. Arce ⁵¹, E. Arena ⁹¹, J-F. Arguin ¹⁰⁷, S. Argyropoulos ⁵⁴, J.-H. Arling ⁴⁸, A.J. Armbruster ³⁶, O. Arnaez ¹⁵⁴, H. Arnold ¹¹³, Z.P. Arrubarrena Tame ¹⁰⁸, G. Artoni ^{74a,74b}, H. Asada ¹¹⁰, K. Asai ¹¹⁷, S. Asai ¹⁵², N.A. Asbah ⁶¹, J. Assahsah ^{35d}, K. Assamagan ²⁹, R. Astalos ^{28a}, R.J. Atkin ^{33a}, M. Atkinson ¹⁶⁰, N.B. Atlay ¹⁸, H. Atmani ^{62b}, P.A. Atmasiddha ¹⁰⁵, K. Augsten ¹³¹, S. Auricchio ^{71a,71b}, A.D. Auriol ²⁰, V.A. Austrup ¹⁶⁹, G. Avner ¹⁴⁹, G. Avolio ³⁶, K. Axiotis ⁵⁶, M.K. Ayoub ^{14c}, G. Azuelos ^{107,aa}, D. Babal ^{28a}, H. Bachacou ¹³⁴, K. Bachas ^{151,q}, A. Bachiu ³⁴, F. Backman ^{47a,47b}, A. Badea ⁶¹, P. Bagnaia ^{74a,74b}, M. Bahmani ¹⁸, A.J. Bailey ¹⁶¹, V.R. Bailey ¹⁶⁰, J.T. Baines ¹³³, C. Bakalis ¹⁰, O.K. Baker ¹⁷⁰, P.J. Bakker ¹¹³, E. Bakos ¹⁵, D. Bakshi Gupta ⁸, S. Balaji ¹⁴⁶, R. Balasubramanian ¹¹³, E.M. Baldin ³⁷, P. Balek ¹³², E. Ballabene ^{70a,70b}, F. Balli ¹³⁴, L.M. Bales ^{63a}, W.K. Balunas ³², J. Balz ⁹⁹, E. Banas ⁸⁵, M. Bandieramonte ¹²⁸, A. Bandyopadhyay ²⁴, S. Bansal ²⁴, L. Barak ¹⁵⁰, E.L. Barberio ¹⁰⁴, D. Barberis ^{57b,57a}, M. Barbero ¹⁰¹, G. Barbour ⁹⁵, K.N. Barends ^{33a}, T. Barillari ¹⁰⁹, M-S. Barisits ³⁶, T. Barklow ¹⁴², R.M. Barnett ^{17a}, P. Baron ¹²¹, D.A. Baron Moreno ¹⁰⁰, A. Baroncelli ^{62a}, G. Barone ²⁹, A.J. Barr ¹²⁵, L. Barranco Navarro ^{47a,47b}, F. Barreiro ⁹⁸, J. Barreiro Guimarães da Costa ^{14a}, U. Barron ¹⁵⁰, M.G. Barros Teixeira ^{129a}, S. Barsov ³⁷, F. Bartels ^{63a}, R. Bartoldus ¹⁴², A.E. Barton ⁹⁰, P. Bartos ^{28a}, A. Basalaeu ⁴⁸, A. Basan ⁹⁹, M. Baselga ⁴⁹, I. Bashta ^{76a,76b}, A. Bassalat ⁶⁶, M.J. Basso ¹⁵⁴, C.R. Basson ¹⁰⁰, R.L. Bates ⁵⁹, S. Batlamous ^{35e}, J.R. Batley ³², B. Batool ¹⁴⁰, M. Battaglia ¹³⁵, D. Battulga ¹⁸, M. Bauge ^{74a,74b}, P. Bauer ²⁴, A. Bayirli ^{21a}, J.B. Beacham ⁵¹, T. Beau ¹²⁶, P.H. Beauchemin ¹⁵⁷, F. Becherer ⁵⁴, P. Bechtel ²⁴, H.P. Beck ^{19,p}, K. Becker ¹⁶⁵, C. Becot ⁴⁸, A.J. Beddall ^{21d}, V.A. Bednyakov ³⁸, C.P. Bee ¹⁴⁴, L.J. Beemster ¹⁵, T.A. Beermann ³⁶, M. Begalli ^{81d,81d}, M. Begel ²⁹, A. Behera ¹⁴⁴, J.K. Behr ⁴⁸, C. Beirao Da Cruz E Silva ³⁶, J.F. Beirer ^{55,36}, F. Beisiegel ²⁴, M. Belfkir ^{115b}, G. Bella ¹⁵⁰, L. Bellagamba ^{23b}, A. Bellerive ³⁴, P. Bellos ²⁰, K. Beloborodov ³⁷, K. Belotskiy ³⁷, N.L. Belyaev ³⁷, D. Benckekroun ^{35a}, F. Bendebba ^{35a}, Y. Benhammou ¹⁵⁰, D.P. Benjamin ²⁹,

M. Benoit ²⁹, J.R. Bensinger ²⁶, S. Bentvelsen ¹¹³, L. Beresford ³⁶, M. Beretta ⁵³, D. Berge ¹⁸,
E. Bergeaas Kuutmann ¹⁵⁹, N. Berger ⁴, B. Bergmann ¹³¹, J. Beringer ^{17a}, S. Berlendis ⁷,
G. Bernardi ⁵, C. Bernius ¹⁴², F.U. Bernlochner ²⁴, T. Berry ⁹⁴, P. Berta ¹³², A. Berthold ⁵⁰,
I.A. Bertram ⁹⁰, S. Bethke ¹⁰⁹, A. Betti ^{74a,74b}, A.J. Bevan ⁹³, M. Bhamjee ^{33c}, S. Bhatta ¹⁴⁴,
D.S. Bhattacharya ¹⁶⁴, P. Bhattarai ²⁶, V.S. Bhopatkar ¹²⁰, R. Bi ^{29,ad}, R.M. Bianchi ¹²⁸,
O. Biebel ¹⁰⁸, R. Bielski ¹²², M. Biglietti ^{76a}, T.R.V. Billoud ¹³¹, M. Bindi ⁵⁵, A. Bingul ^{21b},
C. Bini ^{74a,74b}, S. Biondi ^{23b,23a}, A. Biondini ⁹¹, C.J. Birch-sykes ¹⁰⁰, G.A. Bird ^{20,133},
M. Birman ¹⁶⁷, T. Bisanz ³⁶, E. Bisceglie ^{43b,43a}, D. Biswas ^{168,k}, A. Bitadze ¹⁰⁰, K. Bjørke ¹²⁴,
I. Bloch ⁴⁸, C. Blocker ²⁶, A. Blue ⁵⁹, U. Blumenschein ⁹³, J. Blumenthal ⁹⁹, G.J. Bobbink ¹¹³,
V.S. Bobrovnikov ³⁷, M. Boehler ⁵⁴, D. Bogavac ³⁶, A.G. Bogdanchikov ³⁷, C. Bohm ^{47a},
V. Boisvert ⁹⁴, P. Bokan ⁴⁸, T. Bold ^{84a}, M. Bomben ⁵, M. Bona ⁹³, M. Boonekamp ¹³⁴,
C.D. Booth ⁹⁴, A.G. Borbély ⁵⁹, H.M. Borecka-Bielska ¹⁰⁷, L.S. Borgna ⁹⁵, G. Borissov ⁹⁰,
D. Bortoletto ¹²⁵, D. Boscherini ^{23b}, M. Bosman ¹³, J.D. Bossio Sola ³⁶, K. Bouaouda ^{35a},
J. Boudreau ¹²⁸, E.V. Bouhova-Thacker ⁹⁰, D. Boumediene ⁴⁰, R. Bouquet ⁵, A. Boveia ¹¹⁸,
J. Boyd ³⁶, D. Boye ²⁹, I.R. Boyko ³⁸, J. Bracinik ²⁰, N. Brahimi ^{62d}, G. Brandt ¹⁶⁹,
O. Brandt ³², F. Braren ⁴⁸, B. Brau ¹⁰², J.E. Brau ¹²², K. Brendlinger ⁴⁸, R. Brenner ¹⁶⁷,
L. Brenner ³⁶, R. Brenner ¹⁵⁹, S. Bressler ¹⁶⁷, B. Brickwedde ⁹⁹, D. Britton ⁵⁹, D. Britzger ¹⁰⁹,
I. Brock ²⁴, G. Brooijmans ⁴¹, W.K. Brooks ^{136f}, E. Brost ²⁹, T.L. Bruckler ¹²⁵,
P.A. Bruckman de Renstrom ⁸⁵, B. Brüers ⁴⁸, D. Bruncko ^{28b,*}, A. Bruni ^{23b}, G. Bruni ^{23b},
M. Bruschi ^{23b}, N. Bruscinò ^{74a,74b}, L. Bryngemark ¹⁴², T. Buanes ¹⁶, Q. Buat ¹³⁷,
P. Buchholz ¹⁴⁰, A.G. Buckley ⁵⁹, I.A. Budagov ^{38,*}, M.K. Bugge ¹²⁴, O. Bulekov ³⁷,
B.A. Bullard ⁶¹, S. Burdin ⁹¹, C.D. Burgard ⁴⁸, A.M. Burger ⁴⁰, B. Burghgrave ⁸, J.T.P. Burr ³²,
C.D. Burton ¹¹, J.C. Burzynski ¹⁴¹, E.L. Busch ⁴¹, V. Büscher ⁹⁹, P.J. Bussey ⁵⁹, J.M. Butler ²⁵,
C.M. Buttar ⁵⁹, J.M. Butterworth ⁹⁵, W. Buttinger ¹³³, C.J. Buxo Vazquez ¹⁰⁶, A.R. Buzykaev ³⁷,
G. Cabras ^{23b}, S. Cabrera Urbán ¹⁶¹, D. Caforio ⁵⁸, H. Cai ¹²⁸, Y. Cai ^{14a,14d}, V.M.M. Cairo ³⁶,
O. Cakir ^{3a}, N. Calace ³⁶, P. Calafiura ^{17a}, G. Calderini ¹²⁶, P. Calfayan ⁶⁷, G. Callea ⁵⁹,
L.P. Caloba ^{81b}, D. Calvet ⁴⁰, S. Calvet ⁴⁰, T.P. Calvet ¹⁰¹, M. Calvetti ^{73a,73b},
R. Camacho Toro ¹²⁶, S. Camarda ³⁶, D. Camarero Munoz ²⁶, P. Camarri ^{75a,75b},
M.T. Camerlingo ^{76a,76b}, D. Cameron ¹²⁴, C. Camincher ¹⁶³, M. Campanelli ⁹⁵, A. Camplani ⁴²,
V. Canale ^{71a,71b}, A. Canesse ¹⁰³, M. Cano Bret ⁷⁹, J. Cantero ¹⁶¹, Y. Cao ¹⁶⁰, F. Capocasa ²⁶,
M. Capua ^{43b,43a}, A. Carbone ^{70a,70b}, R. Cardarelli ^{75a}, J.C.J. Cardenas ⁸, F. Cardillo ¹⁶¹,
T. Carli ³⁶, G. Carlino ^{71a}, J.I. Carlotto ¹³, B.T. Carlson ^{128,r}, E.M. Carlson ^{163,155a},
L. Carminati ^{70a,70b}, M. Carnesale ^{74a,74b}, S. Caron ¹¹², E. Carquin ^{136f}, S. Carrá ^{70a,70b},
G. Carratta ^{23b,23a}, F. Carri Argos ^{33g}, J.W.S. Carter ¹⁵⁴, T.M. Carter ⁵², M.P. Casado ^{13,h},
A.F. Casha ¹⁵⁴, E.G. Castiglia ¹⁷⁰, F.L. Castillo ^{63a}, L. Castillo Garcia ¹³, V. Castillo Gimenez ¹⁶¹,
N.F. Castro ^{129a,129e}, A. Catinaccio ³⁶, J.R. Catmore ¹²⁴, V. Cavaliere ²⁹, N. Cavalli ^{23b,23a},
V. Cavasinni ^{73a,73b}, E. Celebi ^{21a}, F. Celli ¹²⁵, M.S. Centonze ^{69a,69b}, K. Cerny ¹²¹,
A.S. Cerqueira ^{81a}, A. Cerri ¹⁴⁵, L. Cerrito ^{75a,75b}, F. Cerutti ^{17a}, A. Cervelli ^{23b}, S.A. Cetin ^{21d},
Z. Chadi ^{35a}, D. Chakraborty ¹¹⁴, M. Chala ^{129f}, J. Chan ¹⁶⁸, W.Y. Chan ¹⁵², J.D. Chapman ³²,
B. Chargeishvili ^{148b}, D.G. Charlton ²⁰, T.P. Charman ⁹³, M. Chatterjee ¹⁹, S. Chekanov ⁶,
S.V. Chekulaev ^{155a}, G.A. Chelkov ^{38,a}, A. Chen ¹⁰⁵, B. Chen ¹⁵⁰, B. Chen ¹⁶³, C. Chen ^{62a},
H. Chen ^{14c}, H. Chen ²⁹, J. Chen ^{62c}, J. Chen ²⁶, S. Chen ¹⁵², S.J. Chen ^{14c}, X. Chen ^{62c},
X. Chen ^{14b,z}, Y. Chen ^{62a}, C.L. Cheng ¹⁶⁸, H.C. Cheng ^{64a}, A. Cheplakov ³⁸,
E. Cheremushkina ⁴⁸, E. Cherepanova ¹¹³, R. Cherkaoui El Moursli ^{35e}, E. Cheu ⁷, K. Cheung ⁶⁵,
L. Chevalier ¹³⁴, V. Chiarella ⁵³, G. Chiarelli ^{73a}, N. Chiedde ¹⁰¹, G. Chiodini ^{69a},
A.S. Chisholm ²⁰, A. Chitan ^{27b}, M. Chitishvili ¹⁶¹, Y.H. Chiu ¹⁶³, M.V. Chizhov ³⁸, K. Choi ¹¹,
A.R. Chomont ^{74a,74b}, Y. Chou ¹⁰², E.Y.S. Chow ¹¹³, T. Chowdhury ^{33g}, L.D. Christopher ^{33g},

K.L. Chu^{64a}, M.C. Chu^{64a}, X. Chu^{14a,14d}, J. Chudoba¹³⁰, J.J. Chwastowski⁸⁵, D. Cieri¹⁰⁹,
 K.M. Ciesla^{84a}, V. Cindro⁹², A. Ciocio^{17a}, F. Cirotto^{71a,71b}, Z.H. Citron^{167,1}, M. Citterio^{70a},
 D.A. Ciubotaru^{27b}, B.M. Ciungu¹⁵⁴, A. Clark⁵⁶, P.J. Clark⁵², J.M. Clavijo Columbie⁴⁸,
 S.E. Clawson¹⁰⁰, C. Clement^{47a,47b}, J. Clercx⁴⁸, L. Clissa^{23b,23a}, Y. Coadou¹⁰¹,
 M. Cobal^{68a,68c}, A. Coccaro^{57b}, R.F. Coelho Barrue^{129a}, R. Coelho Lopes De Sa¹⁰²,
 S. Coelli^{70a}, H. Cohen¹⁵⁰, A.E.C. Coimbra^{70a,70b}, B. Cole⁴¹, J. Collot⁶⁰,
 P. Conde Muiño^{129a,129g}, M.P. Connell^{33c}, S.H. Connell^{33c}, I.A. Connelly⁵⁹, E.I. Conroy¹²⁵,
 F. Conventi^{71a,ab}, H.G. Cooke²⁰, A.M. Cooper-Sarkar¹²⁵, F. Cormier¹⁶², L.D. Corpe³⁶,
 M. Corradi^{74a,74b}, E.E. Corrigan⁹⁷, F. Corriveau^{103,v}, A. Cortes-Gonzalez¹⁸, M.J. Costa¹⁶¹,
 F. Costanza⁴, D. Costanzo¹³⁸, B.M. Cote¹¹⁸, G. Cowan⁹⁴, J.W. Cowley³², K. Cranmer¹¹⁶,
 S. Crépe-Renaudin⁶⁰, F. Crescioli¹²⁶, M. Cristinziani¹⁴⁰, M. Cristoforetti^{77a,77b,c}, V. Croft¹⁵⁷,
 G. Crosetti^{43b,43a}, A. Cueto³⁶, T. Cuhadar Donszelmann¹⁵⁸, H. Cui^{14a,14d}, Z. Cui⁷,
 A.R. Cukierman¹⁴², W.R. Cunningham⁵⁹, F. Curcio^{43b,43a}, P. Czodrowski³⁶, M.M. Czurylo^{63b},
 M.J. Da Cunha Sargedas De Sousa^{62a}, J.V. Da Fonseca Pinto^{81b}, C. Da Via¹⁰⁰, W. Dabrowski^{84a},
 T. Dado⁴⁹, S. Dahbi^{33g}, T. Dai¹⁰⁵, C. Dallapiccola¹⁰², M. Dam⁴², G. D'amen²⁹,
 V. D'Amico¹⁰⁸, J. Damp⁹⁹, J.R. Dandoy¹²⁷, M.F. Daneri³⁰, M. Danninger¹⁴¹, V. Dao³⁶,
 G. Darbo^{57b}, S. Darmora⁶, S.J. Das²⁹, S. D'Auria^{70a,70b}, C. David^{155b}, T. Davidek¹³²,
 D.R. Davis⁵¹, B. Davis-Purcell³⁴, I. Dawson⁹³, K. De⁸, R. De Asmundis^{71a},
 M. De Beurs¹¹³, N. De Biase⁴⁸, S. De Castro^{23b,23a}, N. De Groot¹¹², P. de Jong¹¹³,
 H. De la Torre¹⁰⁶, A. De Maria^{14c}, A. De Salvo^{74a}, U. De Sanctis^{75a,75b}, A. De Santo¹⁴⁵,
 J.B. De Vivie De Regie⁶⁰, D.V. Dedovich³⁸, J. Degens¹¹³, A.M. Deiana⁴⁴, F. Del Corso^{23b,23a},
 J. Del Peso⁹⁸, F. Del Rio^{63a}, F. Deliot¹³⁴, C.M. Delitzsch⁴⁹, M. Della Pietra^{71a,71b},
 D. Della Volpe⁵⁶, A. Dell'Acqua³⁶, L. Dell'Asta^{70a,70b}, M. Delmastro⁴, P.A. Delsart⁶⁰,
 S. Demers¹⁷⁰, M. Demichev³⁸, S.P. Denisov³⁷, L. D'Eramo¹¹⁴, D. Derendarz⁸⁵,
 F. Derue¹²⁶, P. Dervan⁹¹, K. Desch²⁴, K. Dette¹⁵⁴, C. Deutsch²⁴, P.O. Deviveiros³⁶,
 F.A. Di Bello^{74a,74b}, A. Di Ciaccio^{75a,75b}, L. Di Ciaccio⁴, A. Di Domenico^{74a,74b},
 C. Di Donato^{71a,71b}, A. Di Girolamo³⁶, G. Di Gregorio^{73a,73b}, A. Di Luca^{77a,77b},
 B. Di Micco^{76a,76b}, R. Di Nardo^{76a,76b}, C. Diaconu¹⁰¹, F.A. Dias¹¹³, T. Dias Do Vale¹⁴¹,
 M.A. Diaz^{136a,136b}, F.G. Diaz Capriles²⁴, M. Didenko¹⁶¹, E.B. Diehl¹⁰⁵, L. Diehl⁵⁴,
 S. Díez Cornell⁴⁸, C. Diez Pardos¹⁴⁰, C. Dimitriadi^{24,159}, A. Dimitrievska^{17a}, W. Ding^{14b},
 J. Dingfelder²⁴, I-M. Dinu^{27b}, S.J. Dittmeier^{63b}, F. Dittus³⁶, F. Djama¹⁰¹, T. Djjobava^{148b},
 J.I. Djuvsland¹⁶, C. Doglioni^{100,97}, J. Dolejsi¹³², Z. Dolezal¹³², M. Donadelli^{81c},
 B. Dong^{62c}, J. Donini⁴⁰, A. D'Onofrio^{14c}, M. D'Onofrio⁹¹, J. Dopke¹³³, A. Doria^{71a},
 M.T. Dova⁸⁹, A.T. Doyle⁵⁹, M.A. Draguet¹²⁵, E. Drechsler¹⁴¹, E. Dreyer¹⁶⁷,
 I. Drivas-koulouris¹⁰, A.S. Drobac¹⁵⁷, M. Drozdova⁵⁶, D. Du^{62a}, T.A. du Pree¹¹³,
 F. Dubinin³⁷, M. Dubovsky^{28a}, E. Duchovni¹⁶⁷, G. Duckeck¹⁰⁸, O.A. Ducu^{27b}, D. Duda¹⁰⁹,
 A. Dudarev³⁶, M. D'uffizi¹⁰⁰, L. Dufлот⁶⁶, M. Dührssen³⁶, C. Dülsen¹⁶⁹, A.E. Dumitriu^{27b},
 M. Dunford^{63a}, S. Dungs⁴⁹, K. Dunne^{47a,47b}, A. Duperrin¹⁰¹, H. Duran Yildiz^{3a},
 M. Düren⁵⁸, A. Durglishvili^{148b}, B.L. Dwyer¹¹⁴, G.I. Dyckes^{17a}, M. Dyndal^{84a},
 S. Dysch¹⁰⁰, B.S. Dziedzic⁸⁵, Z.O. Earnshaw¹⁴⁵, B. Eckerova^{28a}, M.G. Eggleston⁵¹,
 E. Egidio Purcino De Souza^{81b}, L.F. Ehrke⁵⁶, G. Eigen¹⁶, K. Einsweiler^{17a}, T. Ekelof¹⁵⁹,
 P.A. Ekman⁹⁷, Y. El Ghazali^{35b}, H. El Jarrari^{35c,147}, A. El Moussaouy^{35a}, V. Ellajosyula¹⁵⁹,
 M. Ellert¹⁵⁹, F. Ellinghaus¹⁶⁹, A.A. Elliot⁹³, N. Ellis³⁶, J. Elmsheuser²⁹, M. Elsing³⁶,
 D. Emelianov¹³³, A. Emerman⁴¹, Y. Enari¹⁵², I. Ene^{17a}, S. Epari¹³, J. Erdmann⁴⁹,
 A. Ereditato¹⁹, P.A. Erland⁸⁵, M. Errenst¹⁶⁹, M. Escalier⁶⁶, C. Escobar¹⁶¹, E. Etzion¹⁵⁰,
 G. Evans^{129a}, H. Evans⁶⁷, M.O. Evans¹⁴⁵, A. Ezhilov³⁷, S. Ezzarqtouni^{35a}, F. Fabbri⁵⁹,
 L. Fabbri^{23b,23a}, G. Facini⁹⁵, V. Fadeyev¹³⁵, R.M. Fakhruddinov³⁷, S. Falciano^{74a},

P.J. Falke [ID²⁴](#), S. Falke [ID³⁶](#), J. Faltova [ID¹³²](#), Y. Fan [ID^{14a}](#), Y. Fang [ID^{14a,14d}](#), G. Fanourakis [ID⁴⁶](#),
 M. Fanti [ID^{70a,70b}](#), M. Faraj [ID^{68a,68b}](#), A. Farbin [ID⁸](#), A. Farilla [ID^{76a}](#), T. Faroouque [ID¹⁰⁶](#), S.M. Farrington [ID⁵²](#),
 F. Fassi [ID^{35e}](#), D. Fassouliotis [ID⁹](#), M. Faucci Giannelli [ID^{75a,75b}](#), W.J. Fawcett [ID³²](#), L. Fayard [ID⁶⁶](#),
 P. Federicova [ID¹³⁰](#), O.L. Fedin [ID^{37,a}](#), G. Fedotov [ID³⁷](#), M. Feickert [ID¹⁶⁰](#), L. Feligioni [ID¹⁰¹](#), A. Fell [ID¹³⁸](#),
 D.E. Fellers [ID¹²²](#), C. Feng [ID^{62b}](#), M. Feng [ID^{14b}](#), Z. Feng [ID¹¹³](#), M.J. Fenton [ID¹⁵⁸](#), A.B. Fenyuk [ID³⁷](#),
 L. Ferencz [ID⁴⁸](#), S.W. Ferguson [ID⁴⁵](#), J.A. Fernandez Pretel [ID⁵⁴](#), J. Ferrando [ID⁴⁸](#), A. Ferrari [ID¹⁵⁹](#),
 P. Ferrari [ID¹¹³](#), R. Ferrari [ID^{72a}](#), D. Ferrere [ID⁵⁶](#), C. Ferretti [ID¹⁰⁵](#), F. Fiedler [ID⁹⁹](#), A. Filipčič [ID⁹²](#),
 E.K. Filmer [ID¹](#), F. Filthaut [ID¹¹²](#), M.C.N. Fiolhais [ID^{129a,129c,b}](#), L. Fiorini [ID¹⁶¹](#), F. Fischer [ID¹⁴⁰](#),
 W.C. Fisher [ID¹⁰⁶](#), T. Fitschen [ID²⁰](#), I. Fleck [ID¹⁴⁰](#), P. Fleischmann [ID¹⁰⁵](#), T. Flick [ID¹⁶⁹](#), L. Flores [ID¹²⁷](#),
 M. Flores [ID^{33d}](#), L.R. Flores Castillo [ID^{64a}](#), F.M. Follega [ID^{77a,77b}](#), N. Fomin [ID¹⁶](#), J.H. Foo [ID¹⁵⁴](#),
 B.C. Forland [ID⁶⁷](#), A. Formica [ID¹³⁴](#), A.C. Forti [ID¹⁰⁰](#), E. Fortin [ID¹⁰¹](#), A.W. Fortman [ID⁶¹](#), M.G. Foti [ID^{17a}](#),
 L. Fountas [ID⁹](#), D. Fournier [ID⁶⁶](#), H. Fox [ID⁹⁰](#), P. Francavilla [ID^{73a,73b}](#), S. Francescato [ID⁶¹](#),
 M. Franchini [ID^{23b,23a}](#), S. Franchino [ID^{63a}](#), D. Francis [ID³⁶](#), L. Franco [ID¹¹²](#), L. Franconi [ID¹⁹](#), M. Franklin [ID⁶¹](#),
 G. Frattari [ID²⁶](#), A.C. Freegard [ID⁹³](#), P.M. Freeman [ID²⁰](#), W.S. Freund [ID^{81b}](#), N. Fritzsche [ID⁵⁰](#), A. Froch [ID⁵⁴](#),
 D. Froidevaux [ID³⁶](#), J.A. Frost [ID¹²⁵](#), Y. Fu [ID^{62a}](#), M. Fujimoto [ID¹¹⁷](#), E. Fullana Torregrosa [ID^{161,*}](#),
 J. Fuster [ID¹⁶¹](#), A. Gabrielli [ID^{23b,23a}](#), A. Gabrielli [ID¹⁵⁴](#), P. Gadow [ID⁴⁸](#), G. Gagliardi [ID^{57b,57a}](#),
 L.G. Gagnon [ID^{17a}](#), G.E. Gallardo [ID¹²⁵](#), E.J. Gallas [ID¹²⁵](#), B.J. Gallop [ID¹³³](#), R. Gamboa Goni [ID⁹³](#),
 K.K. Gan [ID¹¹⁸](#), S. Ganguly [ID¹⁵²](#), J. Gao [ID^{62a}](#), Y. Gao [ID⁵²](#), F.M. Garay Walls [ID^{136a,136b}](#), B. Garcia [ID^{29,ad}](#),
 C. García [ID¹⁶¹](#), J.E. García Navarro [ID¹⁶¹](#), J.A. García Pascual [ID^{14a}](#), M. Garcia-Sciveres [ID^{17a}](#),
 R.W. Gardner [ID³⁹](#), D. Garg [ID⁷⁹](#), R.B. Garg [ID¹⁴²](#), S. Gargiulo [ID⁵⁴](#), C.A. Garner [ID¹⁵⁴](#), V. Garonne [ID²⁹](#),
 S.J. Gasiorowski [ID¹³⁷](#), P. Gaspar [ID^{81b}](#), G. Gaudio [ID^{72a}](#), V. Gautam [ID¹³](#), P. Gauzzi [ID^{74a,74b}](#),
 I.L. Gavrilenko [ID³⁷](#), A. Gavrilyuk [ID³⁷](#), C. Gay [ID¹⁶²](#), G. Gaycken [ID⁴⁸](#), E.N. Gazis [ID¹⁰](#),
 A.A. Geanta [ID^{27b,27e}](#), C.M. Gee [ID¹³⁵](#), J. Geisen [ID⁹⁷](#), M. Geisen [ID⁹⁹](#), C. Gemme [ID^{57b}](#), M.H. Genest [ID⁶⁰](#),
 S. Gentile [ID^{74a,74b}](#), S. George [ID⁹⁴](#), W.F. George [ID²⁰](#), T. Geralis [ID⁴⁶](#), L.O. Gerlach [ID⁵⁵](#),
 P. Gessinger-Befurt [ID³⁶](#), M. Ghasemi Bostanabad [ID¹⁶³](#), M. Ghneimat [ID¹⁴⁰](#), A. Ghosal [ID¹⁴⁰](#),
 A. Ghosh [ID¹⁵⁸](#), A. Ghosh [ID⁷](#), B. Giacobbe [ID^{23b}](#), S. Giagu [ID^{74a,74b}](#), N. Giangiacomi [ID¹⁵⁴](#),
 P. Giannetti [ID^{73a}](#), A. Giannini [ID^{62a}](#), S.M. Gibson [ID⁹⁴](#), M. Gignac [ID¹³⁵](#), D.T. Gil [ID^{84b}](#), A.K. Gilbert [ID^{84a}](#),
 B.J. Gilbert [ID⁴¹](#), D. Gillberg [ID³⁴](#), G. Gilles [ID¹¹³](#), N.E.K. Gillwald [ID⁴⁸](#), L. Ginabat [ID¹²⁶](#),
 D.M. Gingrich [ID^{2,aa}](#), M.P. Giordani [ID^{68a,68c}](#), P.F. Giraud [ID¹³⁴](#), G. Giugliarelli [ID^{68a,68c}](#), D. Giugni [ID^{70a}](#),
 F. Giuli [ID³⁶](#), I. Gkialas [ID^{9,i}](#), L.K. Gladilin [ID³⁷](#), C. Glasman [ID⁹⁸](#), G.R. Gledhill [ID¹²²](#), M. Glisic [ID¹²²](#),
 I. Gnesi [ID^{43b,e}](#), Y. Go [ID^{29,ad}](#), M. Goblirsch-Kolb [ID²⁶](#), D. Godin [ID¹⁰⁷](#), S. Goldfarb [ID¹⁰⁴](#), T. Golling [ID⁵⁶](#),
 M.G.D. Gololo [ID^{33g}](#), D. Golubkov [ID³⁷](#), J.P. Gombas [ID¹⁰⁶](#), A. Gomes [ID^{129a,129b}](#), G. Gomes Da Silva [ID¹⁴⁰](#),
 A.J. Gomez Delegido [ID¹⁶¹](#), R. Goncalves Gama [ID⁵⁵](#), R. Gonçalves [ID^{129a,129c}](#), G. Gonella [ID¹²²](#),
 L. Gonella [ID²⁰](#), A. Gongadze [ID³⁸](#), F. Gonnella [ID²⁰](#), J.L. Gonski [ID⁴¹](#), S. González de la Hoz [ID¹⁶¹](#),
 S. Gonzalez Fernandez [ID¹³](#), R. Gonzalez Lopez [ID⁹¹](#), C. Gonzalez Renteria [ID^{17a}](#),
 R. Gonzalez Suarez [ID¹⁵⁹](#), S. Gonzalez-Sevilla [ID⁵⁶](#), G.R. Gonzalvo Rodriguez [ID¹⁶¹](#),
 R.Y. González Andana [ID⁵²](#), L. Goossens [ID³⁶](#), N.A. Gorasia [ID²⁰](#), P.A. Gorbounov [ID³⁷](#), B. Gorini [ID³⁶](#),
 E. Gorini [ID^{69a,69b}](#), A. Gorišek [ID⁹²](#), A.T. Goshaw [ID⁵¹](#), M.I. Gostkin [ID³⁸](#), C.A. Gottardo [ID³⁶](#),
 M. Goughri [ID^{35b}](#), V. Goumarre [ID⁴⁸](#), A.G. Goussiou [ID¹³⁷](#), N. Govender [ID^{33c}](#), C. Goy [ID⁴](#),
 I. Grabowska-Bold [ID^{84a}](#), K. Graham [ID³⁴](#), E. Gramstad [ID¹²⁴](#), S. Grancagnolo [ID¹⁸](#), M. Grandi [ID¹⁴⁵](#),
 V. Gratchev [ID^{37,*}](#), P.M. Gravila [ID^{27f}](#), F.G. Gravili [ID^{69a,69b}](#), H.M. Gray [ID^{17a}](#), M. Greco [ID^{69a,69b}](#),
 C. Grefe [ID²⁴](#), I.M. Gregor [ID⁴⁸](#), P. Grenier [ID¹⁴²](#), C. Grieco [ID¹³](#), A.A. Grillo [ID¹³⁵](#), K. Grimm [ID^{31,m}](#),
 S. Grinstein [ID^{13,t}](#), J.-F. Grivaz [ID⁶⁶](#), E. Gross [ID¹⁶⁷](#), J. Grosse-Knetter [ID⁵⁵](#), C. Grud [ID¹⁰⁵](#), A. Grummer [ID¹¹¹](#),
 J.C. Grundy [ID¹²⁵](#), L. Guan [ID¹⁰⁵](#), W. Guan [ID¹⁶⁸](#), C. Gubbels [ID¹⁶²](#), J.G.R. Guerrero Rojas [ID¹⁶¹](#),
 G. Guerrieri [ID^{68a,68b}](#), F. Guescini [ID¹⁰⁹](#), R. Gugel [ID⁹⁹](#), J.A.M. Guhit [ID¹⁰⁵](#), A. Guida [ID⁴⁸](#), T. Guillemain [ID⁴](#),
 E. Guilloton [ID^{165,133}](#), S. Guindon [ID³⁶](#), F. Guo [ID^{14a,14d}](#), J. Guo [ID^{62c}](#), L. Guo [ID⁶⁶](#), Y. Guo [ID¹⁰⁵](#),
 R. Gupta [ID⁴⁸](#), S. Gurbuz [ID²⁴](#), S.S. Gurdasani [ID⁵⁴](#), G. Gustavino [ID³⁶](#), M. Guth [ID⁵⁶](#), P. Gutierrez [ID¹¹⁹](#),

L.F. Gutierrez Zagazeta [ID127](#), C. Gutschow [ID95](#), C. Guyot [ID134](#), C. Gwenlan [ID125](#), C.B. Gwilliam [ID91](#), E.S. Haaland [ID124](#), A. Haas [ID116](#), M. Habedank [ID48](#), C. Haber [ID17a](#), H.K. Hadavand [ID8](#), A. Hadeif [ID99](#), S. Hadzic [ID109](#), M. Haleem [ID164](#), J. Haley [ID120](#), J.J. Hall [ID138](#), G.D. Hallewell [ID101](#), L. Halser [ID19](#), K. Hamano [ID163](#), H. Hamdaoui [ID35e](#), M. Hamer [ID24](#), G.N. Hamity [ID52](#), J. Han [ID62b](#), K. Han [ID62a](#), L. Han [ID14c](#), L. Han [ID62a](#), S. Han [ID17a](#), Y.F. Han [ID154](#), K. Hanagaki [ID82](#), M. Hance [ID135](#), D.A. Hangal [ID41,y](#), H. Hanif [ID141](#), M.D. Hank [ID39](#), R. Hankache [ID100](#), J.B. Hansen [ID42](#), J.D. Hansen [ID42](#), P.H. Hansen [ID42](#), K. Hara [ID156](#), D. Harada [ID56](#), T. Harenberg [ID169](#), S. Harkusha [ID37](#), Y.T. Harris [ID125](#), N.M. Harrison [ID118](#), P.F. Harrison [ID165](#), N.M. Hartman [ID142](#), N.M. Hartmann [ID108](#), Y. Hasegawa [ID139](#), A. Hasib [ID52](#), S. Haug [ID19](#), R. Hauser [ID106](#), M. Havranek [ID131](#), C.M. Hawkes [ID20](#), R.J. Hawkings [ID36](#), S. Hayashida [ID110](#), D. Hayden [ID106](#), C. Hayes [ID105](#), R.L. Hayes [ID162](#), C.P. Hays [ID125](#), J.M. Hays [ID93](#), H.S. Hayward [ID91](#), F. He [ID62a](#), Y. He [ID153](#), Y. He [ID126](#), M.P. Heath [ID52](#), V. Hedberg [ID97](#), A.L. Heggelund [ID124](#), N.D. Hehir [ID93](#), C. Heidegger [ID54](#), K.K. Heidegger [ID54](#), W.D. Heidorn [ID80](#), J. Heilman [ID34](#), S. Heim [ID48](#), T. Heim [ID17a](#), J.G. Heinlein [ID127](#), J.J. Heinrich [ID122](#), L. Heinrich [ID109](#), J. Hejbal [ID130](#), L. Helary [ID48](#), A. Held [ID168](#), S. Hellesund [ID124](#), C.M. Helling [ID162](#), S. Hellman [ID47a,47b](#), C. Helsens [ID36](#), R.C.W. Henderson [ID90](#), L. Henkelmann [ID32](#), A.M. Henriques Correia [ID36](#), H. Herde [ID142](#), Y. Hernández Jiménez [ID144](#), M.G. Herrmann [ID108](#), T. Herrmann [ID50](#), G. Herten [ID54](#), R. Hertenberger [ID108](#), L. Hervas [ID36](#), N.P. Hessey [ID155a](#), H. Hibi [ID83](#), E. Higón-Rodríguez [ID161](#), S.J. Hillier [ID20](#), I. Hinchliffe [ID17a](#), F. Hinterkeuser [ID24](#), M. Hirose [ID123](#), S. Hirose [ID156](#), D. Hirschbuehl [ID169](#), T.G. Hitchings [ID100](#), B. Hiti [ID92](#), J. Hobbs [ID144](#), R. Hobincu [ID27e](#), N. Hod [ID167](#), M.C. Hodgkinson [ID138](#), B.H. Hodgkinson [ID32](#), A. Hoecker [ID36](#), J. Hofer [ID48](#), D. Hohn [ID54](#), T. Holm [ID24](#), M. Holzbock [ID109](#), L.B.A.H. Hommels [ID32](#), B.P. Honan [ID100](#), J. Hong [ID62c](#), T.M. Hong [ID128](#), Y. Hong [ID55](#), J.C. Honig [ID54](#), A. Hönle [ID109](#), B.H. Hooberman [ID160](#), W.H. Hopkins [ID6](#), Y. Horii [ID110](#), S. Hou [ID147](#), A.S. Howard [ID92](#), J. Howarth [ID59](#), J. Hoya [ID6](#), M. Hrabovsky [ID121](#), A. Hrynevich [ID37](#), T. Hryn'ova [ID4](#), P.J. Hsu [ID65](#), S.-C. Hsu [ID137](#), Q. Hu [ID41,y](#), Y.F. Hu [ID14a,14d,ac](#), D.P. Huang [ID95](#), S. Huang [ID64b](#), X. Huang [ID14c](#), Y. Huang [ID62a](#), Y. Huang [ID14a](#), Z. Huang [ID100](#), Z. Hubacek [ID131](#), M. Huebner [ID24](#), F. Huegging [ID24](#), T.B. Huffman [ID125](#), M. Huhtinen [ID36](#), S.K. Huiberts [ID16](#), R. Hulsken [ID103](#), N. Huseynov [ID12,a](#), J. Huston [ID106](#), J. Huth [ID61](#), R. Hyneman [ID142](#), S. Hyrych [ID28a](#), G. Iacobucci [ID56](#), G. Iakovidis [ID29](#), I. Ibragimov [ID140](#), L. Iconomidou-Fayard [ID66](#), P. Iengo [ID71a,71b](#), R. Iguchi [ID152](#), T. Iizawa [ID56](#), Y. Ikegami [ID82](#), A. Ilg [ID19](#), N. Ilic [ID154](#), H. Imam [ID35a](#), T. Ingebretsen Carlson [ID47a,47b](#), G. Introzzi [ID72a,72b](#), M. Iodice [ID76a](#), V. Ippolito [ID74a,74b](#), M. Ishino [ID152](#), W. Islam [ID168](#), C. Issever [ID18,48](#), S. Istin [ID21a,af](#), H. Ito [ID166](#), J.M. Iturbe Ponce [ID64a](#), R. Iuppa [ID77a,77b](#), A. Ivina [ID167](#), J.M. Izen [ID45](#), V. Izzo [ID71a](#), P. Jacka [ID130,131](#), P. Jackson [ID1](#), R.M. Jacobs [ID48](#), B.P. Jaeger [ID141](#), C.S. Jagfeld [ID108](#), G. Jäkel [ID169](#), K. Jakobs [ID54](#), T. Jakoubek [ID167](#), J. Jamieson [ID59](#), K.W. Janas [ID84a](#), G. Jarlskog [ID97](#), A.E. Jaspán [ID91](#), M. Javurkova [ID102](#), F. Jeanneau [ID134](#), L. Jeanty [ID122](#), J. Jejelava [ID148a,x](#), P. Jenni [ID54,f](#), C.E. Jessiman [ID34](#), S. Jézéquel [ID4](#), J. Jia [ID144](#), X. Jia [ID61](#), X. Jia [ID14a,14d](#), Z. Jia [ID14c](#), Y. Jiang [ID62a](#), S. Jiggins [ID52](#), J. Jimenez Pena [ID109](#), S. Jin [ID14c](#), A. Jinaru [ID27b](#), O. Jinnouchi [ID153](#), P. Johansson [ID138](#), K.A. Johns [ID7](#), D.M. Jones [ID32](#), E. Jones [ID165](#), P. Jones [ID32](#), R.W.L. Jones [ID90](#), T.J. Jones [ID91](#), R. Joshi [ID118](#), J. Jovicevic [ID15](#), X. Ju [ID17a](#), J.J. Junggeburth [ID36](#), A. Juste Rozas [ID13,t](#), S. Kabana [ID136e](#), A. Kaczmarzka [ID85](#), M. Kado [ID74a,74b](#), H. Kagan [ID118](#), M. Kagan [ID142](#), A. Kahn [ID41](#), A. Kahn [ID127](#), C. Kahra [ID99](#), T. Kaji [ID166](#), E. Kajomovitz [ID149](#), N. Kakati [ID167](#), C.W. Kalderon [ID29](#), A. Kamenshchikov [ID154](#), S. Kanayama [ID153](#), N.J. Kang [ID135](#), Y. Kano [ID110](#), S. Kaphle [ID18](#), D. Kar [ID33g](#), K. Karava [ID125](#), M.J. Kareem [ID155b](#), E. Karentzos [ID54](#), I. Karkanas [ID151](#), S.N. Karpov [ID38](#), Z.M. Karpova [ID38](#), V. Kartvelishvili [ID90](#), A.N. Karyukhin [ID37](#), E. Kasimi [ID151](#), C. Kato [ID62d](#), J. Katzy [ID48](#), S. Kaur [ID34](#), K. Kawade [ID139](#), K. Kawagoe [ID88](#), T. Kawamoto [ID134](#), G. Kawamura [ID55](#), E.F. Kay [ID163](#), F.I. Kaya [ID157](#), S. Kazakos [ID13](#), V.F. Kazanin [ID37](#), Y. Ke [ID144](#), J.M. Keaveney [ID33a](#), R. Keeler [ID163](#), G.V. Kehris [ID61](#), J.S. Keller [ID34](#), A.S. Kelly [ID95](#), D. Kelsey [ID145](#), J.J. Kempster [ID20](#), K.E. Kennedy [ID41](#), O. Kepka [ID130](#), B.P. Kerridge [ID165](#),

S. Kersten ¹⁶⁹, B.P. Kerševan ⁹², S. Keshri ⁶⁶, L. Keszeghova ^{28a}, S. Ketabchi Haghighat ¹⁵⁴,
 M. Khandoga ¹²⁶, A. Khanov ¹²⁰, A.G. Kharlamov ³⁷, T. Kharlamova ³⁷, E.E. Khoda ¹³⁷,
 T.J. Khoo ¹⁸, G. Khoriauili ¹⁶⁴, J. Khubua ^{148b}, Y.A.R. Khwaira ⁶⁶, M. Kiehn ³⁶,
 A. Kilgallon ¹²², D.W. Kim ^{47a,47b}, E. Kim ¹⁵³, Y.K. Kim ³⁹, N. Kimura ⁹⁵, A. Kirchhoff ⁵⁵,
 D. Kirchmeier ⁵⁰, C. Kirfel ²⁴, J. Kirk ¹³³, A.E. Kiryunin ¹⁰⁹, T. Kishimoto ¹⁵², D.P. Kisliuk ¹⁵⁴,
 C. Kitsaki ¹⁰, O. Kivernyk ²⁴, M. Klassen ^{63a}, C. Klein ³⁴, L. Klein ¹⁶⁴, M.H. Klein ¹⁰⁵,
 M. Klein ⁹¹, S.B. Klein ⁵⁶, U. Klein ⁹¹, P. Klimek ³⁶, A. Klimentov ²⁹, F. Klimpel ¹⁰⁹,
 T. Klingl ²⁴, T. Klioutchnikova ³⁶, F.F. Klitzner ¹⁰⁸, P. Kluit ¹¹³, S. Kluth ¹⁰⁹, E. Kneringer ⁷⁸,
 T.M. Knight ¹⁵⁴, A. Knue ⁵⁴, D. Kobayashi⁸⁸, R. Kobayashi ⁸⁶, M. Kocian ¹⁴², P. Kodyš ¹³²,
 D.M. Koeck ¹⁴⁵, P.T. Koenig ²⁴, T. Koffas ³⁴, N.M. Köhler ³⁶, M. Kolb ¹³⁴, I. Koletsou ⁴,
 T. Komarek ¹²¹, K. Köneke ⁵⁴, A.X.Y. Kong ¹, T. Kono ¹¹⁷, N. Konstantinidis ⁹⁵, B. Konya ⁹⁷,
 R. Kopeliansky ⁶⁷, S. Koperny ^{84a}, K. Korcyl ⁸⁵, K. Kordas ¹⁵¹, G. Koren ¹⁵⁰, A. Korn ⁹⁵,
 S. Korn ⁵⁵, I. Korolkov ¹³, N. Korotkova ³⁷, B. Kortman ¹¹³, O. Kortner ¹⁰⁹, S. Kortner ¹⁰⁹,
 W.H. Kostecka ¹¹⁴, V.V. Kostyukhin ¹⁴⁰, A. Kotsokechagia ¹³⁴, A. Kotwal ⁵¹, A. Koulouris ³⁶,
 A. Kourkoumeli-Charalampidi ^{72a,72b}, C. Kourkoumelis ⁹, E. Kourlitis ⁶, O. Kovanda ¹⁴⁵,
 R. Kowalewski ¹⁶³, W. Kozanecki ¹³⁴, A.S. Kozhin ³⁷, V.A. Kramarenko ³⁷, G. Kramberger ⁹²,
 P. Kramer ⁹⁹, M.W. Krasny ¹²⁶, A. Krasznahorkay ³⁶, J.A. Kremer ⁹⁹, T. Kresse ⁵⁰,
 J. Kretschmar ⁹¹, K. Kreul ¹⁸, P. Krieger ¹⁵⁴, F. Krieter ¹⁰⁸, S. Krishnamurthy ¹⁰²,
 A. Krishnan ^{63b}, M. Krivos ¹³², K. Krizka ^{17a}, K. Kroeninger ⁴⁹, H. Kroha ¹⁰⁹, J. Kroll ¹³⁰,
 J. Kroll ¹²⁷, K.S. Krowpman ¹⁰⁶, U. Kruchonak ³⁸, H. Krüger ²⁴, N. Krumnack⁸⁰, M.C. Kruse ⁵¹,
 J.A. Krzysiak ⁸⁵, A. Kubota ¹⁵³, O. Kuchinskaia ³⁷, S. Kuday ^{3a}, D. Kuechler ⁴⁸,
 J.T. Kuechler ⁴⁸, S. Kuehn ³⁶, T. Kuhl ⁴⁸, V. Kukhtin ³⁸, Y. Kulchitsky ^{37,a},
 S. Kuleshov ^{136d,136b}, M. Kumar ^{33g}, N. Kumari ¹⁰¹, M. Kuna ⁶⁰, A. Kupco ¹³⁰, T. Kupfer⁴⁹,
 A. Kupich ³⁷, O. Kuprash ⁵⁴, H. Kurashige ⁸³, L.L. Kurchaninov ^{155a}, Y.A. Kurochkin ³⁷,
 A. Kurova ³⁷, E.S. Kuwertz ³⁶, M. Kuze ¹⁵³, A.K. Kvam ¹⁰², J. Kvita ¹²¹, T. Kwan ¹⁰³,
 K.W. Kwok ^{64a}, N.G. Kyriacou ¹⁰⁵, L.A.O. Laatu ¹⁰¹, C. Lacasta ¹⁶¹, F. Lacava ^{74a,74b},
 H. Lacker ¹⁸, D. Lacour ¹²⁶, N.N. Lad ⁹⁵, E. Ladygin ³⁸, B. Laforge ¹²⁶, T. Lagouri ^{136e},
 S. Lai ⁵⁵, I.K. Lakomic ^{84a}, N. Lalloue ⁶⁰, J.E. Lambert ¹¹⁹, S. Lammers ⁶⁷, W. Lampl ⁷,
 C. Lampoudis ¹⁵¹, A.N. Lancaster ¹¹⁴, E. Lançon ²⁹, U. Landgraf ⁵⁴, M.P.J. Landon ⁹³,
 V.S. Lang ⁵⁴, R.J. Langenberg ¹⁰², A.J. Lankford ¹⁵⁸, F. Lanni ³⁶, K. Lantzsch ²⁴, A. Lanza ^{72a},
 A. Lapertosa ^{57b,57a}, J.F. Laporte ¹³⁴, T. Lari ^{70a}, F. Lasagni Manghi ^{23b}, M. Lassnig ³⁶,
 V. Latonova ¹³⁰, T.S. Lau ^{64a}, A. Laudrain ⁹⁹, A. Laurier ³⁴, S.D. Lawlor ⁹⁴, Z. Lawrence ¹⁰⁰,
 M. Lazzaroni ^{70a,70b}, B. Le¹⁰⁰, B. Leban ⁹², A. Lebedev ⁸⁰, M. LeBlanc ³⁶, T. LeCompte ⁶,
 F. Ledroit-Guillon ⁶⁰, A.C.A. Lee⁹⁵, G.R. Lee ¹⁶, L. Lee ⁶¹, S.C. Lee ¹⁴⁷, S. Lee ^{47a,47b},
 T.F. Lee ⁹¹, L.L. Leeuw ^{33c}, H.P. Lefebvre ⁹⁴, M. Lefebvre ¹⁶³, C. Leggett ^{17a}, K. Lehmann ¹⁴¹,
 G. Lehmann Miotto ³⁶, M. Leigh ⁵⁶, W.A. Leight ¹⁰², A. Leisos ^{151,s}, M.A.L. Leite ^{81c},
 C.E. Leitgeb ⁴⁸, R. Leitner ¹³², K.J.C. Leney ⁴⁴, T. Lenz ²⁴, S. Leone ^{73a}, C. Leonidopoulos ⁵²,
 A. Leopold ¹⁴³, C. Leroy ¹⁰⁷, R. Les ¹⁰⁶, C.G. Lester ³², M. Levchenko ³⁷, J. Levêque ⁴,
 D. Levin ¹⁰⁵, L.J. Levinson ¹⁶⁷, M.P. Lewicki ⁸⁵, D.J. Lewis ²⁰, B. Li ^{14b}, B. Li ^{62b}, C. Li^{62a},
 C-Q. Li ^{62c}, H. Li ^{62a}, H. Li ^{62b}, H. Li ^{14c}, H. Li ^{62b}, J. Li ^{62c}, K. Li ¹³⁷, L. Li ^{62c},
 M. Li ^{14a,14d}, Q.Y. Li ^{62a}, S. Li ^{62d,62c,d}, T. Li ^{62b}, X. Li ¹⁰³, Z. Li ^{62b}, Z. Li ¹²⁵, Z. Li ¹⁰³,
 Z. Li ⁹¹, Z. Liang ^{14a}, M. Liberatore ⁴⁸, B. Liberti ^{75a}, K. Lie ^{64c}, J. Lieber Marin ^{81b},
 K. Lin ¹⁰⁶, R.A. Linck ⁶⁷, R.E. Lindley ⁷, J.H. Lindon ², A. Linss ⁴⁸, E. Lipeles ¹²⁷,
 A. Lipniacka ¹⁶, A. Lister ¹⁶², J.D. Little ⁴, B. Liu ^{14a}, B.X. Liu ¹⁴¹, D. Liu ^{62d,62c},
 J.B. Liu ^{62a}, J.K.K. Liu ³², K. Liu ^{62d,62c}, M. Liu ^{62a}, M.Y. Liu ^{62a}, P. Liu ^{14a},
 Q. Liu ^{62d,137,62c}, X. Liu ^{62a}, Y. Liu ⁴⁸, Y. Liu ^{14c,14d}, Y.L. Liu ¹⁰⁵, Y.W. Liu ^{62a},
 M. Livan ^{72a,72b}, J. Llorente Merino ¹⁴¹, S.L. Lloyd ⁹³, E.M. Lobodzinska ⁴⁸, P. Loch ⁷,








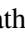









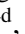




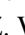





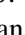

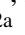
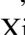



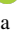

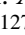
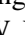




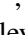
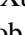



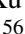


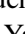









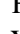

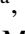




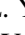
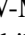



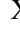
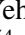
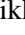

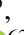


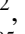




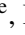
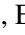
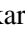

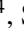


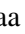






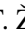





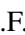
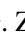





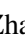

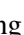


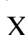
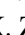
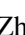
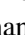



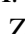


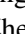

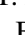
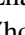

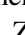


S. Loffredo ^{75a,75b}, T. Lohse ¹⁸, K. Lohwasser ¹³⁸, M. Lokajicek ¹³⁰, J.D. Long ¹⁶⁰,
 I. Longarini ^{74a,74b}, L. Longo ^{69a,69b}, R. Longo ¹⁶⁰, I. Lopez Paz ³⁶, A. Lopez Solis ⁴⁸,
 J. Lorenz ¹⁰⁸, N. Lorenzo Martinez ⁴, A.M. Lory ¹⁰⁸, A. Lösle ⁵⁴, X. Lou ^{47a,47b}, X. Lou ^{14a,14d},
 A. Lounis ⁶⁶, J. Love ⁶, P.A. Love ⁹⁰, J.J. Lozano Bahilo ¹⁶¹, G. Lu ^{14a,14d}, M. Lu ⁷⁹,
 S. Lu ¹²⁷, Y.J. Lu ⁶⁵, H.J. Lubatti ¹³⁷, C. Luci ^{74a,74b}, F.L. Lucio Alves ^{14c}, A. Lucotte ⁶⁰,
 F. Luehring ⁶⁷, I. Luise ¹⁴⁴, O. Lukianchuk ⁶⁶, O. Lundberg ¹⁴³, B. Lund-Jensen ¹⁴³,
 N.A. Luongo ¹²², M.S. Lutz ¹⁵⁰, D. Lynn ²⁹, H. Lyons ⁹¹, R. Lysak ¹³⁰, E. Lytken ⁹⁷, F. Lyu ^{14a},
 V. Lyubushkin ³⁸, T. Lyubushkina ³⁸, H. Ma ²⁹, L.L. Ma ^{62b}, Y. Ma ⁹⁵, D.M. Mac Donell ¹⁶³,
 G. Maccarrone ⁵³, J.C. MacDonald ¹³⁸, R. Madar ⁴⁰, W.F. Mader ⁵⁰, J. Maeda ⁸³, T. Maeno ²⁹,
 M. Maerker ⁵⁰, V. Magerl ⁵⁴, J. Magro ^{68a,68c}, H. Maguire ¹³⁸, D.J. Mahon ⁴¹,
 C. Maidantchik ^{81b}, A. Maio ^{129a,129b,129d}, K. Maj ^{84a}, O. Majersky ^{28a}, S. Majewski ¹²²,
 N. Makovec ⁶⁶, V. Maksimovic ¹⁵, B. Malaescu ¹²⁶, Pa. Malecki ⁸⁵, V.P. Maleev ³⁷,
 F. Malek ⁶⁰, D. Malito ^{43b,43a}, U. Mallik ⁷⁹, C. Malone ³², S. Maltezos ¹⁰, S. Malyukov ³⁸,
 J. Mamuzic ¹³, G. Mancini ⁵³, G. Manco ^{72a,72b}, J.P. Mandalia ⁹³, I. Mandić ⁹²,
 L. Manhaes de Andrade Filho ^{81a}, I.M. Maniatis ¹⁵¹, M. Manisha ¹³⁴, J. Manjarres Ramos ⁵⁰,
 D.C. Mankad ¹⁶⁷, A. Mann ¹⁰⁸, B. Mansoulie ¹³⁴, S. Manzoni ³⁶, A. Marantis ¹⁵¹,
 G. Marchiori ⁵, M. Marcisovsky ¹³⁰, L. Marcoccia ^{75a,75b}, C. Marcon ^{70a,70b}, M. Marinescu ²⁰,
 M. Marjanovic ¹¹⁹, Z. Marshall ^{17a}, S. Marti-Garcia ¹⁶¹, T.A. Martin ¹⁶⁵, V.J. Martin ⁵²,
 B. Martin dit Latour ¹⁶, L. Martinelli ^{74a,74b}, M. Martinez ^{13,t}, P. Martinez Agullo ¹⁶¹,
 V.I. Martinez Outschoorn ¹⁰², P. Martinez Suarez ¹³, S. Martin-Haugh ¹³³, V.S. Martoiu ^{27b},
 A.C. Martyniuk ⁹⁵, A. Marzin ³⁶, S.R. Maschek ¹⁰⁹, L. Masetti ⁹⁹, T. Mashimo ¹⁵²,
 J. Masik ¹⁰⁰, A.L. Maslennikov ³⁷, L. Massa ^{23b}, P. Massarotti ^{71a,71b}, P. Mastrandrea ^{73a,73b},
 A. Mastroberardino ^{43b,43a}, T. Masubuchi ¹⁵², T. Mathisen ¹⁵⁹, N. Matsuzawa ¹⁵², J. Maurer ^{27b},
 B. Maček ⁹², D.A. Maximov ³⁷, R. Mazini ¹⁴⁷, I. Maznas ¹⁵¹, M. Mazza ¹⁰⁶, S.M. Mazza ¹³⁵,
 C. Mc Ginn ^{29,ad}, J.P. Mc Gowan ¹⁰³, S.P. Mc Kee ¹⁰⁵, T.G. McCarthy ¹⁰⁹, W.P. McCormack ^{17a},
 E.F. McDonald ¹⁰⁴, A.E. McDougall ¹¹³, J.A. Mcfayden ¹⁴⁵, G. Mchedlidze ^{148b},
 R.P. McKenzie ^{33g}, T.C. Mclachlan ⁴⁸, D.J. Mclaughlin ⁹⁵, K.D. McLean ¹⁶³, S.J. McMahon ¹³³,
 P.C. McNamara ¹⁰⁴, C.M. Mcpartland ⁹¹, R.A. McPherson ^{163,v}, T. Megy ⁴⁰, S. Mehlhase ¹⁰⁸,
 A. Mehta ⁹¹, B. Meirose ⁴⁵, D. Melini ¹⁴⁹, B.R. Mellado Garcia ^{33g}, A.H. Melo ⁵⁵,
 F. Meloni ⁴⁸, E.D. Mendes Gouveia ^{129a}, A.M. Mendes Jacques Da Costa ²⁰, H.Y. Meng ¹⁵⁴,
 L. Meng ⁹⁰, S. Menke ¹⁰⁹, M. Mentink ³⁶, E. Meoni ^{43b,43a}, C. Merlassino ¹²⁵,
 L. Merola ^{71a,71b}, C. Meroni ^{70a}, G. Merz ¹⁰⁵, O. Meshkov ³⁷, J.K.R. Meshreki ¹⁴⁰, J. Metcalfe ⁶,
 A.S. Mete ⁶, C. Meyer ⁶⁷, J-P. Meyer ¹³⁴, M. Michetti ¹⁸, R.P. Middleton ¹³³, L. Mijović ⁵²,
 G. Mikenberg ¹⁶⁷, M. Mikestikova ¹³⁰, M. Mikuž ⁹², H. Mildner ¹³⁸, A. Milic ¹⁵⁴,
 C.D. Milke ⁴⁴, D.W. Miller ³⁹, L.S. Miller ³⁴, A. Milov ¹⁶⁷, D.A. Milstead ^{47a,47b}, T. Min ^{14c},
 A.A. Minaenko ³⁷, I.A. Minashvili ^{148b}, L. Mince ⁵⁹, A.I. Mincer ¹¹⁶, B. Mindur ^{84a},
 M. Mineev ³⁸, Y. Mino ⁸⁶, L.M. Mir ¹³, M. Miralles Lopez ¹⁶¹, M. Mironova ¹²⁵, T. Mitani ¹⁶⁶,
 A. Mitra ¹⁶⁵, V.A. Mitsou ¹⁶¹, O. Miu ¹⁵⁴, P.S. Miyagawa ⁹³, Y. Miyazaki ⁸⁸, A. Mizukami ⁸²,
 J.U. Mjörnmark ⁹⁷, T. Mkrtchyan ^{63a}, T. Mlinarevic ⁹⁵, M. Mlynarikova ³⁶, T. Moa ^{47a,47b},
 S. Mobius ⁵⁵, K. Mochizuki ¹⁰⁷, P. Moder ⁴⁸, P. Mogg ¹⁰⁸, A.F. Mohammed ^{14a,14d},
 S. Mohapatra ⁴¹, G. Mokgatitwane ^{33g}, B. Mondal ¹⁴⁰, S. Mondal ¹³¹, K. Mönig ⁴⁸,
 E. Monnier ¹⁰¹, L. Monsonis Romero ¹⁶¹, J. Montejo Berlingen ³⁶, M. Montella ¹¹⁸,
 F. Monticelli ⁸⁹, N. Morange ⁶⁶, A.L. Moreira De Carvalho ^{129a}, M. Moreno Llácer ¹⁶¹,
 C. Moreno Martinez ¹³, P. Morettini ^{57b}, S. Morgenstern ¹⁶⁵, M. Morii ⁶¹, M. Morinaga ¹⁵²,
 V. Morisbak ¹²⁴, A.K. Morley ³⁶, F. Morodei ^{74a,74b}, L. Morvaj ³⁶, P. Moschovakos ³⁶,
 B. Moser ³⁶, M. Mosidze ^{148b}, T. Moskalets ⁵⁴, P. Moskvitina ¹¹², J. Moss ^{31,n}, E.J.W. Moyses ¹⁰²,
 S. Muanza ¹⁰¹, J. Mueller ¹²⁸, D. Muenstermann ⁹⁰, R. Müller ¹⁹, G.A. Mullier ⁹⁷, J.J. Mullin ¹²⁷,

D.P. Mungo [id70a,70b](#), J.L. Munoz Martinez [id13](#), D. Munoz Perez [id161](#), F.J. Munoz Sanchez [id100](#),
 M. Murin [id100](#), W.J. Murray [id165,133](#), A. Murrone [id70a,70b](#), J.M. Muse [id119](#), M. Muškinja [id17a](#),
 C. Mwewa [id29](#), A.G. Myagkov [id37,a](#), A.J. Myers [id8](#), A.A. Myers [id128](#), G. Myers [id67](#), M. Myska [id131](#),
 B.P. Nachman [id17a](#), O. Nackenhorst [id49](#), A.Nag Nag [id50](#), K. Nagai [id125](#), K. Nagano [id82](#),
 J.L. Nagle [id29,ad](#), E. Nagy [id101](#), A.M. Nairz [id36](#), Y. Nakahama [id82](#), K. Nakamura [id82](#), H. Nanjo [id123](#),
 R. Narayan [id44](#), E.A. Narayanan [id111](#), I. Naryshkin [id37](#), M. Naseri [id34](#), C. Nass [id24](#), G. Navarro [id22a](#),
 J. Navarro-Gonzalez [id161](#), R. Nayak [id150](#), A. Nayaz [id18](#), P.Y. Nechaeva [id37](#), F. Nechansky [id48](#),
 L. Nedic [id125](#), T.J. Neep [id20](#), A. Negri [id72a,72b](#), M. Negrini [id23b](#), C. Nellist [id112](#), C. Nelson [id103](#),
 K. Nelson [id105](#), S. Nemecek [id130](#), M. Nessi [id36,g](#), M.S. Neubauer [id160](#), F. Neuhaus [id99](#),
 J. Neundorf [id48](#), R. Newhouse [id162](#), P.R. Newman [id20](#), C.W. Ng [id128](#), Y.S. Ng [id18](#), Y.W.Y. Ng [id158](#),
 B. Ngair [id35e](#), H.D.N. Nguyen [id107](#), R.B. Nickerson [id125](#), R. Nicolaidou [id134](#), J. Nielsen [id135](#),
 M. Niemeyer [id55](#), N. Nikiiforou [id36](#), V. Nikolaenko [id37,a](#), I. Nikolic-Audit [id126](#), K. Nikolopoulos [id20](#),
 P. Nilsson [id29](#), H.R. Nindhito [id56](#), A. Nisati [id74a](#), N. Nishu [id2](#), R. Nisius [id109](#), J-E. Nitschke [id50](#),
 E.K. Nkadimeng [id33g](#), S.J. Noacco Rosende [id89](#), T. Nobe [id152](#), D.L. Noel [id32](#), Y. Noguchi [id86](#),
 T. Nommensen [id146](#), M.A. Nomura [id29](#), M.B. Norfolk [id138](#), R.R.B. Norisam [id95](#), B.J. Norman [id34](#),
 J. Novak [id92](#), T. Novak [id48](#), O. Novgorodova [id50](#), L. Novotny [id131](#), R. Novotny [id111](#), L. Nozka [id121](#),
 K. Ntekas [id158](#), E. Nurse [id95](#), F.G. Oakham [id34,aa](#), J. Ocariz [id126](#), A. Ochi [id83](#), I. Ochoa [id129a](#),
 S. Oerdek [id159](#), A. Ogradnik [id84a](#), A. Oh [id100](#), C.C. Ohm [id143](#), H. Oide [id153](#), R. Oishi [id152](#),
 M.L. Ojeda [id48](#), Y. Okazaki [id86](#), M.W. O'Keefe [id91](#), Y. Okumura [id152](#), A. Olariu [id27b](#),
 L.F. Oleiro Seabra [id129a](#), S.A. Olivares Pino [id136e](#), D. Oliveira Damazio [id29](#), D. Oliveira Goncalves [id81a](#),
 J.L. Oliver [id158](#), M.J.R. Olsson [id158](#), A. Olszewski [id85](#), J. Olszowska [id85,*](#), Ö.O. Öncel [id54](#),
 D.C. O'Neil [id141](#), A.P. O'Neill [id19](#), A. Onofre [id129a,129e](#), P.U.E. Onyisi [id11](#), M.J. Oreglia [id39](#),
 G.E. Orellana [id89](#), D. Orestano [id76a,76b](#), N. Orlando [id13](#), R.S. Orr [id154](#), V. O'Shea [id59](#),
 R. Ospanov [id62a](#), G. Otero y Garzon [id30](#), H. Otono [id88](#), P.S. Ott [id63a](#), G.J. Ottino [id17a](#), M. Ouchrif [id35d](#),
 J. Ouellette [id29,ad](#), F. Ould-Saada [id124](#), M. Owen [id59](#), R.E. Owen [id133](#), K.Y. Oyulmaz [id21a](#),
 V.E. Ozcan [id21a](#), N. Ozturk [id8](#), S. Ozturk [id21d](#), J. Pacalt [id121](#), H.A. Pacey [id32](#), K. Pachal [id51](#),
 A. Pacheco Pages [id13](#), C. Padilla Aranda [id13](#), G. Padovano [id74a,74b](#), S. Pagan Griso [id17a](#),
 G. Palacino [id67](#), A. Palazzo [id69a,69b](#), S. Palazzo [id52](#), S. Palestini [id36](#), M. Palka [id84b](#), J. Pan [id170](#),
 T. Pan [id64a](#), D.K. Panchal [id11](#), C.E. Pandini [id113](#), J.G. Panduro Vazquez [id94](#), H. Pang [id14b](#), P. Pani [id48](#),
 G. Panizzo [id68a,68c](#), L. Paolozzi [id56](#), C. Papadatos [id107](#), S. Parajuli [id44](#), A. Paramonov [id6](#),
 C. Paraskevopoulos [id10](#), D. Paredes Hernandez [id64b](#), T.H. Park [id154](#), M.A. Parker [id32](#), F. Parodi [id57b,57a](#),
 E.W. Parrish [id114](#), V.A. Parrish [id52](#), J.A. Parsons [id41](#), U. Parzefall [id54](#), B. Pascual Dias [id107](#),
 L. Pascual Dominguez [id150](#), V.R. Pascuzzi [id17a](#), F. Pasquali [id113](#), E. Pasqualucci [id74a](#), S. Passaggio [id57b](#),
 F. Pastore [id94](#), P. Pasuwan [id47a,47b](#), P. Patel [id85](#), J.R. Pater [id100](#), J. Patton [id91](#), T. Pauly [id36](#),
 J. Pearkes [id142](#), M. Pedersen [id124](#), R. Pedro [id129a](#), S.V. Peleganchuk [id37](#), O. Penc [id36](#), E.A. Pender [id52](#),
 C. Peng [id64b](#), H. Peng [id62a](#), K.E. Penski [id108](#), M. Penzin [id37](#), B.S. Peralva [id81d,81d](#),
 A.P. Pereira Peixoto [id60](#), L. Pereira Sanchez [id47a,47b](#), D.V. Perepelitsa [id29,ad](#), E. Perez Codina [id155a](#),
 M. Perganti [id10](#), L. Perini [id70a,70b,*](#), H. Pernegger [id36](#), S. Perrella [id36](#), A. Perrevoort [id112](#), O. Perrin [id40](#),
 K. Peters [id48](#), R.F.Y. Peters [id100](#), B.A. Petersen [id36](#), T.C. Petersen [id42](#), E. Petit [id101](#), V. Petousis [id131](#),
 C. Petridou [id151](#), A. Petrukhin [id140](#), M. Pettee [id17a](#), N.E. Pettersson [id36](#), A. Petukhov [id37](#),
 K. Petukhova [id132](#), A. Peyaud [id134](#), R. Pezoa [id136f](#), L. Pezzotti [id36](#), G. Pezzullo [id170](#), T.M. Pham [id168](#),
 T. Pham [id104](#), P.W. Phillips [id133](#), M.W. Phipps [id160](#), G. Piacquadio [id144](#), E. Pianori [id17a](#),
 F. Piazza [id70a,70b](#), R. Piegai [id30](#), D. Pietreanu [id27b](#), A.D. Pilkington [id100](#), M. Pinamonti [id68a,68c](#),
 J.L. Pinfeld [id2](#), B.C. Pinheiro Pereira [id129a](#), C. Pitman Donaldson [id95](#), D.A. Pizzi [id34](#),
 L. Pizzimento [id75a,75b](#), A. Pizzini [id113](#), M.-A. Pleier [id29](#), V. Plesanovs [id54](#), V. Pleskot [id132](#),
 E. Plotnikova [id38](#), G. Poddar [id4](#), R. Poettgen [id97](#), L. Poggioli [id126](#), I. Pogrebnyak [id106](#), D. Pohl [id24](#),
 I. Pokharel [id55](#), S. Polacek [id132](#), G. Polesello [id72a](#), A. Poley [id141,155a](#), R. Polifka [id131](#), A. Polini [id23b](#),

C.S. Pollard ¹²⁵, Z.B. Pollock ¹¹⁸, V. Polychronakos ²⁹, E. Pompa Pacchi ^{74a,74b}, D. Ponomarenko ³⁷,
 L. Pontecorvo ³⁶, S. Popa ^{27a}, G.A. Popeneciu ^{27d}, D.M. Portillo Quintero ^{155a}, S. Pospisil ¹³¹,
 P. Postolache ^{27c}, K. Potamianos ¹²⁵, I.N. Potrap ³⁸, C.J. Potter ³², H. Potti ¹, T. Poulsen ⁴⁸,
 J. Poveda ¹⁶¹, M.E. Pozo Astigarraga ³⁶, A. Prades Ibanez ¹⁶¹, M.M. Prapa ⁴⁶, D. Price ¹⁰⁰,
 M. Primavera ^{69a}, M.A. Principe Martin ⁹⁸, M.L. Proffitt ¹³⁷, N. Proklova ¹²⁷, K. Prokofiev ^{64c},
 G. Proto ^{75a,75b}, S. Protopopescu ²⁹, J. Proudfoot ⁶, M. Przybycien ^{84a}, J.E. Puddefoot ¹³⁸,
 D. Pudzha ³⁷, P. Puzo ⁶⁶, D. Pyatiiizbyantseva ³⁷, J. Qian ¹⁰⁵, Y. Qin ¹⁰⁰, T. Qiu ⁹³, A. Quadt ⁵⁵,
 M. Queitsch-Maitland ¹⁰⁰, G. Quetant ⁵⁶, G. Rabanal Bolanos ⁶¹, D. Rafanoharana ⁵⁴,
 F. Ragusa ^{70a,70b}, J.L. Rainbolt ³⁹, J.A. Raine ⁵⁶, S. Rajagopalan ²⁹, E. Ramakoti ³⁷,
 K. Ran ^{48,14d}, V. Raskina ¹²⁶, D.F. Rassloff ^{63a}, S. Rave ⁹⁹, B. Ravina ⁵⁵, I. Ravinovich ¹⁶⁷,
 M. Raymond ³⁶, A.L. Read ¹²⁴, N.P. Readioff ¹³⁸, D.M. Rebutzi ^{72a,72b}, G. Redlinger ²⁹,
 K. Reeves ⁴⁵, J.A. Reidelsturz ¹⁶⁹, D. Reikher ¹⁵⁰, A. Reiss ⁹⁹, A. Rej ¹⁴⁰, C. Rembser ³⁶,
 A. Renardi ⁴⁸, M. Renda ^{27b}, M.B. Rendel ¹⁰⁹, A.G. Rennie ⁵⁹, S. Resconi ^{70a},
 M. Ressegotti ^{57b,57a}, E.D. Resseguie ^{17a}, S. Rettie ⁹⁵, B. Reynolds ¹¹⁸, E. Reynolds ^{17a},
 M. Rezaei Estabragh ¹⁶⁹, O.L. Rezanova ³⁷, P. Reznicek ¹³², E. Ricci ^{77a,77b}, R. Richter ¹⁰⁹,
 S. Richter ^{47a,47b}, E. Richter-Was ^{84b}, M. Ridel ¹²⁶, P. Rieck ¹¹⁶, P. Riedler ³⁶,
 M. Rijssenbeek ¹⁴⁴, A. Rimoldi ^{72a,72b}, M. Rimoldi ⁴⁸, L. Rinaldi ^{23b,23a}, T.T. Rinn ²⁹,
 M.P. Rinnagel ¹⁰⁸, G. Ripellino ¹⁴³, I. Riu ¹³, P. Rivadeneira ⁴⁸, J.C. Rivera Vergara ¹⁶³,
 F. Rizatdinova ¹²⁰, E. Rizvi ⁹³, C. Rizzi ⁵⁶, B.A. Roberts ¹⁶⁵, B.R. Roberts ^{17a},
 S.H. Robertson ^{103,v}, M. Robin ⁴⁸, D. Robinson ³², C.M. Robles Gajardo ^{136f},
 M. Robles Manzano ⁹⁹, A. Robson ⁵⁹, A. Rocchi ^{75a,75b}, C. Roda ^{73a,73b}, S. Rodriguez Bosca ^{63a},
 Y. Rodriguez Garcia ^{22a}, A. Rodriguez Rodriguez ⁵⁴, A.M. Rodríguez Vera ^{155b}, S. Roe ³⁶,
 J.T. Roemer ¹⁵⁸, A.R. Roepe-Gier ¹¹⁹, J. Roggel ¹⁶⁹, O. Röhne ¹²⁴, R.A. Rojas ¹⁶³, B. Roland ⁵⁴,
 C.P.A. Roland ⁶⁷, J. Roloff ²⁹, A. Romaniouk ³⁷, E. Romano ^{72a,72b}, M. Romano ^{23b},
 A.C. Romero Hernandez ¹⁶⁰, N. Rompotis ⁹¹, L. Roos ¹²⁶, S. Rosati ^{74a}, B.J. Rosser ³⁹,
 E. Rossi ⁴, E. Rossi ^{71a,71b}, L.P. Rossi ^{57b}, L. Rossini ⁴⁸, R. Rosten ¹¹⁸, M. Rotaru ^{27b},
 B. Rottler ⁵⁴, D. Rousseau ⁶⁶, D. Rousso ³², G. Rovelli ^{72a,72b}, A. Roy ¹⁶⁰, A. Rozanov ¹⁰¹,
 Y. Rozen ¹⁴⁹, X. Ruan ^{33g}, A. Rubio Jimenez ¹⁶¹, A.J. Ruby ⁹¹, V.H. Ruelas Rivera ¹⁸,
 T.A. Ruggeri ¹, F. Rühr ⁵⁴, A. Ruiz-Martinez ¹⁶¹, A. Rummler ³⁶, Z. Rurikova ⁵⁴,
 N.A. Rusakovich ³⁸, H.L. Russell ¹⁶³, J.P. Rutherford ⁷, K. Rybacki ⁹⁰, M. Rybar ¹³²,
 E.B. Rye ¹²⁴, A. Ryzhov ³⁷, J.A. Sabater Iglesias ⁵⁶, P. Sabatini ¹⁶¹, L. Sabetta ^{74a,74b},
 H.F.W. Sadrozinski ¹³⁵, F. Safai Tehrani ^{74a}, B. Safarzadeh Samani ¹⁴⁵, M. Safdari ¹⁴²,
 S. Saha ¹⁰³, M. Sahinsky ¹⁰⁹, M. Saimpert ¹³⁴, M. Saito ¹⁵², T. Saito ¹⁵², D. Salamani ³⁶,
 G. Salamanna ^{76a,76b}, A. Salnikov ¹⁴², J. Salt ¹⁶¹, A. Salvador Salas ¹³, D. Salvatore ^{43b,43a},
 F. Salvatore ¹⁴⁵, A. Salzburger ³⁶, D. Sammel ⁵⁴, D. Sampsonidis ¹⁵¹, D. Sampsonidou ^{62d,62c},
 J. Sánchez ¹⁶¹, A. Sanchez Pineda ⁴, V. Sanchez Sebastian ¹⁶¹, H. Sandaker ¹²⁴, C.O. Sander ⁴⁸,
 J.A. Sandesara ¹⁰², M. Sandhoff ¹⁶⁹, C. Sandoval ^{22b}, D.P.C. Sankey ¹³³, A. Sansoni ⁵³,
 L. Santi ^{74a,74b}, C. Santoni ⁴⁰, H. Santos ^{129a,129b}, S.N. Santpur ^{17a}, A. Santra ¹⁶⁷,
 K.A. Saoucha ¹³⁸, J.G. Saraiva ^{129a,129d}, J. Sardain ⁷, O. Sasaki ⁸², K. Sato ¹⁵⁶, C. Sauer ^{63b},
 F. Sauerburger ⁵⁴, E. Sauvan ⁴, P. Savard ^{154,aa}, R. Sawada ¹⁵², C. Sawyer ¹³³, L. Sawyer ⁹⁶,
 I. Sayago Galvan ¹⁶¹, C. Sbarra ^{23b}, A. Sbrizzi ^{23b,23a}, T. Scanlon ⁹⁵, J. Schaarschmidt ¹³⁷,
 P. Schacht ¹⁰⁹, D. Schaefer ³⁹, U. Schäfer ⁹⁹, A.C. Schaffer ⁶⁶, D. Schaile ¹⁰⁸,
 R.D. Schamberger ¹⁴⁴, E. Schanet ¹⁰⁸, C. Scharf ¹⁸, V.A. Schegelsky ³⁷, D. Scheirich ¹³²,
 F. Schenck ¹⁸, M. Schernau ¹⁵⁸, C. Scheulen ⁵⁵, C. Schiavi ^{57b,57a}, Z.M. Schillaci ²⁶,
 E.J. Schioppa ^{69a,69b}, M. Schioppa ^{43b,43a}, B. Schlag ⁹⁹, K.E. Schleicher ⁵⁴, S. Schlenker ³⁶,
 K. Schmieden ⁹⁹, C. Schmitt ⁹⁹, S. Schmitt ⁴⁸, L. Schoeffel ¹³⁴, A. Schoening ^{63b},
 P.G. Scholer ⁵⁴, E. Schopf ¹²⁵, M. Schott ⁹⁹, J. Schovancova ³⁶, S. Schramm ⁵⁶,

F. Schroeder ¹⁶⁹, H-C. Schultz-Coulon ^{63a}, M. Schumacher ⁵⁴, B.A. Schumm ¹³⁵, Ph. Schune ¹³⁴, A. Schwartzman ¹⁴², T.A. Schwarz ¹⁰⁵, Ph. Schwemling ¹³⁴, R. Schvienhorst ¹⁰⁶, A. Sciandra ¹³⁵, G. Sciolla ²⁶, F. Scuri ^{73a}, F. Scutti ¹⁰⁴, C.D. Sebastiani ⁹¹, K. Sedlaczek ⁴⁹, P. Seema ¹⁸, S.C. Seidel ¹¹¹, A. Seiden ¹³⁵, B.D. Seidlitz ⁴¹, T. Seiss ³⁹, C. Seitz ⁴⁸, J.M. Seixas ^{81b}, G. Sekhniaidze ^{71a}, S.J. Sekula ⁴⁴, L. Selem ⁴, N. Semprini-Cesari ^{23b,23a}, S. Sen ⁵¹, D. Sengupta ⁵⁶, V. Senthilkumar ¹⁶¹, L. Serin ⁶⁶, L. Serkin ^{68a,68b}, M. Sessa ^{76a,76b}, H. Severini ¹¹⁹, S. Sevova ¹⁴², F. Sforza ^{57b,57a}, A. Sfyrla ⁵⁶, E. Shabalina ⁵⁵, R. Shaheen ¹⁴³, J.D. Shahinian ¹²⁷, N.W. Shaikh ^{47a,47b}, D. Shaked Renous ¹⁶⁷, L.Y. Shan ^{14a}, M. Shapiro ^{17a}, A. Sharma ³⁶, A.S. Sharma ¹⁶², P. Sharma ⁷⁹, S. Sharma ⁴⁸, P.B. Shatalov ³⁷, K. Shaw ¹⁴⁵, S.M. Shaw ¹⁰⁰, Q. Shen ^{62c,5}, P. Sherwood ⁹⁵, L. Shi ⁹⁵, C.O. Shimmin ¹⁷⁰, Y. Shimogama ¹⁶⁶, J.D. Shinner ⁹⁴, I.P.J. Shipsey ¹²⁵, S. Shirabe ⁶⁰, M. Shiyakova ³⁸, J. Shlomi ¹⁶⁷, M.J. Shochet ³⁹, J. Shojaii ¹⁰⁴, D.R. Shope ¹²⁴, S. Shrestha ^{118,ae}, E.M. Shrif ^{33g}, M.J. Shroff ¹⁶³, P. Sicho ¹³⁰, A.M. Sickles ¹⁶⁰, E. Sideras Haddad ^{33g}, A. Sidoti ^{23b}, F. Siegert ⁵⁰, Dj. Sijacki ¹⁵, R. Sikora ^{84a}, F. Sili ⁸⁹, J.M. Silva ²⁰, M.V. Silva Oliveira ³⁶, S.B. Silverstein ^{47a}, S. Simion ⁶⁶, R. Simoniello ³⁶, E.L. Simpson ⁵⁹, N.D. Simpson ⁹⁷, S. Simsek ^{21d}, S. Sindhu ⁵⁵, P. Sinervo ¹⁵⁴, V. Sinetckii ³⁷, S. Singh ¹⁴¹, S. Singh ¹⁵⁴, S. Sinha ⁴⁸, S. Sinha ^{33g}, M. Sioli ^{23b,23a}, I. Siral ¹²², S.Yu. Sivoklov ^{37,*}, J. Sjölin ^{47a,47b}, A. Skaf ⁵⁵, E. Skorda ⁹⁷, P. Skubic ¹¹⁹, M. Slawinska ⁸⁵, V. Smakhtin ¹⁶⁷, B.H. Smart ¹³³, J. Smiesko ³⁶, S.Yu. Smirnov ³⁷, Y. Smirnov ³⁷, L.N. Smirnova ^{37,a}, O. Smirnova ⁹⁷, A.C. Smith ⁴¹, E.A. Smith ³⁹, H.A. Smith ¹²⁵, J.L. Smith ⁹¹, R. Smith ¹⁴², M. Smizanska ⁹⁰, K. Smolek ¹³¹, A. Smykiewicz ⁸⁵, A.A. Snegarev ³⁷, H.L. Snoek ¹¹³, S. Snyder ²⁹, R. Sobie ^{163,v}, A. Soffer ¹⁵⁰, C.A. Solans Sanchez ³⁶, E.Yu. Soldatov ³⁷, U. Soldevila ¹⁶¹, A.A. Solodkov ³⁷, S. Solomon ⁵⁴, A. Soloshenko ³⁸, K. Solovieva ⁵⁴, O.V. Solovyanov ³⁷, V. Solovyev ³⁷, P. Sommer ³⁶, A. Sonay ¹³, W.Y. Song ^{155b}, A. Sopczak ¹³¹, A.L. Soppio ⁹⁵, F. Sopkova ^{28b}, V. Sothilingam ^{63a}, S. Sottocornola ^{72a,72b}, R. Soualah ^{115c}, Z. Soumami ^{35e}, D. South ⁴⁸, S. Spagnolo ^{69a,69b}, M. Spalla ¹⁰⁹, F. Spanò ⁹⁴, D. Sperlich ⁵⁴, G. Spigo ³⁶, M. Spina ¹⁴⁵, S. Spinalli ⁹⁰, D.P. Spiteri ⁵⁹, M. Spousta ¹³², E.J. Staats ³⁴, A. Stabile ^{70a,70b}, R. Stamen ^{63a}, M. Stamenkovic ¹¹³, A. Stampekis ²⁰, M. Standke ²⁴, E. Stanecka ⁸⁵, M.V. Stange ⁵⁰, B. Stanislaus ^{17a}, M.M. Stanitzki ⁴⁸, M. Stankaityte ¹²⁵, B. Stapf ⁴⁸, E.A. Starchenko ³⁷, G.H. Stark ¹³⁵, J. Stark ¹⁰¹, D.M. Starke ^{155b}, P. Staroba ¹³⁰, P. Starovoitov ^{63a}, S. Stärz ¹⁰³, R. Staszewski ⁸⁵, G. Stavropoulos ⁴⁶, J. Steentoft ¹⁵⁹, P. Steinberg ²⁹, A.L. Steinhebel ¹²², B. Stelzer ^{141,155a}, H.J. Stelzer ¹²⁸, O. Stelzer-Chilton ^{155a}, H. Stenzel ⁵⁸, T.J. Stevenson ¹⁴⁵, G.A. Stewart ³⁶, M.C. Stockton ³⁶, G. Stoicea ^{27b}, M. Stolarski ^{129a}, S. Stonjek ¹⁰⁹, A. Straessner ⁵⁰, J. Strandberg ¹⁴³, S. Strandberg ^{47a,47b}, M. Strauss ¹¹⁹, T. Streblner ¹⁰¹, P. Strizenec ^{28b}, R. Ströhmer ¹⁶⁴, D.M. Strom ¹²², L.R. Strom ⁴⁸, R. Stroynowski ⁴⁴, A. Strubig ^{47a,47b}, S.A. Stucci ²⁹, B. Stugu ¹⁶, J. Stupak ¹¹⁹, N.A. Styles ⁴⁸, D. Su ¹⁴², S. Su ^{62a}, W. Su ^{62d,137,62c}, X. Su ^{62a,66}, K. Sugizaki ¹⁵², V.V. Sulim ³⁷, M.J. Sullivan ⁹¹, D.M.S. Sultan ^{77a,77b}, L. Sultanaliyeva ³⁷, S. Sultansoy ^{3b}, T. Sumida ⁸⁶, S. Sun ¹⁰⁵, S. Sun ¹⁶⁸, O. Sunneborn Gudnadottir ¹⁵⁹, M.R. Sutton ¹⁴⁵, M. Svatos ¹³⁰, M. Swiatlowski ^{155a}, T. Swirski ¹⁶⁴, I. Sykora ^{28a}, M. Sykora ¹³², T. Sykora ¹³², D. Ta ⁹⁹, K. Tackmann ^{48,u}, A. Taffard ¹⁵⁸, R. Tafirout ^{155a}, J.S. Tafoya Vargas ⁶⁶, R.H.M. Taibah ¹²⁶, R. Takashima ⁸⁷, K. Takeda ⁸³, E.P. Takeva ⁵², Y. Takubo ⁸², M. Talby ¹⁰¹, A.A. Talyshv ³⁷, K.C. Tam ^{64b}, N.M. Tamir ¹⁵⁰, A. Tanaka ¹⁵², J. Tanaka ¹⁵², R. Tanaka ⁶⁶, M. Tanasini ^{57b,57a}, J. Tang ^{62c}, Z. Tao ¹⁶², S. Tapia Araya ⁸⁰, S. Tapprogge ⁹⁹, A. Tarek Abouelfadl Mohamed ¹⁰⁶, S. Tarem ¹⁴⁹, K. Tariq ^{62b}, G. Tarna ^{27b}, G.F. Tartarelli ^{70a}, P. Tas ¹³², M. Tasevsky ¹³⁰, E. Tassi ^{43b,43a}, A.C. Tate ¹⁶⁰, G. Tateno ¹⁵², Y. Tayalati ^{35e}, G.N. Taylor ¹⁰⁴, W. Taylor ^{155b}, H. Teagle ⁹¹, A.S. Tee ¹⁶⁸, R. Teixeira De Lima ¹⁴², P. Teixeira-Dias ⁹⁴, J.J. Teoh ¹⁵⁴,

K. Terashi ¹⁵², J. Terron ⁹⁸, S. Terzo ¹³, M. Testa ⁵³, R.J. Teuscher ^{154,v}, A. Thaler ⁷⁸,
 O. Theiner ⁵⁶, N. Themistokleous ⁵², T. Thevenaux-Pelzer ¹⁸, O. Thielmann ¹⁶⁹, D.W. Thomas⁹⁴,
 J.P. Thomas ²⁰, E.A. Thompson ⁴⁸, P.D. Thompson ²⁰, E. Thomson ¹²⁷, E.J. Thorpe ⁹³,
 Y. Tian ⁵⁵, V. Tikhomirov ^{37,a}, Yu.A. Tikhonov ³⁷, S. Timoshenko³⁷, E.X.L. Ting ¹, P. Tipton ¹⁷⁰,
 S. Tisserant ¹⁰¹, S.H. Tlou ^{33g}, A. Tnourji ⁴⁰, K. Todome ^{23b,23a}, S. Todorova-Nova ¹³², S. Todt⁵⁰,
 M. Togawa ⁸², J. Tojo ⁸⁸, S. Tokár ^{28a}, K. Tokushuku ⁸², R. Tombs ³², M. Tomoto ^{82,110},
 L. Tompkins ¹⁴², K.W. Topolnicki ^{84b}, P. Tornambe ¹⁰², E. Torrence ¹²², H. Torres ⁵⁰,
 E. Torró Pastor ¹⁶¹, M. Toscani ³⁰, C. Tosciri ³⁹, D.R. Tovey ¹³⁸, A. Traeet¹⁶, I.S. Trandafir ^{27b},
 T. Trefzger ¹⁶⁴, A. Tricoli ²⁹, I.M. Trigger ^{155a}, S. Trincaz-Duvoid ¹²⁶, D.A. Trischuk ²⁶,
 B. Trocmé ⁶⁰, A. Trofymov ⁶⁶, C. Troncon ^{70a}, L. Truong ^{33c}, M. Trzebinski ⁸⁵, A. Trzupiek ⁸⁵,
 F. Tsai ¹⁴⁴, M. Tsai ¹⁰⁵, A. Tsiamis ¹⁵¹, P.V. Tsiarehka³⁷, S. Tsigaridas ^{155a}, A. Tsigotis ^{151,s},
 V. Tsiskaridze ¹⁴⁴, E.G. Tskhadadze^{148a}, M. Tsopoulou ¹⁵¹, Y. Tsujikawa ⁸⁶, I.I. Tsukerman ³⁷,
 V. Tsulaia ^{17a}, S. Tsuno ⁸², O. Tsur¹⁴⁹, D. Tsybychev ¹⁴⁴, Y. Tu ^{64b}, A. Tudorache ^{27b},
 V. Tudorache ^{27b}, A.N. Tuna ³⁶, S. Turchikhin ³⁸, I. Turk Cakir ^{3a}, R. Turra ^{70a}, T. Turtuvshin ³⁸,
 P.M. Tuts ⁴¹, S. Tzamarias ¹⁵¹, P. Tzani ¹⁰, E. Tzovara ⁹⁹, K. Uchida¹⁵², F. Ukegawa ¹⁵⁶,
 P.A. Ulloa Poblete ^{136c}, G. Unal ³⁶, M. Unal ¹¹, A. Undrus ²⁹, G. Unel ¹⁵⁸, J. Urban ^{28b},
 P. Urquijo ¹⁰⁴, G. Usai ⁸, R. Ushioda ¹⁵³, M. Usman ¹⁰⁷, Z. Uysal ^{21b}, V. Vacek ¹³¹,
 B. Vachon ¹⁰³, K.O.H. Vadla ¹²⁴, T. Vafeiadis ³⁶, C. Valderanis ¹⁰⁸, E. Valdes Santurio ^{47a,47b},
 M. Valente ^{155a}, S. Valentinetti ^{23b,23a}, A. Valero ¹⁶¹, A. Vallier ¹⁰¹, J.A. Valls Ferrer ¹⁶¹,
 T.R. Van Daalen ¹³⁷, P. Van Gemmeren ⁶, M. Van Rijnbach ^{124,36}, S. Van Stroud ⁹⁵,
 I. Van Vulpen ¹¹³, M. Vanadia ^{75a,75b}, W. Vandelli ³⁶, M. Vandenbroucke ¹³⁴, E.R. Vandewall ¹²⁰,
 D. Vannicola ¹⁵⁰, L. Vannoli ^{57b,57a}, R. Vari ^{74a}, E.W. Varnes ⁷, C. Varni ^{17a}, T. Varol ¹⁴⁷,
 D. Varouchas ⁶⁶, L. Varriale ¹⁶¹, K.E. Varvell ¹⁴⁶, M.E. Vasile ^{27b}, L. Vaslin⁴⁰, G.A. Vasquez ¹⁶³,
 F. Vazeille ⁴⁰, T. Vazquez Schroeder ³⁶, J. Veatch ³¹, V. Vecchio ¹⁰⁰, M.J. Veen ¹⁰²,
 I. Veliscek ¹²⁵, L.M. Veloce ¹⁵⁴, F. Veloso ^{129a,129c}, S. Veneziano ^{74a}, A. Ventura ^{69a,69b},
 A. Verbytskyi ¹⁰⁹, M. Verducci ^{73a,73b}, C. Vergis ²⁴, M. Verissimo De Araujo ^{81b},
 W. Verkerke ¹¹³, J.C. Vermeulen ¹¹³, C. Vernieri ¹⁴², P.J. Verschuuren ⁹⁴, M. Vessella ¹⁰²,
 M.C. Vetterli ^{141,aa}, A. Vgenopoulos ¹⁵¹, N. Viaux Maira ^{136f}, T. Vickey ¹³⁸,
 O.E. Vickey Boeriu ¹³⁸, G.H.A. Viehhauser ¹²⁵, L. Viganì ^{63b}, M. Villa ^{23b,23a},
 M. Villaplana Perez ¹⁶¹, E.M. Villhauer⁵², E. Vilucchi ⁵³, M.G. Vincter ³⁴, G.S. Virdee ²⁰,
 A. Vishwakarma ⁵², C. Vittori ^{23b,23a}, I. Vivarelli ¹⁴⁵, V. Vladimirov¹⁶⁵, E. Voevodina ¹⁰⁹,
 F. Vogel ¹⁰⁸, P. Vokac ¹³¹, J. Von Ahnen ⁴⁸, E. Von Toerne ²⁴, B. Vormwald ³⁶, V. Vorobel ¹³²,
 K. Vorobev ³⁷, M. Vos ¹⁶¹, J.H. Vosseveld ⁹¹, M. Vozak ¹¹³, L. Vozdecky ⁹³, N. Vranjes ¹⁵,
 M. Vranjes Milosavljevic ¹⁵, M. Vreeswijk ¹¹³, R. Vuillermet ³⁶, O. Vujanovic ⁹⁹, I. Vukotic ³⁹,
 S. Wada ¹⁵⁶, C. Wagner¹⁰², W. Wagner ¹⁶⁹, S. Wahdan ¹⁶⁹, H. Wahlberg ⁸⁹, R. Wakasa ¹⁵⁶,
 M. Wakida ¹¹⁰, V.M. Walbrecht ¹⁰⁹, J. Walder ¹³³, R. Walker ¹⁰⁸, W. Walkowiak ¹⁴⁰,
 A.M. Wang ⁶¹, A.Z. Wang ¹⁶⁸, C. Wang ^{62a}, C. Wang ^{62c}, H. Wang ^{17a}, J. Wang ^{64a},
 P. Wang ⁴⁴, R.-J. Wang ⁹⁹, R. Wang ⁶¹, R. Wang ⁶, S.M. Wang ¹⁴⁷, S. Wang ^{62b}, T. Wang ^{62a},
 W.T. Wang ⁷⁹, W.X. Wang ^{62a}, X. Wang ^{14c}, X. Wang ¹⁶⁰, X. Wang ^{62c}, Y. Wang ^{62d},
 Y. Wang ^{14c}, Z. Wang ¹⁰⁵, Z. Wang ^{62d,51,62c}, Z. Wang ¹⁰⁵, A. Warburton ¹⁰³, R.J. Ward ²⁰,
 N. Warrack ⁵⁹, A.T. Watson ²⁰, M.F. Watson ²⁰, G. Watts ¹³⁷, B.M. Waugh ⁹⁵, A.F. Webb ¹¹,
 C. Weber ²⁹, M.S. Weber ¹⁹, S.M. Weber ^{63a}, C. Wei^{62a}, Y. Wei ¹²⁵, A.R. Weidberg ¹²⁵,
 J. Weingarten ⁴⁹, M. Weirich ⁹⁹, C. Weiser ⁵⁴, C.J. Wells ⁴⁸, T. Wenaus ²⁹, B. Wendland ⁴⁹,
 T. Wengler ³⁶, N.S. Wenke¹⁰⁹, N. Wermes ²⁴, M. Wessels ^{63a}, K. Whalen ¹²², A.M. Wharton ⁹⁰,
 A.S. White ⁶¹, A. White ⁸, M.J. White ¹, D. Whiteson ¹⁵⁸, L. Wickremasinghe ¹²³,
 W. Wiedenmann ¹⁶⁸, C. Wiel ⁵⁰, M. Wielers ¹³³, N. Wieseotte⁹⁹, C. Wiglesworth ⁴²,
 L.A.M. Wiik-Fuchs ⁵⁴, D.J. Wilbern¹¹⁹, H.G. Wilkens ³⁶, D.M. Williams ⁴¹, H.H. Williams¹²⁷,

S. Williams , S. Willocq , P.J. Windischhofer , F. Winklmeier , B.T. Winter , M. Wittgen , M. Wobisch , R. Wölker , J. Wollrath , M.W. Wolter , H. Wolters , V.W.S. Wong , A.F. Wongel , S.D. Worm , B.K. Wosiek , K.W. Woźniak , K. Wraight , J. Wu , M. Wu , M. Wu , S.L. Wu , X. Wu , Y. Wu , Z. Wu , J. Wuerzinger , T.R. Wyatt , B.M. Wynne , S. Xella , L. Xia , M. Xia , J. Xiang , X. Xiao , M. Xie , X. Xie , J. Xiong , I. Xiotidis , D. Xu , H. Xu , H. Xu , L. Xu , R. Xu , T. Xu , W. Xu , Y. Xu , Z. Xu , Z. Xu , B. Yabsley , S. Yacoub , N. Yamaguchi , Y. Yamaguchi , H. Yamauchi , T. Yamazaki , Y. Yamazaki , J. Yan , S. Yan , Z. Yan , H.J. Yang , H.T. Yang , S. Yang , T. Yang , X. Yang , X. Yang , Y. Yang , Z. Yang , W.-M. Yao , Y.C. Yap , H. Ye , J. Ye , S. Ye , X. Ye , Y. Yeh , I. Yeletsikh , M.R. Yexley , P. Yin , K. Yorita , C.J.S. Young , C. Young , M. Yuan , R. Yuan , L. Yue , X. Yue , M. Zaazoua , B. Zabinski , E. Zaid , T. Zakareishvili , N. Zakharchuk , S. Zambito , J.A. Zamora Saa , J. Zang , D. Zanzi , O. Zaplatilek , S.V. Zeibner , C. Zeitnitz , J.C. Zeng , D.T. Zenger Jr , O. Zenin , T. Ženiš , S. Zenz , S. Zerradi , D. Zerwas , B. Zhang , D.F. Zhang , G. Zhang , J. Zhang , J. Zhang , K. Zhang , L. Zhang , P. Zhang , R. Zhang , S. Zhang , T. Zhang , X. Zhang , X. Zhang , Z. Zhang , Z. Zhang , H. Zhao , P. Zhao , T. Zhao , Y. Zhao , Z. Zhao , A. Zhemchugov , X. Zheng , Z. Zheng , D. Zhong , B. Zhou , C. Zhou , H. Zhou , N. Zhou , Y. Zhou , C.G. Zhu , C. Zhu , H.L. Zhu , H. Zhu , J. Zhu , Y. Zhu , Y. Zhu , X. Zhuang , K. Zhukov , V. Zhulanov , N.I. Zimine , J. Zinsser , M. Ziolkowski , L. Živković , A. Zoccoli , K. Zoch , T.G. Zorbas , O. Zormpa , W. Zou , L. Zwalinski .

¹Department of Physics, University of Adelaide, Adelaide; Australia.

²Department of Physics, University of Alberta, Edmonton AB; Canada.

³(^a)Department of Physics, Ankara University, Ankara; (^b)Division of Physics, TOBB University of Economics and Technology, Ankara; Türkiye.

⁴LAPP, Univ. Savoie Mont Blanc, CNRS/IN2P3, Annecy; France.

⁵APC, Université Paris Cité, CNRS/IN2P3, Paris; France.

⁶High Energy Physics Division, Argonne National Laboratory, Argonne IL; United States of America.

⁷Department of Physics, University of Arizona, Tucson AZ; United States of America.

⁸Department of Physics, University of Texas at Arlington, Arlington TX; United States of America.

⁹Physics Department, National and Kapodistrian University of Athens, Athens; Greece.

¹⁰Physics Department, National Technical University of Athens, Zografou; Greece.

¹¹Department of Physics, University of Texas at Austin, Austin TX; United States of America.

¹²Institute of Physics, Azerbaijan Academy of Sciences, Baku; Azerbaijan.

¹³Institut de Física d'Altes Energies (IFAE), Barcelona Institute of Science and Technology, Barcelona; Spain.

¹⁴(^a)Institute of High Energy Physics, Chinese Academy of Sciences, Beijing; (^b)Physics Department, Tsinghua University, Beijing; (^c)Department of Physics, Nanjing University, Nanjing; (^d)University of Chinese Academy of Science (UCAS), Beijing; China.

¹⁵Institute of Physics, University of Belgrade, Belgrade; Serbia.

¹⁶Department for Physics and Technology, University of Bergen, Bergen; Norway.

¹⁷(^a)Physics Division, Lawrence Berkeley National Laboratory, Berkeley CA; (^b)University of California, Berkeley CA; United States of America.

- ¹⁸Institut für Physik, Humboldt Universität zu Berlin, Berlin; Germany.
- ¹⁹Albert Einstein Center for Fundamental Physics and Laboratory for High Energy Physics, University of Bern, Bern; Switzerland.
- ²⁰School of Physics and Astronomy, University of Birmingham, Birmingham; United Kingdom.
- ²¹(^a) Department of Physics, Bogazici University, Istanbul; (^b) Department of Physics Engineering, Gaziantep University, Gaziantep; (^c) Department of Physics, Istanbul University, Istanbul; (^d) Istinye University, Sariyer, Istanbul; Türkiye.
- ²²(^a) Facultad de Ciencias y Centro de Investigaciones, Universidad Antonio Nariño, Bogotá; (^b) Departamento de Física, Universidad Nacional de Colombia, Bogotá; Colombia.
- ²³(^a) Dipartimento di Fisica e Astronomia A. Righi, Università di Bologna, Bologna; (^b) INFN Sezione di Bologna; Italy.
- ²⁴Physikalisches Institut, Universität Bonn, Bonn; Germany.
- ²⁵Department of Physics, Boston University, Boston MA; United States of America.
- ²⁶Department of Physics, Brandeis University, Waltham MA; United States of America.
- ²⁷(^a) Transilvania University of Brasov, Brasov; (^b) Horia Hulubei National Institute of Physics and Nuclear Engineering, Bucharest; (^c) Department of Physics, Alexandru Ioan Cuza University of Iasi, Iasi; (^d) National Institute for Research and Development of Isotopic and Molecular Technologies, Physics Department, Cluj-Napoca; (^e) University Politehnica Bucharest, Bucharest; (^f) West University in Timisoara, Timisoara; (^g) Faculty of Physics, University of Bucharest, Bucharest; Romania.
- ²⁸(^a) Faculty of Mathematics, Physics and Informatics, Comenius University, Bratislava; (^b) Department of Subnuclear Physics, Institute of Experimental Physics of the Slovak Academy of Sciences, Kosice; Slovak Republic.
- ²⁹Physics Department, Brookhaven National Laboratory, Upton NY; United States of America.
- ³⁰Universidad de Buenos Aires, Facultad de Ciencias Exactas y Naturales, Departamento de Física, y CONICET, Instituto de Física de Buenos Aires (IFIBA), Buenos Aires; Argentina.
- ³¹California State University, CA; United States of America.
- ³²Cavendish Laboratory, University of Cambridge, Cambridge; United Kingdom.
- ³³(^a) Department of Physics, University of Cape Town, Cape Town; (^b) iThemba Labs, Western Cape; (^c) Department of Mechanical Engineering Science, University of Johannesburg, Johannesburg; (^d) National Institute of Physics, University of the Philippines Diliman (Philippines); (^e) University of South Africa, Department of Physics, Pretoria; (^f) University of Zululand, KwaDlangezwa; (^g) School of Physics, University of the Witwatersrand, Johannesburg; South Africa.
- ³⁴Department of Physics, Carleton University, Ottawa ON; Canada.
- ³⁵(^a) Faculté des Sciences Ain Chock, Réseau Universitaire de Physique des Hautes Energies - Université Hassan II, Casablanca; (^b) Faculté des Sciences, Université Ibn-Tofail, Kénitra; (^c) Faculté des Sciences Semlalia, Université Cadi Ayyad, LPHEA-Marrakech; (^d) LPMR, Faculté des Sciences, Université Mohamed Premier, Oujda; (^e) Faculté des sciences, Université Mohammed V, Rabat; (^f) Institute of Applied Physics, Mohammed VI Polytechnic University, Ben Guerir; Morocco.
- ³⁶CERN, Geneva; Switzerland.
- ³⁷Affiliated with an institute covered by a cooperation agreement with CERN.
- ³⁸Affiliated with an international laboratory covered by a cooperation agreement with CERN.
- ³⁹Enrico Fermi Institute, University of Chicago, Chicago IL; United States of America.
- ⁴⁰LPC, Université Clermont Auvergne, CNRS/IN2P3, Clermont-Ferrand; France.
- ⁴¹Nevis Laboratory, Columbia University, Irvington NY; United States of America.
- ⁴²Niels Bohr Institute, University of Copenhagen, Copenhagen; Denmark.
- ⁴³(^a) Dipartimento di Fisica, Università della Calabria, Rende; (^b) INFN Gruppo Collegato di Cosenza, Laboratori Nazionali di Frascati; Italy.

- ⁴⁴Physics Department, Southern Methodist University, Dallas TX; United States of America.
- ⁴⁵Physics Department, University of Texas at Dallas, Richardson TX; United States of America.
- ⁴⁶National Centre for Scientific Research "Demokritos", Agia Paraskevi; Greece.
- ⁴⁷(^a) Department of Physics, Stockholm University; (^b) Oskar Klein Centre, Stockholm; Sweden.
- ⁴⁸Deutsches Elektronen-Synchrotron DESY, Hamburg and Zeuthen; Germany.
- ⁴⁹Fakultät Physik, Technische Universität Dortmund, Dortmund; Germany.
- ⁵⁰Institut für Kern- und Teilchenphysik, Technische Universität Dresden, Dresden; Germany.
- ⁵¹Department of Physics, Duke University, Durham NC; United States of America.
- ⁵²SUPA - School of Physics and Astronomy, University of Edinburgh, Edinburgh; United Kingdom.
- ⁵³INFN e Laboratori Nazionali di Frascati, Frascati; Italy.
- ⁵⁴Physikalisches Institut, Albert-Ludwigs-Universität Freiburg, Freiburg; Germany.
- ⁵⁵II. Physikalisches Institut, Georg-August-Universität Göttingen, Göttingen; Germany.
- ⁵⁶Département de Physique Nucléaire et Corpusculaire, Université de Genève, Genève; Switzerland.
- ⁵⁷(^a) Dipartimento di Fisica, Università di Genova, Genova; (^b) INFN Sezione di Genova; Italy.
- ⁵⁸II. Physikalisches Institut, Justus-Liebig-Universität Giessen, Giessen; Germany.
- ⁵⁹SUPA - School of Physics and Astronomy, University of Glasgow, Glasgow; United Kingdom.
- ⁶⁰LPSC, Université Grenoble Alpes, CNRS/IN2P3, Grenoble INP, Grenoble; France.
- ⁶¹Laboratory for Particle Physics and Cosmology, Harvard University, Cambridge MA; United States of America.
- ⁶²(^a) Department of Modern Physics and State Key Laboratory of Particle Detection and Electronics, University of Science and Technology of China, Hefei; (^b) Institute of Frontier and Interdisciplinary Science and Key Laboratory of Particle Physics and Particle Irradiation (MOE), Shandong University, Qingdao; (^c) School of Physics and Astronomy, Shanghai Jiao Tong University, Key Laboratory for Particle Astrophysics and Cosmology (MOE), SKLPPC, Shanghai; (^d) Tsung-Dao Lee Institute, Shanghai; China.
- ⁶³(^a) Kirchhoff-Institut für Physik, Ruprecht-Karls-Universität Heidelberg, Heidelberg; (^b) Physikalisches Institut, Ruprecht-Karls-Universität Heidelberg, Heidelberg; Germany.
- ⁶⁴(^a) Department of Physics, Chinese University of Hong Kong, Shatin, N.T., Hong Kong; (^b) Department of Physics, University of Hong Kong, Hong Kong; (^c) Department of Physics and Institute for Advanced Study, Hong Kong University of Science and Technology, Clear Water Bay, Kowloon, Hong Kong; China.
- ⁶⁵Department of Physics, National Tsing Hua University, Hsinchu; Taiwan.
- ⁶⁶IJCLab, Université Paris-Saclay, CNRS/IN2P3, 91405, Orsay; France.
- ⁶⁷Department of Physics, Indiana University, Bloomington IN; United States of America.
- ⁶⁸(^a) INFN Gruppo Collegato di Udine, Sezione di Trieste, Udine; (^b) ICTP, Trieste; (^c) Dipartimento Politecnico di Ingegneria e Architettura, Università di Udine, Udine; Italy.
- ⁶⁹(^a) INFN Sezione di Lecce; (^b) Dipartimento di Matematica e Fisica, Università del Salento, Lecce; Italy.
- ⁷⁰(^a) INFN Sezione di Milano; (^b) Dipartimento di Fisica, Università di Milano, Milano; Italy.
- ⁷¹(^a) INFN Sezione di Napoli; (^b) Dipartimento di Fisica, Università di Napoli, Napoli; Italy.
- ⁷²(^a) INFN Sezione di Pavia; (^b) Dipartimento di Fisica, Università di Pavia, Pavia; Italy.
- ⁷³(^a) INFN Sezione di Pisa; (^b) Dipartimento di Fisica E. Fermi, Università di Pisa, Pisa; Italy.
- ⁷⁴(^a) INFN Sezione di Roma; (^b) Dipartimento di Fisica, Sapienza Università di Roma, Roma; Italy.
- ⁷⁵(^a) INFN Sezione di Roma Tor Vergata; (^b) Dipartimento di Fisica, Università di Roma Tor Vergata, Roma; Italy.
- ⁷⁶(^a) INFN Sezione di Roma Tre; (^b) Dipartimento di Matematica e Fisica, Università Roma Tre, Roma; Italy.
- ⁷⁷(^a) INFN-TIFPA; (^b) Università degli Studi di Trento, Trento; Italy.
- ⁷⁸Universität Innsbruck, Department of Astro and Particle Physics, Innsbruck; Austria.
- ⁷⁹University of Iowa, Iowa City IA; United States of America.

- ⁸⁰Department of Physics and Astronomy, Iowa State University, Ames IA; United States of America.
- ⁸¹(^a) Departamento de Engenharia Elétrica, Universidade Federal de Juiz de Fora (UFJF), Juiz de Fora; (^b) Universidade Federal do Rio De Janeiro COPPE/EE/IF, Rio de Janeiro; (^c) Instituto de Física, Universidade de São Paulo, São Paulo; (^d) Rio de Janeiro State University, Rio de Janeiro; Brazil.
- ⁸²KEK, High Energy Accelerator Research Organization, Tsukuba; Japan.
- ⁸³Graduate School of Science, Kobe University, Kobe; Japan.
- ⁸⁴(^a) AGH University of Science and Technology, Faculty of Physics and Applied Computer Science, Krakow; (^b) Marian Smoluchowski Institute of Physics, Jagiellonian University, Krakow; Poland.
- ⁸⁵Institute of Nuclear Physics Polish Academy of Sciences, Krakow; Poland.
- ⁸⁶Faculty of Science, Kyoto University, Kyoto; Japan.
- ⁸⁷Kyoto University of Education, Kyoto; Japan.
- ⁸⁸Research Center for Advanced Particle Physics and Department of Physics, Kyushu University, Fukuoka ; Japan.
- ⁸⁹Instituto de Física La Plata, Universidad Nacional de La Plata and CONICET, La Plata; Argentina.
- ⁹⁰Physics Department, Lancaster University, Lancaster; United Kingdom.
- ⁹¹Oliver Lodge Laboratory, University of Liverpool, Liverpool; United Kingdom.
- ⁹²Department of Experimental Particle Physics, Jožef Stefan Institute and Department of Physics, University of Ljubljana, Ljubljana; Slovenia.
- ⁹³School of Physics and Astronomy, Queen Mary University of London, London; United Kingdom.
- ⁹⁴Department of Physics, Royal Holloway University of London, Egham; United Kingdom.
- ⁹⁵Department of Physics and Astronomy, University College London, London; United Kingdom.
- ⁹⁶Louisiana Tech University, Ruston LA; United States of America.
- ⁹⁷Fysiska institutionen, Lunds universitet, Lund; Sweden.
- ⁹⁸Departamento de Física Teórica C-15 and CIAFF, Universidad Autónoma de Madrid, Madrid; Spain.
- ⁹⁹Institut für Physik, Universität Mainz, Mainz; Germany.
- ¹⁰⁰School of Physics and Astronomy, University of Manchester, Manchester; United Kingdom.
- ¹⁰¹CPPM, Aix-Marseille Université, CNRS/IN2P3, Marseille; France.
- ¹⁰²Department of Physics, University of Massachusetts, Amherst MA; United States of America.
- ¹⁰³Department of Physics, McGill University, Montreal QC; Canada.
- ¹⁰⁴School of Physics, University of Melbourne, Victoria; Australia.
- ¹⁰⁵Department of Physics, University of Michigan, Ann Arbor MI; United States of America.
- ¹⁰⁶Department of Physics and Astronomy, Michigan State University, East Lansing MI; United States of America.
- ¹⁰⁷Group of Particle Physics, University of Montreal, Montreal QC; Canada.
- ¹⁰⁸Fakultät für Physik, Ludwig-Maximilians-Universität München, München; Germany.
- ¹⁰⁹Max-Planck-Institut für Physik (Werner-Heisenberg-Institut), München; Germany.
- ¹¹⁰Graduate School of Science and Kobayashi-Maskawa Institute, Nagoya University, Nagoya; Japan.
- ¹¹¹Department of Physics and Astronomy, University of New Mexico, Albuquerque NM; United States of America.
- ¹¹²Institute for Mathematics, Astrophysics and Particle Physics, Radboud University/Nikhef, Nijmegen; Netherlands.
- ¹¹³Nikhef National Institute for Subatomic Physics and University of Amsterdam, Amsterdam; Netherlands.
- ¹¹⁴Department of Physics, Northern Illinois University, DeKalb IL; United States of America.
- ¹¹⁵(^a) New York University Abu Dhabi, Abu Dhabi; (^b) United Arab Emirates University, Al Ain; (^c) University of Sharjah, Sharjah; United Arab Emirates.
- ¹¹⁶Department of Physics, New York University, New York NY; United States of America.

- ¹¹⁷Ochanomizu University, Otsuka, Bunkyo-ku, Tokyo; Japan.
- ¹¹⁸Ohio State University, Columbus OH; United States of America.
- ¹¹⁹Homer L. Dodge Department of Physics and Astronomy, University of Oklahoma, Norman OK; United States of America.
- ¹²⁰Department of Physics, Oklahoma State University, Stillwater OK; United States of America.
- ¹²¹Palacký University, Joint Laboratory of Optics, Olomouc; Czech Republic.
- ¹²²Institute for Fundamental Science, University of Oregon, Eugene, OR; United States of America.
- ¹²³Graduate School of Science, Osaka University, Osaka; Japan.
- ¹²⁴Department of Physics, University of Oslo, Oslo; Norway.
- ¹²⁵Department of Physics, Oxford University, Oxford; United Kingdom.
- ¹²⁶LPNHE, Sorbonne Université, Université Paris Cité, CNRS/IN2P3, Paris; France.
- ¹²⁷Department of Physics, University of Pennsylvania, Philadelphia PA; United States of America.
- ¹²⁸Department of Physics and Astronomy, University of Pittsburgh, Pittsburgh PA; United States of America.
- ¹²⁹^(a)Laboratório de Instrumentação e Física Experimental de Partículas - LIP, Lisboa;^(b)Departamento de Física, Faculdade de Ciências, Universidade de Lisboa, Lisboa;^(c)Departamento de Física, Universidade de Coimbra, Coimbra;^(d)Centro de Física Nuclear da Universidade de Lisboa, Lisboa;^(e)Departamento de Física, Universidade do Minho, Braga;^(f)Departamento de Física Teórica y del Cosmos, Universidad de Granada, Granada (Spain);^(g)Departamento de Física, Instituto Superior Técnico, Universidade de Lisboa, Lisboa; Portugal.
- ¹³⁰Institute of Physics of the Czech Academy of Sciences, Prague; Czech Republic.
- ¹³¹Czech Technical University in Prague, Prague; Czech Republic.
- ¹³²Charles University, Faculty of Mathematics and Physics, Prague; Czech Republic.
- ¹³³Particle Physics Department, Rutherford Appleton Laboratory, Didcot; United Kingdom.
- ¹³⁴IRFU, CEA, Université Paris-Saclay, Gif-sur-Yvette; France.
- ¹³⁵Santa Cruz Institute for Particle Physics, University of California Santa Cruz, Santa Cruz CA; United States of America.
- ¹³⁶^(a)Departamento de Física, Pontificia Universidad Católica de Chile, Santiago;^(b)Millennium Institute for Subatomic physics at high energy frontier (SAPHIR), Santiago;^(c)Instituto de Investigación Multidisciplinario en Ciencia y Tecnología, y Departamento de Física, Universidad de La Serena;^(d)Universidad Andres Bello, Department of Physics, Santiago;^(e)Instituto de Alta Investigación, Universidad de Tarapacá, Arica;^(f)Departamento de Física, Universidad Técnica Federico Santa María, Valparaíso; Chile.
- ¹³⁷Department of Physics, University of Washington, Seattle WA; United States of America.
- ¹³⁸Department of Physics and Astronomy, University of Sheffield, Sheffield; United Kingdom.
- ¹³⁹Department of Physics, Shinshu University, Nagano; Japan.
- ¹⁴⁰Department Physik, Universität Siegen, Siegen; Germany.
- ¹⁴¹Department of Physics, Simon Fraser University, Burnaby BC; Canada.
- ¹⁴²SLAC National Accelerator Laboratory, Stanford CA; United States of America.
- ¹⁴³Department of Physics, Royal Institute of Technology, Stockholm; Sweden.
- ¹⁴⁴Departments of Physics and Astronomy, Stony Brook University, Stony Brook NY; United States of America.
- ¹⁴⁵Department of Physics and Astronomy, University of Sussex, Brighton; United Kingdom.
- ¹⁴⁶School of Physics, University of Sydney, Sydney; Australia.
- ¹⁴⁷Institute of Physics, Academia Sinica, Taipei; Taiwan.
- ¹⁴⁸^(a)E. Andronikashvili Institute of Physics, Iv. Javakhishvili Tbilisi State University, Tbilisi;^(b)High Energy Physics Institute, Tbilisi State University, Tbilisi;^(c)University of Georgia, Tbilisi; Georgia.

- ¹⁴⁹Department of Physics, Technion, Israel Institute of Technology, Haifa; Israel.
- ¹⁵⁰Raymond and Beverly Sackler School of Physics and Astronomy, Tel Aviv University, Tel Aviv; Israel.
- ¹⁵¹Department of Physics, Aristotle University of Thessaloniki, Thessaloniki; Greece.
- ¹⁵²International Center for Elementary Particle Physics and Department of Physics, University of Tokyo, Tokyo; Japan.
- ¹⁵³Department of Physics, Tokyo Institute of Technology, Tokyo; Japan.
- ¹⁵⁴Department of Physics, University of Toronto, Toronto ON; Canada.
- ¹⁵⁵(^a) TRIUMF, Vancouver BC; (^b) Department of Physics and Astronomy, York University, Toronto ON; Canada.
- ¹⁵⁶Division of Physics and Tomonaga Center for the History of the Universe, Faculty of Pure and Applied Sciences, University of Tsukuba, Tsukuba; Japan.
- ¹⁵⁷Department of Physics and Astronomy, Tufts University, Medford MA; United States of America.
- ¹⁵⁸Department of Physics and Astronomy, University of California Irvine, Irvine CA; United States of America.
- ¹⁵⁹Department of Physics and Astronomy, University of Uppsala, Uppsala; Sweden.
- ¹⁶⁰Department of Physics, University of Illinois, Urbana IL; United States of America.
- ¹⁶¹Instituto de Física Corpuscular (IFIC), Centro Mixto Universidad de Valencia - CSIC, Valencia; Spain.
- ¹⁶²Department of Physics, University of British Columbia, Vancouver BC; Canada.
- ¹⁶³Department of Physics and Astronomy, University of Victoria, Victoria BC; Canada.
- ¹⁶⁴Fakultät für Physik und Astronomie, Julius-Maximilians-Universität Würzburg, Würzburg; Germany.
- ¹⁶⁵Department of Physics, University of Warwick, Coventry; United Kingdom.
- ¹⁶⁶Waseda University, Tokyo; Japan.
- ¹⁶⁷Department of Particle Physics and Astrophysics, Weizmann Institute of Science, Rehovot; Israel.
- ¹⁶⁸Department of Physics, University of Wisconsin, Madison WI; United States of America.
- ¹⁶⁹Fakultät für Mathematik und Naturwissenschaften, Fachgruppe Physik, Bergische Universität Wuppertal, Wuppertal; Germany.
- ¹⁷⁰Department of Physics, Yale University, New Haven CT; United States of America.
- ^a Also Affiliated with an institute covered by a cooperation agreement with CERN.
- ^b Also at Borough of Manhattan Community College, City University of New York, New York NY; United States of America.
- ^c Also at Bruno Kessler Foundation, Trento; Italy.
- ^d Also at Center for High Energy Physics, Peking University; China.
- ^e Also at Centro Studi e Ricerche Enrico Fermi; Italy.
- ^f Also at CERN, Geneva; Switzerland.
- ^g Also at Département de Physique Nucléaire et Corpusculaire, Université de Genève, Genève; Switzerland.
- ^h Also at Departament de Física de la Universitat Autònoma de Barcelona, Barcelona; Spain.
- ⁱ Also at Department of Financial and Management Engineering, University of the Aegean, Chios; Greece.
- ^j Also at Department of Physics and Astronomy, Michigan State University, East Lansing MI; United States of America.
- ^k Also at Department of Physics and Astronomy, University of Louisville, Louisville, KY; United States of America.
- ^l Also at Department of Physics, Ben Gurion University of the Negev, Beer Sheva; Israel.
- ^m Also at Department of Physics, California State University, East Bay; United States of America.
- ⁿ Also at Department of Physics, California State University, Sacramento; United States of America.
- ^o Also at Department of Physics, King's College London, London; United Kingdom.
- ^p Also at Department of Physics, University of Fribourg, Fribourg; Switzerland.

- ^q Also at Department of Physics, University of Thessaly; Greece.
- ^r Also at Department of Physics, Westmont College, Santa Barbara; United States of America.
- ^s Also at Hellenic Open University, Patras; Greece.
- ^t Also at Institucio Catalana de Recerca i Estudis Avancats, ICREA, Barcelona; Spain.
- ^u Also at Institut für Experimentalphysik, Universität Hamburg, Hamburg; Germany.
- ^v Also at Institute of Particle Physics (IPP); Canada.
- ^w Also at Institute of Physics, Azerbaijan Academy of Sciences, Baku; Azerbaijan.
- ^x Also at Institute of Theoretical Physics, Ilia State University, Tbilisi; Georgia.
- ^y Also at Lawrence Livermore National Laboratory, Livermore; United States of America.
- ^z Also at The Collaborative Innovation Center of Quantum Matter (CICQM), Beijing; China.
- ^{aa} Also at TRIUMF, Vancouver BC; Canada.
- ^{ab} Also at Università di Napoli Parthenope, Napoli; Italy.
- ^{ac} Also at University of Chinese Academy of Sciences (UCAS), Beijing; China.
- ^{ad} Also at University of Colorado Boulder, Department of Physics, Colorado; United States of America.
- ^{ae} Also at Washington College, Maryland; United States of America.
- ^{af} Also at Yeditepe University, Physics Department, Istanbul; Türkiye.
- * Deceased